AFCRL TR-60-199

LOW REFLECTION ABSORBERS FOR ELECTROMAGNETIC WAVES

E. Meyer and R. Pottel
(Translated by F Vilbig)

November 1960

ELECTRONICS RESEARCH DIRECTORATE
AIR FORCE CAMBRIDGE RESEARCH LABORATORIES
AIR FORCE RESEARCH DIVISION (ARDC)
UNITED STATES AIR FORCE
BEDFORD MASS.

Requests for additional copies by Agencies of the Department of Defense, their contractors and other Government agencies should be directed to the

Armed Services Technical Information Agency
Arlington Hall Station
Arlington 12, Virginia

Department of Defense contractors must be established for ASTIA services, or have their "need-to-know" certified by the cognizant military agency of their project or contract.

All other persons and organizations should apply to the:

U. S. DEPARTMENT OF COMMERCE
OFFICE OF TECHNICAL SERVICES,
WASHINGTON 25, D. C.

AFCRL-TR-60-199

LOW REFLECTION ABSORBERS FOR ELECTROMAGNETIC WAVES

(REFLEXIONSARME ABSORBER FUER ELEKTROMAGNETISCHE WELLEN)

Translation by F. Vilbig from a German manuscript for the book "Fortschritte der Hochfrequenztechnik" edited by the Akademische Verlagsgesellschaft, Frankfurt - Main (Germany), 1960.

Erwin Meyer and Reinhard Pottel
Goettingen, Germany
III. Physikalisches Institut der Universitat

Project 4610
Task 46102

COMMUNICATION SCIENCES LABORATORY
ELECTRONICS RESEARCH DIRECTORATE
AIR FORCE CAMBRIDGE RESEARCH LABORATORIES
AIR FORCE RESEARCH DIVISION (ARDC)
UNITED STATES AIR FORCE
BEDFORD MASS.

ABSTRACT

Low reflecting absorbers for electromagnetic waves in the range of m- and cm- wavelengths are used in research - f. expl. for coating the walls of test rooms - and in radar technique. The major aspect of the development of absorbers is the elimination of reflections which under vertical incidence of waves on plane surfaces occur at almost all dissipative materials. This reduction of reflections may be attained in different ways: by a continual transition from free space into the absorbing material, by using resonance arrangements, or with the help of certain absorbing substances with uniform, spatial distribution.

Wedge-, pyramid-, and rib-absorbers; foil-, layer-, dipole-, slit-, and loop-absorbers; absorbers with low density material and $\varepsilon = \mu$ - absorbers: These various absorbers resulting from the three basic principles of reduction of reflections are treated with respect to the dependence of their reflection coefficients on frequency, angle of incidence, and direction of polarization and finally the thickness of the arrangement. Numerous theoretical and experimental data indicate the most favorable design and the range of application of the individual absorbers.

In addition to the statements put forward for absorbers for electromagnetic waves short remarks are made concerning the corresponding absorbers for air - or water-borne sound, which are physically closely related to the electromagnetic absorbers and have in part been prototypes for the latter. Finally test methods for low reflection absorbers (measurement in the free field and in the echo chamber) and their application in electromagnetically oanechoic rooms are discussed.

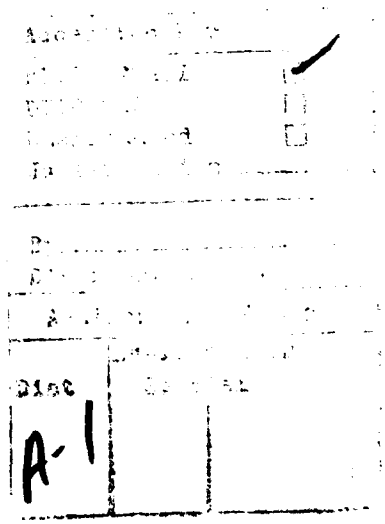

TABLE OF CONTENTS

TABLE OF CONTENTS (Cont.)

SUMMARY OF SYMBOLS

A = Degree of absorption

C = Capacity

d = Layer thickness, absorber thickness

E = Electrical field strength

F = Surface area

G = Conductance

g, h = Grid constants

H = Magnetic field strength

L = Inductivity

l = Length

Q = Quality

R = Ohmic resistance

r = Complex reflection factor

V = Volume

W = Complex input impedance

x = Plane coordinate

Y = Complex input admittance

Z_o = Wave impedance

α = Attenuation constant

β = Phase constant

γ = Complex propagation constant ($\alpha + i\beta$)

δ = Thickness of foil

$\delta_\varepsilon, \delta_\mu$ = Loss angles

ε = $\varepsilon' - i\varepsilon''$ complex relative dielectric constant

ε_o = Influence constant

ϑ = Angle of incidence

λ = Wave length

μ = $\mu' - i\mu''$ complex relative permeability

μ_o = Induction constant

ν = Frequency

σ = Conductivity

τ = Reverberation time

ψ = Polarization angle

ω = Circular frequency

Other terms not frequently used are explained in the text.

LOW REFLECTION ABSORBERS FOR ELECTROMAGNETIC WAVES

by

E. Meyer and R. Pottel

1. INTRODUCTION

1.1 Purpose of Poorly-reflecting Absorbers and Goal of their Development

The rapidly progressing development in the field of electromagnetic waves in the dm- and cm-portion of the wave spectrum during the last two decades invited the attention also to configurations which reflect electromagnetic waves as poorly as possible, and which absorb the entered energy along a path as short as possible. This holds true especially for waves which travel in free space. For measuring purposes it is often desirable to make nonreflecting a certain wall, a ceiling, or even all walls of a room. In the latter case, a so-called free-space room is obtained. Also in practical applications, the employment of radar for instance, it may be desirable to let disappear, that is, to make nonreflecting certain objects such as structures on ships, funnels, or the like, which may happen to be near the point of measurement. Finally, one thinks of military applications, such as to camouflage targets by coating with a nonreflecting substance and simultaneous erection of mock-up targets for erroneous results for enemy radar direction finding.

Nonreflecting configurations are important not only in the free space but also for guided waves; they are needed for measurements in coaxial cables and wave guides. The nonreflecting terminal plays a vital part in this measuring technique.

It has been mentioned already, that the desire for nonreflecting absorbers is connected mainly with the development of the cm-waves. However, nonreflecting configurations are not limited to this part of the wave spectrum. It is possible to produce these also for considerable greater wave lengths, but in this case, their layer thickness is much bigger and therefore bulky. As far as the authors know, configurations have been created in the form of wedge-shaped or "Schacht" absorbers. (compare Sections 2 and 3) which are effective up to wave lengths of several meters.

Important factors for the development of absorbers are the frequency bandwidth, the influence of the angle of incidence and polarization, as well as the thickness of the absorbing layers. First some remarks about the frequency bandwidth in which they operate. Wide-band absorbers, effective over several octaves, are constructed almost exclusively in the form of wedges and are used expecially for wall-covering of nonreflecting rooms; their thickness is big. In case of fixed wave lengths, or such with small variations only, small-band absorbers constructed of resonant structures can be of value; their thickness is much smaller and their bandwidth is, as a rule, below an octave.

Important is also the dependence from the angle of incidence and the direction of polarization. The general requirement is that the reflection be greatly independent from the angle of incidence and the polarization direction of the wave.

1.2 The Reflection Factor as a Function of the Input Impedance, the Angle of Incidence and the Direction of Polarization

Let us consider first a plane wave which strikes an absorber normally. The configuration may have the complex input impedance W defined by the quotient of electrical and magnetic field strength taking into the consideration the phase at the input of the absorber configuration. Furthermore, let Z_0 be the wave impedance of the free medium opposing a planar wave; it is always so that in all practical applications the free space (air) will be in front of the configuration. Z_0 is the ratio of electrical field strength to magnetic field strength within the propagating planar wave; its value

(for air) amounts to 377 ohms. From the two factors the reflection factor r becomes

$$r = \frac{W - Z_0}{W + Z_0}$$

Instead of the reflection factor, which is related to the amplitudes of the incident and the reflected waves, often the degree of reflection $|r^2|$ is used which is based upon the ratio of energies. Finally, it is customary to note a reflection attenuation in db as 10 times the logarithm of the quotient of the reflected energy at 100 percent reflection, and the amount of the reflected energy from the test object.

The above formula shows immediately which possibilities a reflection factor of ± 1 provides, namely the cases $W = 0$, or $W = \infty$. Out of these two, for electro-magnetic waves only the case $W = 0$ can be realized easily by use of a metal plate. The case $W = \infty$ is for practical purposes "fictitous", perhaps in a plane with a distance of $\lambda/4$ in front of a metal plate.

The input impedance of an absorber depends, in general, strongly upon the wave length. The less it is dependent, and the closer its value is to the wave impedance Z_0, the wider is the bandwidth of the absorber and the lower its reflection. Taking the above into account, an absorber is considered to be good when $|r|$ is below 0.1. As effective frequency bandwidth, that frequency interval is specified where $|r|$ is smaller than 0.1. The value $|r| = 0.1$ defines the two limiting frequencies. The relation between the reflection factor (amount and phase) and input impedance (amount and phase, or real and imaginary part, respectively) is taken from the known diagrams which are based upon conformal mapping.[1]

In the case of the reflection of an obliquely incident electro-magnetic wave, the polarization direction of the wave has to be taken into consideration, i.e., the position of the electrical field strength vector, either parallel ($\parallel$) or vertical ($\perp$) as referenced to the plane of incidence. If γ is the incidence angle, referenced to the normal direction, the corresponding formulae become

$$r_{||} = \frac{W - Z_0 \cos\vartheta}{W + Z_0 \cos\vartheta}$$

$$r_{\perp} = \frac{W - Z_0 / \cos\vartheta}{W + Z_0 / \cos\vartheta} \quad .$$

In general, the input impedance W will depend here upon the angle of incidence ϑ.

From the above formulae it can be seen that the absorber can be made non-reflecting for a vertical incidence, as mentioned before. However, it is possible to match the input impedance for any desired angle of incidence at least for one of the two polarization directions. This matching does not apply, in general, for the other polarization direction unless the absorber is made independent from the polarization. Of course, also in the latter case the reflection factor's dependence from the angle of incidence remains valid. Using the best of the presently known absorbers, the reflection factor can be made small only for a certain range of angles, for example between 0^{o} and 60^{o}.

Here the question arises how the reflection from absorption configurations develops for one polarization direction as function of the angle of incidence if the reflection has been made as small as possible for all angles for the other polarization direction. A similar problem is how much the reflection factor depends upon the angle of incidence if it is desired that the reflection factor is to be equal for both polarization directions. In both cases, laws can be quoted which will be mentioned in the discussion about the different types of absorbers.

In addition to the normal and oblique reflection, the "back-scatter" or "radar" reflection is also introduced, i.e., that portion of the power of the incident wave is considered which is reflected back into the direction of incidence, or in other words, is reflected back into the direction of the transmitter.

1.3 Comparison of Electromagnetic and Acoustical Absorbers

For a study of absorption methods of electro-magnetic waves, also the older acoustical methods can be considered for purposes of comparison; since the acoustical absorbers exist in an uncounted variety and are employed especially for the regulation of the reverberation in theaters and concert halls as well as a means of reducing noise in noisy rooms. Last, it is well to mention that some types of acoustical absorbers served as prototypes for the development of the respective electro-magnetic absorbers. Moreover, the acoustical absorbers play an important role not only for the sound in air but also for the sound in water.

When using the acoustical absorbers for purposes of comparison, it is well to remember that the field of sound -- having only one vector: the particle velocity, and only one scalar: the sound pressure -- is composed differently as the electro-magnetic field with its two vectors, the electric and the magnetic field. But with regard to the reflection and its relation to the impedances, the same relationship exists. For a normal sound incidence of a plane wave, as before is

$$r = \frac{W - Z_0}{W + Z_0} \quad .$$

In air sound techniques, the case $W = \infty$ as reference value for a reflection of 100 percent can be realized extremely simply by use of a rigid wall (normal velocity ≈ 0) while the case $W = 0$ can be realized in a simple manner only in water through a free liquid surface. $Z_{0\ air}$ has in the mgs system a value of 420 acoustical ohms, $Z_{0\ water}$ amounts to 1.5×10^6 acoustical ohms. The big difference between the two values proves that in one case the "hard" termination, in the other case the "soft" termination can be achieved.

Since in shear-stress free media such as air and water, no polarized sound waves exist, the polarization directions, as mentioned in the preceding chapter are obsolete. In contrast, the dependence from the angle of incidence ϑ is retained in the form

$$r = \frac{W - Z_0/\cos\vartheta}{W + Z_0/\cos\vartheta} .$$

In general, W depends here upon the angle of incidence. Only in the so-called Rayleigh's model of a sound absorber, where no sound propagation occurs in the interior parallel to the surface, W is independent from the angle of incidence.

With respect to a classification of the electro-magnetic absorbers it is not uninteresting to describe briefly the different classes of acoustical absorbers.

The acoustical absorbers, which are most frequently employed, belong to the class of homogenous substances with planar faces where the material constants provide the best matching to the medium as well as a relative high attenuation of the entered wave. Here, the porous acoustical absorbers are to be mentioned whose flow resistances in the pores cause the interior losses.

To the aforementioned class belongs also an absorber type, which has been tried repeatedly to manufacture for underwater technique, likewise having smooth (planar) surfaces and high internal losses. Let us consider a rubber-like elastic substance whose Poisson's number lies close to C.5, then its characteristic impedance is

$$Z_M = \sqrt{\frac{\varrho}{K}} = \sqrt{\frac{|\varrho|}{|K|}} \times e^{(j/2)(\delta_\varrho - \delta_K)}$$

where K and ϱ are the complex compressibility and density, and δ_K and δ_ϱ are the pertaining loss angles. Freedom from reflection is given when $\delta_\varrho = \delta_K$ and $\sqrt{\frac{|\varrho|}{K}}$ equals the wave impedance of the medium, that is, the wave impedance of the water, provided the thickness of the layer is sufficiently high in order to avoid the influence of the reflection of the entered wave from the rear side of the absorber. Such an absorber type has its counterpart in the so-called $\varepsilon = \mu$ absorber (see Section 4).

In general, the thickness and the internal attenuation of these absorbers will not be sufficiently big enough so that the wave, penetrating the absorber, is reflected with a rather high intensity from the absorber rear side. Consequently, interference results between the wave, (having penetrated the absorber material, and then being

reflected) with the wave reflected at the input side, or in other words, resonance, or antiresonance, respectively, causes a reflection factor which changes with the frequency.

With the type of absorber just described, it is not possible to achieve small reflections over a wide band of frequencies. For this purpose, another type of absorber is used which has a high internal attenuation, too. It has, however, no planar faces extended toward the medium because it cannot be matched with the surrounding medium due to its high internal attenuation; it must rather provide a gradual transition toward the medium, mostly in geometric form. This is the type of the so-called "wedge-absorber". The geometric transition takes place usually in the form of a wedge, but also the conical or pyramidal form is employed.

Nonreflecting rooms for acoustical measurements are covered according to this principle[2] where for sound porous substances are chosen, as a rule, such as glass or mineral fibers. The lower limiting frequency is given by the lengths of the wedges. There is no upper limiting frequency. With this type of absorber an excellent "wide-band-absorber" exists.

This absorber type has been used recently also as an electro-magnetic absorber for the decorating of nonreflecting rooms. By proper use of materials the acoustic and electric effectiveness has been combined successfully.

Instead of the geometrical transition of the absorber structure, it is possible to select principally also a gradual transition of the material properties with planar limitation of the layer; this method, however, presents considerable technical difficulties, and remains, therefore, meaningless for practical purposes.

Finally, a third class of acoustical absorbers can be defined, namely those with a limited frequency band. They are generally constructed in the form of resonant circuits. Typical examples of this class are the "plate absorber", e.g., wooden plates with a certain distance before a rigid wall, or "hole-absorber", that is, plates with numerous holes, likewise at a certain distance in front of a rigid wall. The plates in

the first case, or the air "pistons" in the holes in the second case, represent the resonant mass, the air cushion between wall and plate represent the spring action of an acoustic-mechanical resonance circuit. Accordingly, such a configuration has a more or less wide resonance-like curve of sound absorption with respect to the frequency depending upon its attenuation.

It is apparent that a wider frequency band by adding of more resonant circuits can be achieved -- in the above case by connecting several plates in series. A similar development has been achieved for under-water absorbers.

This type can be defined as "resonant absorber". Transferring the principles gained in the acoustics to the electromagnetic absorbers has resulted in particularly interesting electromagnetic absorbers (compare Section 3).

1.4 Systematic Classification of Absorbers

Each absorber for electromagnetic waves must contain energy-dissipating substances. An energy-dissipating substance is defined in this case as having the property to convert a portion of the incident electromagnetic energy into heat, the electromagnetic energy being taken from the electromagnetic field of the wave. The action of the wave on the absorbing substance causes line currents, or electrical or magnetic polarization, respectively. Each one of these elementary processes is always accompanied by an electromagnetic radiation. Usually, an incident wave produces, therefore, a reflected wave at a planar face of the energy-dissipating substance.

The determining factor in the development of absorbers is the reduction or elimination of the reflected radiation produced by the wave striking the absorber material, that is, the most complete transition of the incident wave into the energy-dissipating substance. The realization of this goal depends upon the basic structure of the absorbing material (value of losses, dielectric and magnetic properties), and particularly upon its arrangement in space.

The underlying principle of elimination of the reflected radiation by arranging the absorbing materials suitably in space can be seen from the following configuration:

A planar wave strikes normally a wide-stretched plane upon which the absorbing material is distributed very thinly in relation to the wave length. From this plane, a reflected wave is radiated, the amplitude and phase of which depends upon the nature and the distribution of the absorbing material. Parallel to this plane, another plane is now being erected which is likewise covered with absorbing material and being able to reflect on its own accord. The kind of absorbing material, the manner of its distribution on these planes, and especially the distance between the planes can be chosen so that the entire configuration becomes nonreflecting.

The absorbing material across the two planes can be distributed either uniformly (for instance in the form of foils) or nonuniformly (perhaps in the form of dipoles), while the distance between the planes amounts to fractions of a wave length (for instance, a quarter wave length). As the rear plane of the two aforementioned planes, also a metal plate can be used. The number of reflecting planes does not necessarily have to be restricted to two. Foil and dipole absorbers belong into this group.

The principle of reflection reduction, mentioned above, may be expressed even more generally by the requirement that there must be a reciprocal action of two or more individually reflecting planes located parallel to each other. The absorbing material, causing the reflection of each plane, does not have to be concentrated in these planes, as described before, but may be distributed uniformly between these planes. As reflecting plane either an interface between the free space and an absorbing material, homogeneous in depth, can be effective, or an interface between different absorbing materials also homogeneous in depth. This is the case with the " $\lambda/4$ layer-absorbers" and "multi-layer absorbers". A multi-layer absorber, consisting of very many and very thin layers, differs hardly from an inhomogeneous absorber with continuous distribution in depth of its absorbing material. With both, the absorption increases slowly from small values with increasing penetration. Therefore, the absorbers with an inhomogeneous structure have to be accorded the same underlying principle, for instance the wedge-absorbers when only as limiting cases.

The absorbers with a homogeneous structure do not follow the above principle of reflection depression which could be defined as interference principle. Here, only the properties of the absorbing material are responsible for the reflection reduction.

In order to achieve a classification of absorbers, it seems convenient to consider the spacial distribution of the absorbing material within the absorber along the direction of a vertically incident wave, and especially the irregularities of the distribution. Imagine the density of the absorbing material with respect to the depth of penetration when graphically represented, and count the irregularities of the curves. Adjacent irregularities, which have a very small distance from each other compared with the wave length, are to be counted only as one irregularity (for instance foil thickness). Furthermore, only those irregularities are significant which are actually reached by the wave.

There are no irregularities to be observed on the absorbers with an inhomogeneous structure, as will be discussed in Section 2, such as the rib-shaped, and wedge-shaped, and pyramid-shaped absorbers.

The absorbers with a homogeneous structure of Section 4 posses an irregularity as determined by their planar interface.

The distribution of the absorbing material in all remaining absorbers is marked by two or more irregularities, where a planar metallic interface has to be counted also as an irregularity. An absorber configuration (for instance the above mentioned basic configuration) with at least two irregularities having a distance from each other comparable to the wave length, displays "resonant properties", that is, the input impedance depends strongly upon the frequency. Such a configuration shall be defined here as "resonant structure of the first kind" (or resonant layer). Also a single absorbing plane may possess resonant properties, namely if it consists, for instance, of an energy-dissipating grid of dipoles, or is made of a foil with resonant slots. In this case, the term "resonant structure of the second kind" (or resonator layer) is used. Section 3 is devoted to absorbers having resonant structures.

2. WIDE-BAND ABSORBERS OF INHOMOGENEOUS STRUCTURE

2.1 Absorbing Materials and Principle of Gradual Transition from Absorber to Free Space

The absorbers, to be discussed in this section, require materials which cause great electrical losses, and have therefore a high dielectric constant, or materials which cause great magnetic losses. Having this property, energy is primarily extracted from the electric or magnetic field of the incident wave. It is especially important to have absorbing materials whose electrical or magnetic properties can be changed at will very easily. This change can be best accomplished by use of artificial dielectrics or magnetic substances, that is, with loss-free dielectric carrier substances which contain respective filling materials such as graphite powder, or iron powder. Such substances have been investigated thoroughly.[3] Measurements with paraffin as carrier substance and with kinds of graphite with different purity (98 and 99.5 percent) up to 20 percent volume as filling substance are considered first. With $\lambda = 3$ cm wave length, the following have been measured: ε, μ, $\mathrm{tg}\delta_\varepsilon$, and $\mathrm{tg}\,\delta_\mu$.

Figure 2.1 contains a summary of the results. With increasing graphite content, the dielectric constant increases (the graphite particles represent induced macroscopic dipoles) but more important for this discussion is the increase in the electrical attenuation factor, especially in the case of the purer graphite. In contrast to this, the slight change of permeability and the small increase of the magnetic loss angle is insignificant. The drawn curve for the dielectric constant in Fig. 2.1 is calculated according to a theory by Lewin.[4]

Similar measurements have been taken with an artificial ferro-magnetic substance with iron powder as addition to paraffin. In particular, carbonyl iron powder and two other kinds of iron powder with grain diameters of 2×10^{-4} cm, and 50×10^{-4} cm have been used (Fig. 2.2). The results, again for $\lambda = 3$ cm, show that the permeability as well as the dielectric constant increases with increasing amounts of iron powder. Remarkable, however, is the high factor of magnetic loss $\mathrm{tg}\delta_\mu$ which reaches about 0.4, while $\mathrm{tg}\delta_\varepsilon$ is very low due to the high electrical conductivity of iron.

In the same manner, many other metals and semiconductors in powdered form have been investigated; but the two aforementioned cases provide the highest attenuation so that practically only graphite and iron powder are suitable for construction of absorbers. Two volume-percent of filled-in substances represent for iron a density of 0.145 g/cm^3, for graphite 0.04 g/cm^3; using paraffin as carrier substance at 3 cm wave length, an attenuation of 75 db/m for iron powder and 45 db/m for graphite powder has been obtained.

According to Lewin's theory, which confirms itself in this respect also quantitatively, the angle of loss increases with the size of the grain of the filled-in substance, reaches a maximum and decreases again. The dielectric constant and the permeability show the respective dispersion curve. A strong increase of the losses can be achieved when, by considerable greater dimensions of the added particles (perhaps through small wires with a length of $\lambda/2$), resonant effects come into being at certain wave lengths.

The wave impedance of a strongly energy-dissipating substance differs conditionally from that of free space in that matching becomes impossible with a planar and smooth surface of the configuration; an incident wave will be reflected the more strongly, the higher the attenuation of the wave is within the substance. An exception are only those substances with $\varepsilon = \mu$ (Section 4) which, having a planar surface, let pass the incident wave without reflection into the interior of the substance where the wave is being absorbed if attenuation and layer thickness are great enough. Such substances do not, or do not yet, exist for use in the cm or dm portion of the spectrum.

The same situation can be found in acoustics. The strongly energy-dissipating, porous substances, employed here, have mostly a very high flow resistance, and differ thereby in their properties from those of air so that a reflection-free transition of the incident sound wave into the substance is impossible with planar surface. The solution of this problem is simple. The transition must take place gradually, that is, in the geometrical sense in such a way that with the extension of the absorbing materials in depth the cross-sectional area of air decreases and that of the material increases until

finally the material solely fills the cross-section. The transition length must lie in the order of magnitude of the respective wave length.[2]

The same solution can be used in the electromagnetic case. Suitable geometric transitions are the same as in the acoustics, namely wedges, pyramids, or suitably sharpened ribs.

There is a second possibility of matching. Instead of the geometrical transition, a "material" transition is used, that is, a gradual change of the properties of the substance is initiated and a planar entrance plane is retained. This possibility offers many advantages for its employment, however, it is hardly employed due to technical production difficulties.

2.2 About the Determination of the Transition Form

The determining factor in the development of absorbers with a gradual transition is -- by given material properties -- the length of the transition, since associated with it is the important question of the layer thickness. Here, from the beginning it is to be expected that the length of the transition must be in the order of magnitude of the wave length of the incident wave. Pyramid-shaped, or wedge-shaped absorbers have been used to experimentally investigate this problem for electromagnetic waves, about which will be reported in Section 2, 2.3.

If the form of transition is of interest, it is simpler to investigate the wave propagation on transmission lines with locally varying attenuation in restriction to one-dimensional line phenomena. Such a configuration is then, so to speak, an "Analog computer" for poorly reflecting absorbers. This is valuable since -- even with restriction to one-dimensional phenomena -- the complicated transitions are beyond a direct numerical calculation.

K. L. Lenz[5] has conducted experiments of this kind not with a homogeneous line but with a low-pass filter consisting of 32 π-sections with a limiting frequency of 1.5 Mc in a frequency range up to 300 Kc, so that at this frequency still four sections cover one-quarter wave length. The attenuation takes place at fixed values of inductivity and

capacity according to the desired transition by staggered cross resistances parallel to the capacities of the low-pass filter.

The input impedance is being measured with the end of the network short circuited, and is being compared with the wave impedance of the undamped system. From this, the reflection factor is derived immediately. If L', C', G(x) are the inductivity, the capacity, and the conductance per unit length, and L is the total length of the transmission line, then the voltage distribution is given by the differential equation

$$\frac{d^2 U}{d\,(x/L)^2} = \gamma^2 L^2 U$$

where $\gamma = \sqrt{j\omega L' (G'(x) + j\omega C')}$ with ω denoting the circular frequency.

The linear increase belongs to the few attenuation functions on the line which permit a full integration of the above differential equation. Figure 2.3a and b show two measurement examples for the circle diagram of the input impedance, where a total attenuation of 1.5 or 3 Neper, respectively, is linearly distributed along the network, the measured resistances and reactances are, as already mentioned, referenced to the wave impedance of the undamped network. The parameter is not the frequency but the reciprocal value of the pertaining wave length in the undamped line referenced to the total length of the line $(1/\lambda_0)$. The curves are obtained by measurements; the points are calculated. Also plotted are the curves of constant reflection factor. A reflection factor of 10 percent is derived for the length of the network of $0.7\lambda_0$. If slight excesses of this value are permitted, then a total length of $0.5\lambda_0$ is already sufficient.

While the linear increase in attenuation can be found numerically, the advantage of the Lenz method becomes apparent when dealing with complicated attenuation distributions. Figure 2.4 is based upon an exponential course. The attenuation starts at the input of the line with 0.29 Neper, and according to the law exp. 2.73 x/L, increases up to a final value of 4.37 Neper, Such a course is more suitable with

respect to the lower limiting frequency than the case where the attenuation for X = 0 starts with the value 0. For $L = 0.35\ \lambda_o$, the 10 percent limit of the reflection factor will be reached. By summarizing the optimum attenuation distributions, measured by Lenz it can be seen that the differences are not too big.

Extensive calculations for exponential transitions of the material properties of one dimensional inhomogeneous absorbing layers for electromagnetic and acoustic waves are given by K. Walther.[13] The reflection factor /r/ of such layers is calculable from a Riccati-differential equation. K. Walther has determined some of its solutions with an analog computer. With increasing ratio of layer thickness to free space wavelength the reflection factor shows the expected decrease in the form of strongly damped oscillations. The smallest absorber thicknesses d, beyond /r/ does not exceed 0.1 (0.14), are near $d/\lambda_o > 0.35$ (0.28). They are slightly larger than the d/λ_o-values measured with other inhomogeneous constructed wide band absorbers, e.g., wedge-type absorbers.

2.3 Wedge and Pyramid Absorbers

The favorable layer thickness of somewhat more than $1/3\lambda$, as established by the model experiments and the provisions of the previous paragraph can practically not be reached for the electromagnetic absorbers with the principle of a gradual transition.

In this chapter, real absorbers with wedge-like shape, or pyramid-like shape shall be discussed, like the ones which were investigated by H. G. Haddenhorst[6] at 3.4 kmc/s. The measurements were taken with paraffin as dielectric carrier material (compare 2.1). The cross-sectional forms used are summarized in Fig. 2.5; the transition of the length T is followed by a layer of compact material of the length S with a metal plate in the rear. Since the mixture of paraffin-graphite has been varied in order to cause a change in the dielectric properties of the test material, Fig. 2.6 summarizes the increase of the attenuation (Neper/cm) with the concentration of graphite (Vol. percent). Changing the graphite concentration from 5 to 40 volume

percent causes an increase in attenuation from 0.5 db/cm to 18 db/cm. The measurements were taken in the wave guide (TE_{10} mode) with guide wave length of 13.3 cm (wave length in free space 8.75 cm), in other words, in this experiment the incidence angle of the radiation was about 45^{o} onto the test pieces. The edges of the wedges may lie parallel or vertical to the E-vector in the wave guide. Such a difference in polarization does not exist when a pyramid-shaped absorber is chosen. If the E-vector lies parallel to the edges then the space between the wedges act as "wave guides below the cut-off frequency". Due to the additional imaginary attenuation, the reflection is being enlarged. This is different when the E-vector is vertical to the edges; here one deals with "energy-dissipating parallel plate TEM-Lines". With the same transition length this difference affects favorably the latter's polarization, resulting in a considerable greater reduction of the reflection factor.

The investigation of the required length of the transition from air to the paraffin-graphite-objects is simple. As already mentioned, the length of the transition must supposedly be greater, the higher the content of graphite, since then the dielectric with its wave impedance differs more markedly from that of free space. When being measured, the part S of the configuration has such a length for the different contents of graphite that the reflection of the entered wave at the rear end becomes negligible. Figure 2.7 shows that the length of the pyramid transition T increases with increasing contents of graphite. Between 10 and 40 percent graphite, the length of the pyramid increases approximately from 5 to 15 cm, if small reflection values are to be obtained.

From a practical point of view, the total smallest layer thickness for a given wave length is more interesting than the length of the transition. The parameter for this series of experiments is again the contents of graphite, which determines the optimum length of the pyramid (T for $/r/ = 0.1$ from Fig. 2.7). The pyramids, with a length as determined above, are followed by a sufficiently long compact layer consisting of the same paraffin-graphite misture. These structures with a metal

plate at their read end, serve for measurements of the reflection factor depending upon the total length. Hereby, the test pieces are reduced in steps, that is, first the parallel-epiped part is shortened and finally also the length of the pyramids is reduced. The results for the various contents of graphite are summarized in Fig. 2.8. As abscissa, the total length d = S + T is drawn. The point, where the configuration configuration consists solely of the wedge, has been specially designated (d ≙ T). Small and big amounts of graphite additives result in greater values of the total length since in one case the attenuation is lower per unit length, and in the other case the required length of the transition is greater. Those total lengths, where the reflection factor reaches a value of 10 percent, are pictured in Fig. 2.9 in dependence of the graphite contents. The optimum length in the case of paraffin and the aforementioned type of graphite lies between 20 and 25 percent content and amounts to about 7 cm, thus being somewhat smaller than the wave length in free space. Since this value holds for an incidence angle of 45°, it can be assumed that at this polarization (vertical to the plane of incidence), the layer thickness for vertical incidence and an amplitude reflection of 10 percent may be still smaller. The same conclusion can be drawn, probably, for the other direction of polarization (parallel to the plane of incidence).

At this point, the acoustical absorbers in the form of wedges or pyramids should be briefly recalled. They consist of air sound, as a rule, of porous substances, mineral wool, glass wool, and similar substances, whose statistically distributed flow resistances correspond to the graphite particles in a carrier material. Also in the acoustics, the goal is, naturally, to achieve layer thicknesses as small as possible for a given low limiting frequency. Already very early experiments showed that a reflection factor of 10 percent can be obtained with a layer thickness of 1 m at 80 cps. This means that the length of the absorber may even be below one-quarter wave length of the limiting frequency.

If it is desired to combine acoustical and electrical absorption, that is, to create an acoustically and electrically nonreflecting room, then small particles of graphite will

be inserted into the pores of the porous glass wool or mineral wool. Such wedges, impregnated with graphite, can be used for electrical dm-waves also with a smaller content of graphite, for instance 1 vol. percent.[7]

At the end of this chapter, it is well to mention an absorber type frequently used in the United States. As a carrier material for graphite serves a web of animal hair and rubber threads, being cut for example in the form of a pyramid structure.

2.4 The Rib-Shaped Absorber

Already in the year 1940, a poorly reflecting absorber has been introduced into water sound techniques which operates upon the principle of the gradual transition and requires only relatively small material. It consists of thin plates, toothed at the front side - shortly referred to as ribs - which are made of an energy-dissipating rubber-like material. The ribs are arranged in a relatively small distance to each other, and parallel to the direction of the approaching sound wave; between them is water. At this arrangement, the sound enters canals, the walls of which, namely the ribs, offer the sound a complex impedance consisting of a real and imaginary part. In the canals, the entered sound is attenuated as described, for instance, by the theories of Morse and Cremer for sound absorbing tubes.[10] Figure 2.10 shows what results can be achieved by use of such an absorber configuration under water. Oppanol* ribs with dimensions and distances as listed in Fig. 2.10 posses a frequency curve of the reflection factor which over more than two octaves remains below 10 percent. The lower limiting frequency is given by the layer thickness ($1 \approx \lambda$); the upper limiting frequency is introduced by the fact that the width of the canal becomes comparable to the wave length, and the incoming wave is not influenced any more by the absorbing walls due to a certain beam-forming in the canal center. The configuration, therefore, has reached almost an optimum design by the employment of smaller ribs between the larger one.

The configuration, described above, can be employed in principle with electromagnetic absorbers. The thin, energy-dissipating and compressible ribs are re-

* trade name of a rubber-like material

placed by thin dielectric plates which are covered with graphite and posses therefore a certain loss resistance.[11] It is difficult to produce plates, covered externally with graphite, or containing graphite throughout, which have a pure ohmic resistance in the cm-band. Almost all of the materials of this kind posses an additional capacitive reactance component which at times is in the order of the effective resistance.

Using λ = 3 cm, H. Sauer[11] has investigated the wave propagation between thin graphite-containing plates at different distances between the plates, and different surface resistivities.* The plate bundle had not been cut in wedge form at the incident plane, but was arranged rectangularly as shown in Fig. 2.11.

The electrical vector of the wave, striking the test piece normally, was parallel to the plates. The electrical field intensity (the square of the amplitude) had been measured in front of and between the plates. In front of the plates, a standing wave occurred, between the plates the intensity decreases rapidly with increasing depth. The determining factors in both cases are the surface resistivity $R_{\square}$ (30 - 215 ohms/square) and the distance between the plates (12 - 16 mm). Also here, it can be seem immediately that the mismatch to the free field is the more distinct, the greater the attenuation becomes within the canals.

The summary about the relationships between attenuation in db/cm, the distance between plates d (8, 12, 16, 20 and 24 mm) and the surface resistivities of the plates $R_{\square}$ (30, 80, 100, 160, 215, and 325 ohms/square) is given in Fig. 2.12. With a distance between the plates greater than $\lambda/2$, the attenuation disappears for the plate surface resistivities zero and infinity; between them, a maximum is located. A practical dimensioning for λ = 3 cm is as follows: Distance between plates 2 cm; plate surface resistivities 150 ohms/square, which gives an attenuation of 10 db/cm. It is interesting to note that with greater widths of the canals, for instance 24 mm, and with greater plate surface resitivities, for instance 215 ohms, the decrease in field strength in the canal center is greater than along the graphite plates.

---

* - resistance between the opposing edges of a square piece of foil.

With this, an experimental basis for the construction of a rib-absorber is given. On the input side, the matching of the parallel plate medium with the free space has to be taken care of, perhaps as in the case of the underwater sound absorbers, by use of a gradual geometric transition. In order to become independent from the polarization of the incident wave, two crossed systems are used, standing perpendicular to each other. Such an absorber, consisting of graphitized foils 100 mm long, 60 mm transition length, 24 mm distance between foils, 200 ohms/square surface resistivity, with an area of 1 m^2 has been tested with normally incident waves with respect to its reflection factor at different wave lengths (Fig. 2.13). Despite the different rear terminations, the reflection factors between 2 and 14 cm wave lengths remain almost below 5 percent, that is, 99.75 percent of the incident energy is being absorbed. According to an extrapolation in Fig. 2.13, it can be assumed that perhaps the limiting wave length λ_{gr} at which the reflection factor reaches 10 percent, equals twice the amount of the total layer thickness, that is, up to 20 cm ($1/\lambda_{gr} = 0.5$).

The graphitized foils can be included in a foamed lossless material (dielectric constant near 1), or the walls of suitably formed cavities in the interior of the foamed material can be graphitized directly. Such a wide-band absorber, as illustrated in Fig. 2.14, is easy to produce and may, like a picture, be hung on the wall of those rooms which are to become nonreflecting.

Finally, it should be mentioned here that also cone-shaped or pyramid-shaped hollow bodies can be used as absorbers when their external surfaces are coated with a layer of graphite; in that manner graphitized "paper bags" may be good absorbers.

At the end of this chapter, the question arises how the reflection factor depends upon the angle of incidence, and how the polarization direction influences this dependence. K. Walther[12] concerned himself with questions of this kind, theoretically and experimentally (compare 3.1, 3.2). If a thin absorber -- for instance an absorber with a 377-ohm foil in a distance of $\lambda/4$ in front of a metal plate, or a $\lambda/4$-layer absorber -- is equally matched at each incidence angle for each polarization

direction to free space then the reflection factor follows an incidence angle law in the form $\frac{1 - \cos \alpha}{1 + \cos \alpha}$, that is, it remains -- precise matching at normal incidence provided -- below 10 percent up to an angle of incidence of 35°. This assumption of an equally well matching for each incidence angle and each polarization direction is, however, unrealistic insofar as the physical data of the absorber would have to be adjusted individually for each angle, for instance, one would have to change the distance of the 377-ohms foil from the rear of the metal plate, or the losses of the $\lambda/4$-layer would have to be varied. No practical thin absorber exists which fulfills the above requirements; with this, only the attainable optimum is demonstrated (compare also 3.1, Fig. 3.4).

If one deals not with a thin absorber but in contrast with an infinitely extended homogeneous medium where $\varepsilon = \mu$, and which has a small loss factor as well as a planar face, then the reflection is indepepdent from the polarization, and it remains below 10 percent between the incidence angles of 0 and 35° even with very high values of the product of $|\varepsilon \cdot \mu|$. However, the smaller this product, i.e., the smaller the refraction quotient, the greater is the range of angles where the reflection for each polarization direction remains below 10 percent, for instance, for $|\varepsilon \cdot \mu| = 1.02$, a limiting angle of 80° exists.

It is obvious to assume that the absorbers with gradual transitions, discussed in this chapter, take an intermediate position between a very thin and a thick absorber as far as the angle dependence is concerned. This subject has been investigated experimentally by K. Walther,[12] namely with a rib-absorber of the above mentioned type. The layer thickness was 9.5 cm and the length of the transition 3.5 cm, measurements have been taken with a wave length of 3.7 cm. The distance between the ribs, the grid constant so to speak, of the arrangement was 1.5 cm, thereby being below $\lambda/2$ of the used test wave length, so that no diffraction phenomena could occur.

In Fig. 2.15, the reflection factors in dependence upon the incidence angle are plotted at the two polarization directions $E_\perp$ and $E_\parallel$, namely first, when the rib system is parallel or normal to the incidence plane and secondly, when it is below 45°.

The differences are not great for different positions of the rib absorber, but for the two polarization directions. In addition to the geometrical reflection also the back scatter reflection is shown which is very small, as could be expected. The angular function $\frac{1-\cos\gamma}{1+\cos\gamma}$ is also plotted for the purpose of comparison.

The most significant result is that the above mentioned limiting angle of 35^{o} for a 10 percent reflection has increased considerably when using the absorbers with gradual transitions approximately to 55^{o} in this particular case. It can be assumed that the angle range increases further if the layer thickness of the absorber is increased, that is, if the transition is made even smoother than in the model, upon which Fig. 2.15 is based. The differences in the dependence of $E_{\perp}$ and $E_{||}$ as per Fig. 2.15 may be due in the case of the parallel polarization that not only one of the two rib systems is responsible for the absorption but also that with increasing angle of incidence a steadily increasing component of $E_{||}$ is projected into the direction of the second rib system and thereby both strip systems become effective.

3. ABSORBERS WITH "RESONANT STRUCTURES"

The term "resonant structures" has been mentioned already in the Introduction (1.4). Resonant Structures in this sense are called all those absorber components which show individually a strong frequency dependence of the reflection. Two configurations are used. The one is composed of two reflecting planes, one parallel behind the other, each of which possesses a reflection factor greatly independent from the frequency (for instance a dielectric plate with two planar faces which represent a resonant layer for wave lengths below a limiting value). The other configuration consists solely of a single reflecting plane with a reflection factor strongly dependent from the frequency (for instance a dipole grid or reflecting foil with resonant structure can naturally be effective over a small frequency range only. Wide-band, poorly-reflecting absorbers have to be composed of several resonant structures.

3.1 The "377-ohms-Foil Absorber" and the Multi-Foil Absorbers

The simplest absorber having only one resonant structure of the first kind is the "377-ohms-foil" absorber. The two reflecting planes are realized by a thin homogeneous resistance foil with 377 ohms surface resistivity* and a metal plate located parallel behind in a distance of $\lambda/4$ (Fig. 3.1). The space between foil and metal plate can be filled with a loss-free dielectric with the constant ε'_1 for the purpose of the reduction of the absorber thickness. The distance between the two is then decreased to $\lambda/4\sqrt{\varepsilon'_1}$.

A thin, planar conducting layer (thickness δ, conductivity σ_1), at a distance d_1 in front of the metal plate covered with a loss-free dielectric (dielectric constant ε'_1) up to the conducting layer has for a normal incident wave an input admittance, as related to the foil plane of $Y^{(1)}$:

$$Y^{(1)} = \frac{Y_o \sqrt{\varepsilon'_1}}{j \operatorname{tg} \frac{2\pi}{\lambda} \sqrt{\varepsilon'_1}\, d_1} + G_1 \qquad (3.1)$$

It is composed additively of the admittance, which in the foil plane is given solely by the metal plate (first link) and the conductance of the conducting foil, $G_1 = \sigma_1 \delta$.

$1/Y_o = Z_o = \sqrt{\mu_o/\varepsilon_o} = 337$ ohms is the wave impedance of free space. This relation (Eq. 3.1) is based upon the provision that the conducting layer is very thin as compared to the wave length within the layer ($\frac{2\pi}{\lambda} \left| \sqrt{\varepsilon'_s - i\varepsilon''_s} \right| \delta << 1$) and that the displacement current within the layer can be neglected. ($\varepsilon''_s = \frac{\sigma}{\varepsilon_o \omega} >> \varepsilon'_s$).

This shall hold true for all foils to be discussed in the following. For the wave length $\lambda_r = 4\sqrt{\varepsilon'_1}\, d_1$ the input admittance becomes real. λ_r shall designate the resonant wave length and ω_r shall be the resonant frequency.

---

* The surface resistivity is defined as the resistance between two opposite edges of a squared piece of the thin conducting foil with the thickness δ and the specific conductivity σ: $R_\square = 1/\sigma\delta$.

With $G_1^{-1} = 377$ ohms, the input admittance becomes $Y = Y_o$ when $\lambda = \lambda_r$, that is, the arrangement is nonreflecting. The admittance contribution, solely introduced by the metal plate in Eq. 3.1 at frequencies ω near ω_r becomes in the first order of approximation

$$\frac{Y}{Y_o} \approx i \cdot \sqrt{\varepsilon_1'} \frac{\pi}{2} \cdot \frac{\omega - \omega_r}{\omega_r} \tag{3.2}$$

This frequency dependence corresponds approximately to the one of the admittance Y_p of a parallel-resonant circuit with the inductivity L and the capacity C in the vicinity of its resonant frequency, $\omega_r = 1/\sqrt{LC}$:

$$Y_p \sqrt{\frac{L}{C}} = i \left(\frac{\omega}{\omega_r} - \frac{\omega_r}{\omega}\right) \approx 2i \cdot \frac{\omega - \omega_r}{\omega_r} \tag{3.3}$$

As an analog circuit for the input admittance of a 377-ohms-foil-absorber in the vicinity of the resonant frequency, a parallel resonant circuit can be used, damped by the parallel resistance $R_F = 377$ ohms with the inductance $L = 8 \mu_o d/r^2$ and the capacitance $C = \varepsilon_o \varepsilon_1' d/2$ (Fig. 3.1).

The reflection factor of the 377-ohms-foil-absorber becomes for a normal incident wave, in dependence upon the wave length:

$$r = \frac{-\sqrt{\varepsilon_1'}}{2i \operatorname{tg}\left(\frac{\pi}{2} \frac{\lambda_r}{\lambda}\right) + \sqrt{\varepsilon_1'}} \tag{3.4}$$

The absolute amount of the reflection factor is graphically represented in Fig. 3.2 in dependence from $\frac{\lambda_r}{\lambda} = \frac{\omega}{\omega_r}$ for different loss-free intermediate-layer dielectrics ($\varepsilon_1' = 1, 2, 4$). The highest possible frequency range in which $/r/ \leq 0.1$ is achieved for $\varepsilon_1' = 1$. Its band-width is determined by the ratio of the limiting frequencies 1 : 1.28. This value cannot be surpassed by choosing the surface resistivity so as to deviate slightly from $R_F = 377$ ohms, and thereby a vanishing reflection for $\omega = \omega_r$ is waived. The thinner the absorber becomes by increasing the dielectric constant of the intermediate layer ε_1', the smaller the frequency range of the absorber.

The dependence of the reflection factor from the incident angle ϑ is discussed first for very thin one-foil absorbers; for the dielectric constant of the loss-free dielectric layer between the foil and the metal plate stands $\varepsilon_1' >> 1$. The foil with the surface resistivity R_F is located in front of the metal plate in a distance $d = \lambda/4\sqrt{\varepsilon_1}$. The reflection factor can then be expressed in the case of parallel or vertical position, respectively, of the electric field strength vector of a planar, linearly polarized wave with respect to the incidence plane:[12]

$$r_{\parallel} = \frac{R_F - Z_0 \cos\vartheta}{R_F + Z_0 \cos\vartheta}; \quad r_{\perp} = \frac{R_F - Z_0/\cos\vartheta}{R_F + Z_0/\cos\vartheta} \qquad (3.5), (3.6)$$

For any given angle ϑ_1 it is possible to obtain $r_{\parallel}(\vartheta_1) = 0$, or $r_{\perp}(\vartheta_1) = 0$ by selecting the surface resitivity according to $R_f = Z_0/\cos\vartheta_1$, or $R_F = Z_0/\cos\vartheta_1$, respectively. In both cases, for the mismatched polarization direction at the incidence angle ϑ_1 is

$$|r_1| = \frac{1 - \cos^2\vartheta_1}{1 + \cos^2\vartheta_1} \qquad (3.7)$$

A uniform match for both polarization directions requires for all angles $R_F = Z_0$. The reflection factor depends upon the incidence angle according to

$$|r_2| = \frac{1 - \cos\vartheta}{1 + \cos\vartheta} \qquad (3.8)$$

The functions $|r_1(\vartheta_1)|$ and $|r_2(\vartheta)|$ are represented graphically in Fig. 3.3. The highest possible angular range of absorber effectiveness, in which $|r| \leq 0.1$ is independent from the polarization direction, is obtained by selection of ϑ_1 according to $|r_1| = 0.1$ to $\vartheta_1 = 25^\circ$, with matching for one polarization direction. With an equal matching for both polarization directions, the highest possible angular range of absorber effectiveness can be determined by $|r_2| = 0.1$ to $\vartheta_2 = 35^\circ$.

These statements are based upon the fact that the foil due to the high dielectric constant of the loss-free intermediate layer is located at a position of maximum electrical field strength practically independent from the incidence angle in front of the metal plate. On the other hand, with values of ε_1' near 1, the angular range of the absorber effectiveness is smaller than listed above. With $R_F = Z_0$, then it holds for $|r|^2$ with respect to ϑ and ε_1':

$$|r_{\parallel}|^2 = \frac{\varepsilon_1'^2 \cos^2\vartheta + (\varepsilon_1' - \sin^2\vartheta)\,(1 - \cos\vartheta)^2\, tg^2\left(\frac{\pi}{2}\sqrt{1 - \frac{\sin^2\vartheta}{\varepsilon_1'}}\right)}{\varepsilon_1'^2 \cos^2\vartheta + (\varepsilon_1' - \sin^2\vartheta)\,(1 + \cos\vartheta)^2\, tg^2\left(\frac{\pi}{2}\sqrt{1 - \frac{\sin^2\vartheta}{\varepsilon_1'}}\right)} \qquad (3.9)$$

$$|r_{\perp}|^2 = \frac{(\varepsilon_1' - \sin^2\vartheta) + (1 - \cos\vartheta)^2\, tg^2\left(\frac{\pi}{2}\sqrt{1 - \frac{\sin^2\vartheta}{\varepsilon_1'}}\right)}{(\varepsilon_1' - \sin^2\vartheta) + (1 + \cos\vartheta)^2\, tg^2\left(\frac{\pi}{2}\sqrt{1 - \frac{\sin^2\vartheta}{\varepsilon_1'}}\right)} \qquad (3.10)$$

Figure 3.4 shows $|r_{\parallel}(\vartheta)|$ and $|r_{\perp}(\vartheta)|$ for $\varepsilon_1' = 1$ and $\varepsilon_1' \to \infty$. From this, it can be seen that the angular range of the absorber effectiveness in the case of $\varepsilon_1' = 1$ amounts only to approximate 26^0 for both polarization directions.

For the construction of the 377-ohms-foil-absorbers and also for the multi-foil absorbers, to be discussed later, graphite-containing paper or plastic foils are normally used for the cm-wave portion. As loss-free intermediate layer dielectrics, plexiglass, Trolitul* or hand foam substances such as foam-Trolitul* or Moltopren* are used. Higher values of the dielectric constant can be obtained by implanting of aluminum powder into the foam substances.[3] The surface impedance of graphite containing foil is frequently not real. The (mostly capacitive) imaginary part can be compensated for by selecting the distance between the foil and the metal plate slightly differing from $d = \lambda/4\sqrt{\varepsilon'}$.

* - trade names

In the dm- and m-wave portion, the resistance foil in front of the metal plate can be replaced by a net (grid) of mesh wire which contains in its meshes suitably selected ohmic resistances.[14,15,16] In order to achieve a greater bandwidth than the one provided by the 377-ohms-foil-absorber with its single resonant structure of the first kind, it is necessary to combine two or more resonant structures. In the following part of this chapter, absorbers shall be discussed which have been developed from the single foil absorber by adding of a loss-free and additional energy-dissipating resonant structures of the first kind.[17] The first and simplest further development is to place a loss-free dielectric plate (dielectric constant ε'_2) with a thickness of d_2 directly in front of a conducting foil which in turn is located in the distance d_1 in front of a metal plate (Fig. 3.5). The electrical lengths $d_1\sqrt{\varepsilon'_1}$ and $d_2\sqrt{\varepsilon'_2}$ must coincide. As shown by the curve of the frequency dependence of the reflection factor in the Figs. 3.5a and b, the original point of resonance (Fig. 3.2) obtained without a dielectric plate, has been doubled. At the center frequency $_m$ of the absorption range $d_1\sqrt{\varepsilon'_1} = \lambda/4$, and the input admittance is real. At the two symmetrically located resonant frequencies $\omega_{1,2} = (1 \pm \Delta)\,\omega_m$, a capacitive or inductive admittance value of the same magnitude is being added to the ohmic surface conductance value in the plane of the foil. The dielectric front plate, the electrical thickness of which $d_2\sqrt{\varepsilon'_2}$ at the center frequency also being $\lambda/4$, causes, while acting as transformation agent, that the above mentioned reactive admittance values at ω_1, ω_2 do not re-appear in the input plane of the front plate. Since the front plate steps down the ohmic conductance value of the foil, $Z_0/R_F > 1$ must be chosen for the optimum matching. Between the points of resonance with $|r| = 0$, the reflection factor goes through a maximum, which height depends upon the ratio $\frac{1-\Delta}{1+\Delta}$ of the two resonant frequencies and the values of the dielectric constants of the two loss-free dielectric layers. The smaller these values are, the lower is the maximum, as shown in the curves in Figs. 3.5 a and b, which differ from each other by different resonant frequency ratios, values of the dielectric constants and conductance values of the foils.

Not until $\frac{1+\Delta}{1-\Delta} < 2$ and the smallest obtainable values of ε'_1, ε'_2, the reflection maximum can be reduced to $|r| = 0.1$. The widest possible bandwidth, which corresponds to a ratio of the limiting frequencies of approximately 1 : 2.3, necessitates a total absorber thickness d_{tot} of approx. 1/4 of the highest wave length of the absorption range. With lesser thicknesses, which can be achieved with greater values of dielectric constants ε'_1, ε'_2, a narrowing of the absorber range is associated.

The single-foil absorber, discussed above, possesses with its two resonant layers - namely the rear-side dielectric layer terminating in a metal, and the second dielectric layer terminating in a low conducting foil - two absorption points which correspond to the two resonators coupled together. With each additional coupled resonator, a new resonant frequency appears. Correspondingly, every more loss-free dielectric plate, with a terminating low-conducting rear foil which is to be positioned in front of the single foil absorber with dielectric front plate, creates a new absorption frequency provided the conductance values of the foils and the intermediate dielectrics are properly selected. The input admittance of such a multi-foil arrangement are easy to obtain if the transformation equation for a loss-free dielectric plate is employed step by step and by using the fact as expressed in Eq. (3.1) that the ohmic conductance of a foil is to be added to the admittance of the plane in which the foil is placed. The admittance $Y^{(n-1)}$, which is offered by a reflecting plane to a normal incident wave, is being transformed by a loss-free dielectric plate -- positioned in front, with the dielectric constant ε'_n and the thickness d_n within the value $Y^{(n)}$ of the plate input plane according to

$$Y^{(n)} = Y_n \frac{Y^{(n-1)} + iY_n \operatorname{tg} \beta_n d_n}{Y_n + iY^{(n-1)} \operatorname{tg} \beta_n d_n}, \qquad \text{with } Y_n = \sqrt{\varepsilon'_n} \cdot Y_o = \frac{\sqrt{\varepsilon'_n}}{Z_o}$$

$$\text{and } \beta_n = \frac{2\pi}{\lambda}\sqrt{\varepsilon'_n} \qquad (3.11)$$

The input admittance $Y^{(1)}$, already mentioned in Eq. (3.1) for the single foil absorber with one resonant layer, can be obtained from Eq. (3.11) with $Y^{(o)} = \infty$ for the

metallic termination, and by addition of G_1. The input admittance $Y^{(2)}$ of the single-foil absorber with two resonant layers (Fig. 3.5) becomes according to Eq. (3.11)

$$Y^{(2)} = Y_2 \frac{Y^{(1)} + iY_2 \operatorname{tg}\beta_2 d_2}{Y_2 + iY^{(1)} \operatorname{tg}\beta_2 d_2} \qquad \begin{matrix}(\text{with } Y^{(1)} \\ (3.1))\end{matrix} \text{ according to} \qquad (3.12)$$

If a loss-free dielectric plate with the dielectric constant ε'_3 and the thickness d_3 is placed in front, having a foil at the rear with the surface conductance G_2, then at the input of the entire configuration

$$Y^{(3)} = Y_3 \frac{(Y^{(2)} + G_2) + iY_3 \operatorname{tg}\beta_3 d_3}{Y_3 + i(Y^{(2)} + G_2) \operatorname{tg}\beta_3 d_3} \qquad \begin{matrix}(\text{with } Y^{(2)} \text{ according} \\ \text{to } (3.12))\end{matrix} \qquad (3.13)$$

Correspondingly, also $Y^{(4)}$, $Y^{(5)}$, etc., can be found. The conditions for matching are: $\operatorname{Re}(Y^{(n)}) = Y_o$, $\operatorname{Im}(Y^{(n)}) = 0$ at the n frequencies ω_1, ω_2, ... ω_n. With the plate thicknesses d_1, d_2, ... d_n, the dielectric constants ε'_1, ε'_2, ... ε'_n, and the foil surface conductances G_1, G_2, ... G_{n-1}, 3n-1 parameters for fulfilling of the 2 n matching requirements are available. The absorption frequencies and n-1 of the parameters can be given, however, only limited since the resulting values must be $\varepsilon'_1 \geq 1$, and $G_1 > 0$. The matching conditions can be numerically simply evaluated only for those absorbers with three or four resonant layers besides for the foil absorbers with two resonant layers which has been done by H. J. Schmitt.[17] The results are shown in Figs. 3.6 and 3.7 where the value of the reflection factor is plotted with respect to the frequency for the two last-mentioned absorbers. Between the absorption points, the reflection factor does not increase beyond 0.1. The limiting frequency ratios amount to 1 : 3.6, and 1 : 4.6, respectively, under the provision $r \leq 0.1$. The absorber thickness amounts to 1/4 and 1.3 $\lambda_{max.}$ resp. This explains the considerable advantage of the multi-foil absorber over the wedge absorber (see Sec. 2) which requires at least a thickness of 1/2 λ_{max}. A disadvantage of the multi-foil

absorber is the required care in construction since the adherence to the calculated values is very important. In contrast, the dimensioning of a wedge absorber is very uncritical.

Figure 3.8 shows the frequency curve of the reflection factor with two different incidence directions, as measured on a tri-foil absorber with four resonant layers by H. J. Schmitt.[17] With increasing incidence angles, the absorption range shifts to higher frequencies and becomes smaller.

When dimensioning multi-foil absorbers with identical intermediate layers ($\varepsilon'_1 = \varepsilon'_2 \ldots \varepsilon'_n$, $d_1 = d_2 = \ldots d_n$, and harmonically selected absorption frequencies ($\omega_1 : \omega_2 : \ldots \omega_n = 1 : 2 : \ldots n$) it can be noticed that with an increasing number of layers, the required values of dielectric constants approach 1 while the thickness of the total absorber seems to approach 1/2 λ_o (λ_o = the greatest absorbtion wave length) (Fig. 3.9). Within a multi-foil absorber, the required surface conductance of the foils decreases monotonously in direction to the input plane ($G_1 > G_2 > \ldots G_{n-1}$). From these facts it becomes apparent that with an increase of layers the multi-foil absorber approaches more and more the type of absorber which is composed inhomogeneously (gradual transition type).

An absorber which leads from the multi-foil absorber to the inhomogeneous absorber with gradual transition, is represented by the "electrical swamp" developed by Jaumann as discussed in (Ref. 18). Here a great number of conducting foils are arranged in distinctive distances parallel to each other in front of a metallic wall. The foil conductivity increases steadily toward the metal wall. The arrangement and the reflection factor with respect to the wave length is shown in Fig. 3.10. Due to the distances between the foils a distinctly marked upper limiting frequency can be noticed in contrast to the absorbers with gradual transitions (wedge absorber!).

The principle of the single-foil or multi-foil absorber is found also among the acoustical absorbers. In air sound techniques a thin porous foil or a tightly knit mesh net in the distance of $\lambda/4$ in front of a sound hard wall is corresponding to the 377-

ohms-foil-absorber. The porous foil is thereby brought into the plane of maximum velocity amplitude and draws energy from the wave field by the foil's flow resistance of 420 mgs units.

A thin layer, made of wax or rubber, placed at a distance of $\lambda/4$ in front of a sound soft wall can be used for the absorption of sound waves in water. The foil, being located at the pressure maximum, absorbs by its compression losses.

Multi-foil absorbers for sound waves in air have been mentioned already by Maljushinez.[19]

3.2 The "$\lambda/4$-layer" Absorber and the Multi-Layer Absorber

The layer absorbers consist, like the foil absorbers, of one or several resonant structures of the first kind, that is, the reflecting planes of the resonant structures have a reflection factor widely independent from the frequency. In contrast to the foil absorbers, however, the layer absorber's absorbing material is uniformly distributed within the area between the reflecting planes of each resonant structure. As resonant structures serve plane-parallel plates, made of energy-dissipating material which acts dielectrically, magnetically, or in both ways, and may have the relatively complex dielectric constant $\varepsilon = \varepsilon' - i\varepsilon''$ and permeability $\mu = \mu' - i\mu''$.

Such a plate with the thickness d, which is located directly in front of a metal plate (Fig. 3.11) has with respect to a normal incident wave the reflection factor

$$r = \frac{\sqrt{\mu/\varepsilon}\ \mathrm{tgh}\,(2\pi i\ \sqrt{\varepsilon\mu}\,d/\lambda) - 1}{\sqrt{\mu/\varepsilon}\ \mathrm{tgh}\,(2\pi i\ \sqrt{\varepsilon\mu}\,d/\lambda) + 1} \qquad (3.14)$$

The reflected wave consists of the wave components 1 and 2 (Fig. 3.11). The wave component 1 results from the partial reflection from the front of the layer. The wave, which penetrated the layer, is being reflected several times in the layer and attenuated there. It produces the wave component 2, which is phase shifted with respect to 1. The phase shift amounts to π when the layer thickness d coincides approximately with a quarter wave length in the layer material. In addition, if the reflection at the front side and the attenuation within the layer are tuned in such a way that the wave

components 1 and 2 possess the same amplitudes, then 1 and 2 cancel each other. The "$\lambda/4$-layer absorber causes a complete absorption. For this purpose the values d, ε, and μ must fulfill the requirement

$$\sqrt{\mu/\varepsilon}\ \mathrm{tgh}\ (2\pi i\sqrt{\varepsilon\mu}\,d/\lambda) \cdot 1 \qquad (3.15)$$

With a given ratio d/λ, two of the parameters, ε', ε'', μ', μ'' are still available. The required real and imaginary part of the dielectric constant of a solely dielectrically acting absorbing material ($\mu' = 1$, $\mu'' \approx 0$) can be seen in Fig. 3.11 for layer thicknesses of $d = 0.01\,\lambda$ to $0.3\,\lambda$. In case that the absorbing material shall have only magnetic losses (ε' = constant, $\varepsilon'' = 0$, for instance metal powder mixtures), then μ' and μ'' have to be selected according to the diagram of Fig. 3.12. The characteristic curve of the reflection factor with respect to the frequency is shown in Fig. 3.13 for an absorber with only one resonant structure as obtained from a "$\lambda/4$-layer" absorber consisting of a carbonyl iron powder mixture with magnetic and electrical losses. The ratio of the limiting frequencies of the absorption range ($|r| \leq 0.1$) amounts here to 1 : 1.15 with an absorber thickness of about 1/30 wave length in free space. $\lambda/4$-layer absorbers made of electrical and magnetic energy-dissipating substances show a slightly greater bandwidth than absorbers of the same thickness made of magnetically ineffective materials. The relative frequency bandwidth of the latter absorbers is plotted against the ratio between layer thickness and wave length in free space, the bandwidth is slightly smaller than the one for the 377-ohms-foil-absorber which has the same thickness. The $\lambda/4$-layer absorber has been mentioned in 1938 by Daellenbach and Kleinsteuber.[20]

The influence of the incidence angle upon the reflection factor of $\lambda/4$-layer absorbers has been investigated by K. Walther.[12] The dielectric constant ε and the permeability μ of the layer material can be selected in such a way that for a given incidence angle α_1 the reflection factor becomes zero for either the parallel or normal position of the electrical field strength vector referred to the plane of incidence while it differs from zero at the respective perpendicular polarization.

Also, an equal matching for both polarization directions can be achieved. The dependence of the reflection factor from the incidence angle can only be described clearly under the provision $|\varepsilon \mu| \geq 1$. Then, the same relations exist as those pertinent to the thin foil-absorber with one resonant layer (see 3.1): If for a given angle ϑ_1, matching is accomplished for one polarization direction, then for the other polarization direction the reflection factor $|r_1| = (1 - \cos^2 \vartheta_1)/(1 + \cos^2 \vartheta_1)$; the reflection factor has the same value for both polarization directions $|r_2| = (1 - \cos \vartheta)/(1 + \cos \vartheta)$ when the absorber is completely matched for vertical incidence. (see Eq. 3.15). For incidence angles $\vartheta \leq 35^{\circ}$, is in this case $|r_2| \leq 0.1$.

In the same manner as for the foil absorber, the frequency bandwidth of the layer absorber can be increased by the addition of similar resonant layers, being positioned in front of each other. Several energy-dissipating plates with different, suitably dimensioned dielectric and magnetic properties are to be used. However, the numerical calculation of the multi-layer absorbers is more difficult due to the losses in each plate than the one for the foil absorbers with several resonant structures. It seems quite possible to employ one-dimensional filter-type transmission lines as an analogous calculator, as used by Lenz[5] for inhomogeneous wide-band absorbers. (see 2.2) Lenz discussed also an attenuation course which could be attributed to a three-layer absorber. The three layers have, counted from the terminating metal plate, the thicknesses $d_1 = 0.297d$; $d_2 = 0.359d$; $d_3 = 0.344d$, where d is the total thickness of the absorber. For the conductivities σ_i holds

$$\sigma_1 d = 1.85 \times 10^{-2} \Omega^{-1}; \quad \sigma_2 d = 0.615 \times 10^{-2} \Omega^{-1}, \text{ and}$$

$$\sigma_3 d = 0.308 \times 10^{-2} \Omega^{-1},$$

the losses being uniformly distributed in each layer and ε' assumed to be 1. But it is also possible to locate the absorbing material concentrated at distinct planes oriented in parallel to the direction of wave propagation. A three-layer absorber, constructed

in this manner, was mentioned by Lenz[5] as "chimney-absorber". Fig. 3.15 shows a cut view of it. The chimney walls may be produced from graphitized hard paper plates and must have surface restivities R_F, which have to be calculated from the above presented conductivity values according to $R_F = 1/\;\!W$ with W denoting the foil distance. J. Deutsch and P. Thust report measurements of the reflection factor of such chimney-absorbers.[29] One of their experimental results is presented in Fig. 3.15. The reflection factor in dependence of frequency is plotted for an absorber with total thickness d = 90 cm, with the chimney widths $W_1 = 12.5$ cm, $W_2 = W_3 =$ 25 cm and with the surface restivities $R_{F1} = 400\,\Omega$, $R_{F2} = 600\,\Omega$, $R_{F3} = 1200\,\Omega$ of the chimney walls. In the frequency range 150 mc/s to about 3500 mc/s the reflection factor does not exceed 0.1. The frequency dependence of the reflection factor as calculated by Lenz[5] is also plotted in Fig. 3.15 for comparison. The calculated value of the upper limiting wavelength and the value derived from the measurement are equal to three times the absorber thickness. The increase of the reflection factor towards higher frequencies (in the present case above 3.5 kmc/s) is caused mainly by the fact, that at these frequencies (if $\lambda < 2W$) the chimneys act like waveguides thereby reducing the attenuation (look for Fig. 2.12).

In the case of a multi-layer absorber, with - in contrast to the chimney absorber - uniformly distributed losses in each layer, a short wavelength limit of the absorption range need not to exist as expressive as e.g., among the foil absorbers in Fig. 3.5, 3.6, 3.7.

A total reflection will generally not be achieved since with decreasing wave length the wave does not advance to the metallic termination. The resonant layers located closest to the metal plate, become step by step ineffective with decreasing wave length. In the extreme case, the reflection factor is solely determined by the surface reflection of the outermost layer. This can be kept very small when the absorber can be sufficiently thick so that the attenuation from layer to layer toward the metal plate has to increase only slowly, like this is the case with the wedge absorber.

Single- or multi-layer absorbers are known for decades for sound in air or water. The absorption is caused by the flow resistance of a porous material in front of a sound hard wall, or in a material with compression losses in front of a sound soft termination, resp.

3.3 Single-Dipole and Multi-Dipole Absorbers

For the foil and layer absorbers (see 3.1 or 3.2 respectively) only those resonant structures are being used whose reflecting planes do not show a strong dependence from the frequency (first kind). The dipole absorber, and also those absorbers still to be discussed in Section 3.4 distinguish themselves by that they contain in addition resonant structures which consist of a single reflecting plane with a reflection factor strongly depending upon the frequency (second kind).

The explanation of the single-dipole absorber[21] is based upon the 337-ohms-foil-absorber (3.1) where a thin conducting foil with the surface resistivity of 377 ohms is located in the electrical distance $d\sqrt{\varepsilon'}$ in front of a metal plate. For wave lengths in the vicinity of the resonant wave length $\lambda_r = 4d\sqrt{\varepsilon'}$, the frequency curve of the input admittance corresponds to that of a damped parallel-resonant circuit, according to Fig. 3.1. The sharp rise of the reflection factor for the wave lengths on both sides of the resonant wave length (see Fig. 3.2) is caused by the capacitive or inductive reactance of the parallel-tuned circuit outside of its resonance. In case the parallel foil resistance outside the resonance would become complex with a suitable sign, the absorbing range could be increased by compensation of the reactances. This is possible if to the ohmic resistances of 377 ohms an additional series-tuned circuit is connected in series (see Fig. 3.16a) being tuned to the same frequency as the parallel-resonant circuit. The admittance Y_p of the parallel-resonant circuit increases with increasing frequency while the imaginary part of the admittance Y_s of the damped series circuit decreases. The inclinations of both frequency curves are both the same numerically in the vicinity of the resonant frequency ω_r when the parallel inductance L_1, the parallel capacity C_p, the series inductance L_s, the series

capacitance C_s and the ohmic resistance $R_s = Z_o = 377$ ohms are related to each other according to

$$\frac{1}{L_p C_p} = \frac{1}{L_s C_s} = \omega_o^2 \quad ; \quad \sqrt{\frac{L_s}{C_s}} = Z_o^2 \sqrt{\frac{C_p}{L_p}} \qquad (3.16)$$

The real part of Y_s remains in the first approximation constant in the vicinity of ω_r equal to Z_o^{-1}. The input impedance of the two-circuit configuration in Fig. 3.16 a is accordingly in the first approximation independent from the frequency and equals Z_o. To make the admittance of the parallel-resonant circuit at the resonant frequency ω_r corresponding to that of the metal plate in a distance $d = \lambda_r / 4\sqrt{\varepsilon'}$ the following condition must exist

$$\sqrt{\frac{L_p}{C_p}} = \frac{4}{\pi} \frac{Z_o}{\sqrt{\varepsilon'}} \qquad (3.17)$$

The series connection R_s, L_s, C_s can be replaced by a grid of energy-dissipating dipoles with the length $\lambda_r/2$ which is being placed in front of the metal plate in a distance of $d = \lambda_r/4\sqrt{\varepsilon'}$ instead of the 377-ohms foil (Fig. 3.16 c). The electric field strength vector of the wave to be absorbed must be directed parallel to the dipole axes. The dependence from the polarization can be avoided by use of dipole crosses or circular disks. The dipole grid is defined by the two grid constants g and h according to Fig. 3.18. Best suited for energy-dissipating dipoles are stripes made of homogeneous graphitized plastic foil (see 3.1) with the width g'. The surface resistivity of the graphite foil, the density of the dipole grid and the dipole strip width must be selected in such a way that the grid plane has an r-f surface resistivity of 377 ohms. For this purpose, the foil resistance must be considerably below 377 ohms. Due to the attenuation and the mutual influence of the dipoles, the dipole length L deviates slightly from $\lambda_r/2$. At a fixed foil resistance the dipole strip width g' determines the inclination of the frequency curve of Im (Y_s) at resonance. (see Fig. 3.17)

Figure 3.16 shows the frequency curve of the reflection factor for single-dipole absorbers in the range $0 \leq \frac{\omega}{\omega_r} \leq 2$. The reflection factor has been calculated for different damping resistances R_s from the input impedance Z_i of the analog circuit (b) shown also in Fig. 3.16. With $R_s = 0.8\ Z_o$, the absorption range ($|r| \leq 0.1$) has its widest expansion; the two resonant points of the system of two coupled resonant structures become very apparent. The limiting frequency-ratio of the absorption range amounts approximately to 1 : 1.8. In addition, Fig. 3.16 shows points of actual measurements on a dipole absorber at 3 cm wave length, which confirms that the presentation of the analog circuit is correct.

It is known from the network theory[28] that a combination of parallel and series-resonant circuit according to Fig. 3.16 a can be designed in such a way that its impedance is completely independent from the frequency and equals R_s, when the ohmic resistance of the order R_s is connected in series to the parallel-resonant circuit (as shown in dotted lines in Fig. 3.16a). However, the analog circuit cannot be realized to that amount with ultra-high frequency resonant structures.

Figure 3.16 shows the most favorable curve of the reflection factor in dependence from the frequency for a single-dipole absorber of the thickness $d = \lambda_r/4$ ($\varepsilon' = 1$). The bandwidth of the absorber is being reduced when a loss-free layer with a higher dielectric constant ($\varepsilon' > 1$) is inserted between dipole grid and metal plate, whereby the absorber is made thinner.

The acoustical analog to the single-dipole absorber is, for sound in water, a plane arrangement of air bubbles, which are located in a distance of $\lambda/4$ in front of a sound-soft wall. The air bubbles located at the pressure maximum which correspond to the electrical dipoles execute pulsed oscillations as "monopoles" and possess the same resonant frequency as the $\lambda/4$ layer. The resonant frequency is determined by the surrounding, oscillating medium mass and by the spring action of the embedded air. The attenuation is of thermal origin.

In a practical design, called "Alberich", a covered hole-foil, made of rubber, is located in front of an iron plate. Here, the air bubbles are "frozen in" so to speak. The parallel-resonant circuit is realized not by a $\lambda/4$ layer but by the rubber spring and the mass of the terminating wall, i.e., by concentrated circuit elements.

Some results of measurements should be quoted concerning the dependence of the reflection factor from the incidence angle.[21] The measured curve of the reflection factor with the incidence angle at vertical ($\perp$) and parallel ($\parallel$) position of the electrical field strength vector to the incidence plane is plotted in Fig. 3.18 for two dipole absorbers with different dielectric constants of their intermediate layer. Here, it becomes apparent -- similar as for the 377-ohms-foil-absorber and the $\lambda/4$-layer absorber -- that with increasing angle the reflection factor increases slower, the higher the intermediate-layer-dielectric-constant has been chosen. In contrast to the 377-ohms-foil- absorber and the $\lambda/4$-layer absorber (see Fig. 3.3 in 3.1), the angular range of effectiveness ($|r| \leq 0.1$) of the dipole absorber is considerably smaller for parallel polarization (15°) than for vertical polarization ($25 - 30^{\circ}$). The reason for this is that at parallel polarization the dipole grid acts differently upon an obliquely incident wave than a homogeneous foil or the surface of a dielectric plate because the integral surface impedance of the dipole grid changes with the incidence angle.

The steep rise of the dipole absorber's reflection factor with increasing incidence angle at parallel polarization has been counteracted by Kurtze and Neumann[22] in the following manner: In addition to the grid of $\lambda/2$ long dipoles which are located in the distance of $\lambda/4$ in front of the metal plate -- the dipole axis being in the grid plane ("transversal-dipole-grid") -- a grid consisting of $\lambda/4$ long, energy-dissipating dipoles is added which stands normally on the metal plate in the gaps of the first grid, the dipoles being in contact with the metal plate ("longitudinal dipole grid"). With normal incidence, this longitudinal dipole grid is ineffective since the electrical field strength does not have a component in the direction of the axis of the longitudinal

dipoles. With increasing incidence angle the electrical longitudinal component increases at the expense of the transversal component. The absorption of the longitudinal dipole grid increases, that of the transversal dipole grid decreases. This has been measured for both dipole grids individually in front of the metal plate and is illustrated in Fig. 3.19 by the curve of the reflection factor with respect to the incidence angle. The reflection factor of the combination of both grids (Fig. 3.19) shows a steep rise first beginning above 60^{o}.

The single-dipole absorber with the dipoles having a length of $\lambda_r/2$ in a distance of $\lambda_r/4$ in front of the metal plate becomes more and more ineffective with decreasing wave length and reflects completely at a wave length $\lambda = \lambda_r/2$, since then, a node of the electrical field in front of the metal plate is located in the dipole grid plane. A complete absorption is achieved again when an additional grid consisting of energy dissipating $\lambda_r/4$ long dipoles is inserted in front of the metal plate at a distance of $\lambda_r/8$. (Fig. 3.21a). Such a dual-dipole absorber has been investigated by H. J. Schmitt and W. Futtermenger.[23] The dimensioning of such an absorber is more difficult as compared to the single-dipole absorber since the higher tuned grid D_2 influences the properties of the low-tuned grid D_1. The latter has to be arranged differently, therefore, as for the single-dipole absorber. For the investigation of the conditions for a favorable dimensioning which is hard to find numerically, a model filter circuit operated in the a-f region has been substituted for the dual-dipole absorber. It was built according to the analog circuit in Fig. 3.20c. The reflection factor, calculated with the requirement of complete matching at the frequencies ω_r and $2\omega_r$ is plotted with respect to the frequency in Fig. 3.20c. For comparison, also the curves for the single dipole absorber (b) and the 377-ohms-foil absorber (a) have been added. Between the two resonant nodes $\frac{\omega}{\omega_r} = 1$ and $\frac{\omega}{\omega_r} = 2$, the reflection factor of the dual-dipole absorber can hardly be reduced below 0.16. Figure 3.21b shows several reflection curves as obtained from the measurements on the model analogue circuit. The lowest curve has a maximum of 0.12 in the center of the absorbing range. The frequencies

at the extreme "$|r| = 0.1$-limits" of the absorption range have the ratio 1 : 2.7. With actual dual-dipole absorbers of similar bandwidths, Schmitt and Futtermenger could not achieve $|r| < 0.2$ in the center of the absorbing range as shown in Fig. 3.21c by the measured curve for a dual-dipole absorber which had been designed for a wave length of 3 to 15 cm.

The sole employment of multi-dipole absorbers appears not suitable for broad-band absorber arrangements due to the difficult manufacturing in comparison to the wedge absorbers of the simpler absorbers with only two resonant structures. It is conceivable to combine multi-dipole absorbers with wedge absorbers in complete analogy to the corresponding acoustical absorber systems (wedges consisting of porous materials with slotted resonators behind them[7]). As far as lower frequencies are concerned the effectiveness of the wedge absorbers is limited by the required length of wedges. The purpose of the resonant absorbers would be to absorb waves of such low frequencies, which are passing the wedges to a great amount; this could possibly be achieved without heavy spacial requirements due to the more favorable ratio of layer thickness to the wave wave length. Small reflections, being present at the dual-dipole absorber, are insignificant in this case since the wedge absorbers in front of the resonant absorber already reduce the reflection.

3.4 Slotted-foil Absorber, the Slotted-foil Dipole Absorber and the Loop Absorber

The resonant structure, being complementary to the grid consisting of energy-dissipating dipoles with the length $\lambda/2$, is a plane, energy-dissipating foil with $\lambda_r/2$ long slots. To a wave whose electrical field strength vector lies parallel to the dipole axes, the dipole grid offers an impedance having the same frequency dependence as that of a damped series-resonant circuit in the vicinity of the resonant frequency. The impedance of the slotted foil corresponds in its frequency curve to that of a damped parallel-resonant circuit in the vicinity of the resonant frequency ω_r (Fig. 3.22) in case the electrical field strength vector is perpendicular to the slots. The slotted foil is resonant at a slot length of slightly below $\lambda/2$. The impedance of the

foil is capacitive when the slot length is greater than $\lambda/2$. A strongly capacitive energy-dissipating foil offers the possibility to construct a very thin absorber. In order to compensate for the capacitive reactance, the foil has to be placed in front of a metal plate with suitable distance much smaller than $\lambda/4$ where strongly inductive reactance value $Y_L = Y_0/itg\ \frac{2\pi}{\lambda} \cdot d \approx \lambda/(Ci Z_0 \cdot 2\pi d)$ is present ($Z_0 = 377$ ohms). At the resonant wavelength λ_r, Y_L should equal the imaginary part $Y_C = i\ \frac{2\pi}{\lambda}\ C$ of the foil admittance, so that $C = \lambda_r^2/4\pi^2\, d\, Z_0$. The input susceptance of the slotted foil at a distance d in front of the metal plate is then given by

$$Y = \frac{i}{2\pi Z_0 d}\ \frac{\lambda_r^2 - \lambda^2}{\lambda} \qquad (3.18)$$

The r-f conductivity of the foil is strongly reduced by the slots. In order to obtain an effective resistance of 377 ohms, a foil must be used which has very little surface resistivity (15 ohms, for instance). The accurate adjustment of the real part of the input impedance is being done by changing the density of the slots. The advantage of the low thickness of this "slotted-foil-absorber" developed by F. Wiekhorst[24] is balanced by the disadvantage of the very small bandwidth as can be seen from the diagram of the reflection factor above the wave length in Fig. 3.23a. The curve has been measured in the 3.3 cm wave length region at an absorber whose slotted foil was located in a distance of 0.2mm(0.006 λ!) in front of the metal plate and which was covered with a 0.5 mm thick rubber foil in order to increase the capacitive reactance (total absorber thickness 0.03 λ!). The foil with 15 ohms surface resistivity contained 6 x 19 slots in an area of 150 x 150 mm^2; the slots were 18 mm long ($> \lambda/2$) and 1.8 mm wide. The forced reduction of the bandwidth with decreasing thickness can be seen from Eq. 3.18: At the resonant wave length the input susceptance Y passes through zero steeper, for smaller d; big $dY/d\lambda$ expresses small bandwidths.

The effective frequency range of the slotted-foil absorber can be increased slightly by a manipulation proposed by Wiekhorst.[24] Between the slotted foil and the metal plate a grid is placed consisting of energy-dissipating dipoles approximately $\lambda/2$ long, the

axes of which in the grid plane are located perpendicularly to the slots. Thereby, the short circuit plane behind the foil is not fixed any more, but varies with the frequency. In Eq. 3.18 d changes in such a way that dependence from the frequency Y remains low in a narrow frequency range. More precisely, the dipole grid with the admittance frequency curve of a series-resonant circuit causes a limited compensation of the opposite admittance-frequency-dependence of the parallel-resonant circuit which is formed by the slotted foil and the metal plate. The relations are here similar to the ones of the single-dipole absorber (3.3). In order to avoid a dependence from the polarization Wiekhorst used for an actual design of the "slotted-foil-dipole-absorber" a foil with circular slots instead of the linear slots, and a grid made of dipole crosses which were cut from a foil with 25 ohms surface resistivity. The absorber for 3.6 cm wave length has a total thickness of 2 mm ($\approx 0.06\lambda$). Figure 23b shows the dependence of its reflection factor from the wave length. Due to the remarkable steep increase at the sides of the absorbing range, the bandwidth does not depend here upon how much reflection is tolerated unlike many other absorbers. The limiting frequency-ratio amounts to 1 : 1.12 while it was only 1 : 1.03 for the thinner simple slotted-foil absorber. (see Fig. 3.23a). Besides the more difficult dimensioning, the advantage of the slotted-foil absorber with respect to other absorbers with resonant structures seems to be the fact that an equally low reflection factor can be achieved over the whole absorption range.

The loop absorber[25] is an absorber where the energy of the incident wave is extracted from the field in a very small distance ($< \lambda/4$) in front of the metal plate similar to the slotted-foil absorber. By means of small loop antennas at the front side of the metal plate, the absorption elements sitting in the metal plate are coupled to the magnetic field in front of the metal plate (Fig. 3.24). As absorbing elements small energy-dissipating coaxial cable pieces are used which are short circuited on one side. They act capacitive since their length L_1 is between $\lambda/4$ and $\lambda/2$. At their open end the internal conductor converts into the loop which can be considered as a short circuited parallel wire circuit. It is shorter than $\lambda/4$ and acts inductively in the plate plane.

Therefore, the equivalent circuit of a loop absorber element is drawn accordingly in Fig. 3.24. The losses of the coaxial resonators are taken care of by some iron powder at the shirt circuited end of the coaxial cable piece. The tuning of the resonators is determined by the length of the coaxial line L_1 and the length of the loop L_2. With a fixed resonant frequency, variations of these two values as well as variations of the amount of iron powder influence the resonant resistance. Finally, the input impedance of the overall absorber depends also upon the density with which the resonators are distributed on the metal plate. For an absorber, operating at a wave length of 3.18 cm, the following values proved to be favorable: length of coaxial line piece L_1 = 10.6 mm, length of loop L_2 = 2.5 mm; iron powder quantity 1.6 mg and resonator density N = 1.12 resonators per L cm^2 of absorber area. Figure 3.25a shows the dependence of the reflection factor from the wave length at an incidence angle of 15^o. The bandwidth is considerably smaller than that of all absorbers discussed so far.

The dependence of the reflection factor from the incidence angle is illustrated in Fig. 3.25b. The limiting angle with /r/ = 0.1 is around 22^o for vertical polarization. The loop absorber becomes fully effective only when the magnetic field strength vector is normal upon the loop plane. If it is desired to avoid the so caused polarization dependence, then a second grid of resonators has to be inserted between the first ones; the coupling loops of the second grid must be turned 90^o against the first one.

The dimensioning of the discussed loop absorber is difficult indeed, since its properties depend very sensitively upon the given measures; the bandwidth is very small. In spite of this, the significance should not be overlooked which lies in the completely different composition of the loop absorber in comparison to the other absorbers with resonant structures. At the latter ones, all absorbing structures and all those which influence the frequency curve are arranged in front of the metal plate which terminates the absorber in the rear. The design of the loop absorber makes it possible to relocate the absorbing and frequency-determining elements to a high degree in or behind the metal plate. Certain applications may permit to house there several resonant

structures without regard to their geometrical dimensions, so that a greater bandwidth may be achieved with the loop absorber as well. The complicated, multi-circuit absorbing system does not form a sensitive cover of the metal plate any more, but is located securely behind it.

As an acoustical analog of the loop absorbers, the "hole absorber" for sound in air can be considered, i.e., a punched plate located in a small distance ($< \lambda/4$) before a rigid wall. The air, vibrating in the holes, is the mass. The relatively small (as compared to the wave length) cavity between the punched plate and the terminating wall acts as a spring. The damping of this mechanical resonant circuit is caused by the friction of the air in the holes, or takes place in an additional porous material in the vicinity of the holes. The equivalent electrical circuits for the electromagnetic loop absorber and the acoustical hole absorber are in dualism to each other, i.e., the substitute circuit for the hole absorber is a series-resonant circuit. The reason for this is that in the electrical case a completely conducting plane is assumed where the electrical field collapses, while in the case of the acoustical absorber the reference plane is a rigid wall where the normal component of the velocity amplitude disappears.

3.5 About the Realization of Thin and Wide-Band Absorbers.

A very important goal of the absorber development is the creation of very thin absorber arrangements but nevertheless being effective over a wide range. Reviewing the absorbers with resonant structures, one comes to the result that the bandwidth of the absorber is smaller, the thinner it is attempted to build them. This fact leads to the question if basically a large frequency range of effectiveness and a small absorber thickness can be combined. An accurate answer including all absorbers has not been found yet.

In case of a particular absorber type, the $\lambda/4$ layer absorber with only electrical or magnetic losses, has been investigated by Pottel.[26] The $\lambda/4$-layer absorber can be constructed as thin as desired by use of a layer material with a suitable high dielectric constant ε or permeability μ. The idea is close at hand to use a material

whose dielectric constant or its permeability varies in such a way with the frequency that the wave length within the material remains independent from the frequency, being equal to the four-fold layer thickness, and that the attenuation occurs suitably. For that purpose, the dielectric constant or the permeability must decrease with increasing frequency namely in the manner as shown in Fig. 3.11 and 3.12. With a fixed layer thickness d the abscissa scale in these illustrations transforms into the frequency scale by multiplication with c/d, or $c/\varepsilon' d$ respectively (c = speed of light). It can be demonstrated that the required frequency course of the values ε and μ cannot be realized by resonant and relaxation processes. The reason for this is that the real and imaginary part of the dielectric constant as well as the permeability are not independent from each other but that with respect to their frequency courses they are tied together by common relations, the so-called Kramers-Kronig relations.[27] The frequency curves of the dielectric constant and the permeability, respectively, shown in Fig. 3.11 and 3.12 ($\varepsilon' d/\lambda > 0.01$!) for $\lambda/4$-layer-absorbers, being effective without dependence from the frequency, oppose the laws which are contained in the Kramers-Kronig relations. Thin $\lambda/4$-layer absorbers and at the same time effective over a wide range are basically impossible according to this, if only magnetic losses in the case $\varepsilon' d > 0.01$ <u>or</u> only electrical losses are present.

The Kramers-Kronig relations are based merely upon the fact that the polarization of a material caused by a suddenly switched on electric or magnetic field lags in time or occurs instantaneously with the switch-on of the field, however, it does not occur sooner and that the polarization depends linearly upon the field. These statements, however, are not restricted to the molecular electric or magnetic oscillating structures of a material capable of being polarized. They also can be applied to the polarization or the current in macroscopic resonant structures, possibly for the energy-dissipating dipole grids (3.3), or energy-dissipating slotted foils (3.4). Between the real and imaginary part of the admittance of these arrangements, there must exist similar tie-ins like the Kramers-Kronig relations. By these, the frequency dependences of these ad-

mittances are governed by certain regulations. Probably, these regulations prevent that perhaps the energy-dissipating dipole grid of a thin dipole absorber or the energy-dissipating slotted foil of a thin foil absorber or a combination thereof, might have a frequency curve of the admittance which compensates for the frequency curve of the admittance transposed from the metal plate into the dipole or slotted foil plane over a wide range of frequencies. Quantitive investigations are still missing.

The results of Pottel[26] about the bandwidth of thin /4-layer-absorbers don't include the special case $\text{tgh}\,(2\pi j\sqrt{\varepsilon\mu'}\,d/\lambda) \approx 2\pi j\sqrt{\varepsilon\mu}\,d/\lambda$ in Eq. (3.15). Thereby Eq. (3.15) determines the permeability of the layer material according to $u' \approx 0$; $\mu'' \approx (2\pi d/\lambda)^{-1}$, while no prescription exists for the frequency dependence of the dielectric constant. The dielectric constant is, however, limited to $(|\varepsilon| + \varepsilon'')d/\lambda \leq 0.01$ thus the matching condition (3.15) being fulfilled with deviations below 2 percent in this special case. The above required frequency variation of the permeability ($\mu'' \sim \omega^{-1}$; $\mu' \approx 0$) occurs at ferromagnetic materials, e.g., ferrites, in the range of the so-called natural ferromagnetic resonance[30] possibly over a frequency interval 1 : 10. If also the dielectric constant of such a ferromagnetic material is sufficiently low a very thin and at the same time broad band absorber may be realizable (Helberg). This absorber with $\mu'' = (2\pi d/\lambda)^{-1}$ is the "magnetic analog" of the 377-ohms-foil absorber, having $\varepsilon'' = (2\pi d/\lambda)^{-1}$.

4. ABSORBERS OF HOMOGENEOUS STRUCTURE

The term "absorbers of homogeneous structure" shall apply to all those absorber arrangements which the absorbing material is plane limited toward the free space, where inside -- at least in the direction normal to the surface -- the material is homogeneously distributed, and forms no resonant structure.

If the absorbing material is only dielectrically effective, that is, only electrical losses are present, then it stands for the reflection factor with normal incidence to the boundary plane

$$r = \frac{1 - \varepsilon}{1 + \varepsilon}$$

where $\varepsilon = \varepsilon' - i\varepsilon''$ stands for the relative complex dielectric constant of the material. A small reflection can be achieved here only with materials of small density, that is, with low dielectric effectiveness. Configurations of this type form the first group of absorbers with homogeneous structure.

The second group consists of dielectric and magnetic effective materials. The reflection factor with a wave incidence normal to the boundary plane is

$$r = \frac{\sqrt{\mu / \varepsilon' - 1}}{\sqrt{\mu / \varepsilon' + 1}}$$

where $\mu = \mu' - j\mu''$ stands for the relative complex permeability. The reflection at the boundary plane disappears for $\mu = \varepsilon$.

4.1 Absorbers with Small Material Density

The absorbers of this group cannot be made nonreflecting principally since due to the required material losses ε'' must be > 0 and mostly also $\varepsilon' > 1$ is related. A small reflection at the surface plane can be achieved only by employment of weak-absorbing materials where ε'' is low and ε' is around 1. Since absorbers are used frequently to camouflage strongly reflecting objects, the most unfavorable case is given when a metal plate is located behind the absorber. In order to achieve despite the weak absorption a small reflection, a great absorber thickness must be taken into account. If the reflection factor is desired to be $|r| \leq 0.1$, for the thickness of the absorbers metallically in the rear, in relation to the wave length λ in space, the following must be true

$$\frac{d}{\lambda} \geq - \frac{1}{2\alpha\lambda} \cdot \ln (0.1 - |r_1|).$$

where

$$r_1 = \frac{1 + |\varepsilon| - \sqrt{2\,(|\varepsilon| + \varepsilon')}}{1 + |\varepsilon| + \sqrt{2\,(|\varepsilon| + \varepsilon')}}$$ is the reflection at the boundary place

$$\alpha\lambda = 2\pi\sqrt{\frac{1}{2} \cdot (|\varepsilon| - \varepsilon')}$$ is the attenuation exponent.

ε' and ε'' must be selected in such a way that $|r_1| < |r| \leq 0.1$. The condition for d is reached by disregarding members of the order of magnitude $|r|^2$.

As materials with small losses and a dielectric constant around 1, only materials with small density can be considered. For practical purposes, light loss-free substances are used, for instance foam materials, loosely packed glass-wool or hair balls in which the energy-dissipating material, frequently graphite, is inserted, finely distributed and with the necessary concentration. In case of foamy material, the graphite powder is mixed with the liquid primary substance. Graphite powder is blown into the glass-wool.[7] The hair ball is soaked with graphite containing diluted glue.[8]

The absorbers are effective to a large degree independent from the frequency if their thickness is sufficiently large. The reflecting termination, in most of all cases present, causes an upper extreme wave length. This dependence from the wave length is expressed in the relation for the absorber thickness.

If the reflecting termination is not taken into consideration, the dependence of the reflection factor from the incidence angle - when the electrical field strength vector is in the incidence plane ($\parallel$) or normal ($\perp$) to it - becomes

$$r_{\parallel} = \frac{\sqrt{\varepsilon - \sin^2\vartheta} - \varepsilon\cos\vartheta}{\sqrt{\varepsilon - \sin^2\vartheta} + \varepsilon\cos\vartheta}; \quad r_{\perp} = \frac{\cos\vartheta - \sqrt{\varepsilon - \sin^2}}{\cos\vartheta + \sqrt{\varepsilon - \sin^2}}$$

In the acoustics there are corresponding absorbers made of cotton-wool having a low flow resistance.

4.2 $\varepsilon = \mu$ Absorbers

A material element, electrically a. d ferro-magnetically polarizable, ' ₅ very small with respect to the wave length, transmits an electrical as well as a etic

dipole radiation when influenced by an electromagnetic wave. With respect to the dipole axes, both radiation fields have the same spatial structure if one imagines the electric and magnetic field to be interchanged. The dipole axes are perpendicular to each other. The superposition of the two secondary radiation fields takes place opposite in phase in that direction from where the exciting wave came. If the amplitudes of the two dipole radiations are equal, then there is no back radiation. In extended material, whose dielectric constant and permeability coincide numerically in the real and imaginary part, the amplitudes of the electric and magnetic elementary dipole radiations are correspondingly of equal value. This is the reason why the plane surface of such a material does not reflect when $\varepsilon' = \mu'$ and ε'' and μ'' when being hit normally from a plane wave.

There are severe difficulties opposing the creation of materials whose relatively complex dielectric constant and permeability coincide numerically at frequencies over 1 kmc/s. However, it would be particularly interesting to possess such materials for absorbers at frequencies above 1 kmc/s. In general, the real parts of the dielectric constant of electrically energy-dissipating materials are considerably above 1 (for instance, $\varepsilon' = 10$). Due to the therefore required high permeability only ferro-magnetic materials can be considered. When being magnetized by alternating magnetic fields two mechanisms are effective: the domain wall displacement and the domain rotation. The displacement of domain walls, which causes great permeabilities at low frequencies, is hardly or not effective at all at frequencies above 1 kmc/s. Here, the magnetization is accomplished almost exclusively by domain rotation which leads, however, only at frequencies closely below the ferro-magnetic resonance to noticeable real parts μ' above 1 of the permeability and to magnetic losses (μ''). However, the higher the resonant frequency, the smaller are μ' and μ''. A compensation is only possible by an increased saturation-magnetization.

The ferro-magnetic metals, especially iron, posses the highest value of saturation magnetization. They can be used only as a fine powder imbedded in isolation

material since otherwise radio frequencies do not penetrate deep enough. Such metallic powder mixtures, however, possess hardly electrical losses so that ε'' cannot be made equal to μ''. An increase of the electrical losses by suitable additives (for instance graphite) causes in turn an inadmissible increase of ε''.

A suitable adjustment of the electrical losses is, in contrast, possible with the nonmetallic, ferro-magnetic ferrites. Yet their magnetic saturation point is too low in order to achieve a sufficiently high permeability above 1 kmc/s.

The above considerations are related to homogeneous, isotropic ferro-magnetic substances. By use of these, the construction of an absorber could not be accomplished for frequencies above 1 kmc/s as far as is known from the literature. Below 1 kmc/s, it would be principally possible. Homogeneous isotropic-composed $\varepsilon = \mu$ absorbers would be independent from the polarization at any incidence. The dependence of the reflection factor from the incidence angle would be according to

$$(r_{||})_{\varepsilon=u} = \frac{\sqrt{1 - \frac{\sin^2 \vartheta}{\varepsilon^2}} - \cos \vartheta}{\sqrt{1 - \frac{\sin^2 \vartheta}{\varepsilon^2}} + \cos \vartheta} \quad ; \quad (r_{\perp})_{\varepsilon=\mu} = -(r_{||})_{\varepsilon=\mu} \; .$$

With some of the ferromagnetic substances the matching of dielectric constant and permeability could be enforced also above 1 kmc/s if the homogeneous, isotropic primary material is formed anisotropic in a suitable manner.[31] However, freedom from reflection can be achieved only for one polarization direction. Two different types of anisotropy shall be mentioned here.

One is of geometrical origin and is based upon a sub-division of the primary material (iron powder mixture) into thin, parallel layers separated from each other by small gaps. For a wave, which is propagating parallel to the layer planes with an electric field strength vector normal upon it, this parallel-layer medium possesses a dielectric constant which, in contrast to that of the solid primary material, is decreased much more than the permeability. The dielectric polarization of thin plates in the normal direction is opposed by a strong de-electrification while practically no

de-magnetization occurs, since the magnetic field strength vector lies in the plane of the layers. This artificial decrease of the dielectric constant enables a matching of the real parts of ε' and μ' by proper selection of the layer thickness and the distance between the layers. A matching of the imaginary parts of ε'', μ'' is not achievable since no considerable electrical losses are present. It remains therefore a residual reflection. At such an arrangement, planely limited to 3.9 cm thickness, the reflection factor was 0.12 in the wave spectrum between 6 to 12 cm while the transmission factor increased from 0.15 to 0.40 with increasing wave length. For practical usage the attenuation ($\alpha\lambda \approx$ 23 db) is too small, and cannot be increased without an increase of the reflection factor.

The introduction of the aforementioned, geometrically-based anisotropy enables a strong decrease of the dielectric constant, while the dielectric properties of the employed, homogeneous, ferro-magnetic materials (ferrite) remain unchanged in the case of the second type of anisotropy. For the anisotropy here, an externally applied static magnetic field is responsible, the direction of which is perpendicular upon the direction of propagation and perpendicular to the magnetic field strength vector of the wave. By proper choice of its strength the occurrence of ferro-magnetic resonance can be achieved at the desired working frequency. The ferro-magnetic resonance is so marked that the permeability takes on relatively high values. In such a way, u can be made equal to up to frequencies of approximately 5 kmc/s (ferrites have an $\varepsilon' \approx 11$). At a wave length of 7.3 cm, r = 0 and the attenuation $\alpha\lambda \approx 500$ db has been measured at a pre-magnetized plate. The ratio of the limiting frequencies of the absorption range amounted, however, only to 1 : 1.18. Especially because of the required static magnetic field such an $\varepsilon = \mu$ absorber has only theoretical value; at least it can be used for nonreflecting termination of cables.

5. MEASUREMENTS OF POORLY-REFLECTING ABSORBERS. NONREFLECTING ROOMS

5.1 About Measurement of Poorly-reflecting Absorbers

It is self-explanatory that poorly-reflecting absorbers which are to be used in free space ought to be tested in free space. Here, not only the dependence of the reflection factor from the frequency but also its dependence from the direction of incidence and the polarization of the incident wave has to be investigated. Such tests become simpler, the smaller the wave length becomes, and the more one approaches optical relations, that is, the incident radiation can be received strongly beamed and the reflected radiation can be received directionally. Also, a second advantage is apparent at small wave lengths. In order to conduct dependable reflection measurements, the test piece must be big as compared to the wave length; a usable measure is for a wave length of $\lambda = 3$ cm for instance an area of 30 by 30 cm. The more oblique the wave incidence becomes, the bigger must be the dimensions of the test piece which for the absorber development creates difficulties in the construction of the test pieces. For preliminary measurements, small physical dimensions must suffice.

When taking measurements in the free field (Fig. 5.1) it is recommended, as already mentioned, to use beams of small diverging diameters both for transmitting and receiving; as far as possible measurements have to be taken in the far field or at least at the border of near and far field. This requirement is also good for the reflection field of the test piece proper. The comparison object with a 100-percent reflection must be always a metal plate of the same physical dimensions as the test piece. Great importance is given to the straightness of the two reflection surfaces because of eventual focusing or defocusing effects of curvatures and the like. The field measurements have to be carried out in the out-of-doors or in the nonreflecting room, so that no disturbing reflections occur originating from walls and the like. There is, however, still another possibility to separate the disturbing reflections from the surroundings from the reflections of the test piece: The test piece is made to move with a sufficient speed, for

instance either swinging to and fro, or the test piece is mounted on a rotating arm. The signal to be utilized, shifted in frequency by the Doppler effect, is by use of a modulation process easy to separate from the disturbing reflection caused by objects at rest.

Three-dimensional field tests made sense, of course, only in the cm-band or in the adjacent dm-wave-band due to the small dimensions of the test pieces. The same holds true for two-dimensional investigations in a flat room, i.e., in a room which is composed of well-conducting, plane metal plates on two opposite sides, for instance top and bottom. The lateral walls are made nonreflecting by suitably located absorbers. The distance between the metal plates is smaller than $\lambda/2$ if the arrangement is to work as a TEM-guide with the electrical vector being vertical upon the metal plates. The distance is greater than $\lambda/2$ if it is a waveguide of the type of H_{10}-wave, the electrical vector parallel to the plates.

While an investigation of the dependence of the reflection factor from the incidence angle is still possible in the flat measuring device with the lateral damping, this possibility is not available with one-dimensional conductors (strip line or wave guide). Considering the strip line, here the wave hits vertically the absorber test piece located at the end of the line, while in the wave guide, as is well known, the incidence angle depends upon the relation between the reference frequency ν to the cut-off frequency ν_{gr}. With increasing approach toward the cut-off frequency, the incident angle ϑ approaches 90^{o} ($\cos\vartheta = \sqrt{1 - (\frac{\nu_{gr}}{\nu})^2}$). This should be taken into consideration when transferring results of measurements in the wave guide to the free field. One can express this difference, in other words, the reflection investigation of an absorber test piece in the wave guide is related to a different wave resistance than that of the free space. Finally, the attention is to be invited to the fact that the field strength distribution across the cross section of the wave guide differs from that of the free space, for instance, at the H_{10} wave, the sine-like curve of the electrical field strength across the cross-section. Test pieces, which are not composed homogeneously, must therefore be fixed with their respective characteristic elements at symmetrical points of the field

strength distribution across the cross-section. Such a difficulty is not encountered when using the strip-line whose field distribution approaches almost the free space as compared to other wave types; here certain complications are introduced by border disturbances of the open line especially at the test piece.

While the optical procedure may be preferred as a rule, for the determination of incident and reflected energies in the two- and three-dimensional arrangements, the determination of the reflection factor can be done only using the method of the standing wave in the one-dimensional arrangement. The waviness of the field strength, the ratio between maximum and minimum of the standing wave of the line determines the amount of the reflection, the displacement of the field strength-minimum position by the test piece as compared to a known termination (short circuit for instance) determines the phase of the reflection. For measurement surveys, a directional coupler can be used instead of a measuring line.

The measurements of absorbers in lines leads also to the question, how transmission lines themselves are to be terminated nonreflectingly. To begin with the wave guide: Here, one uses mainly the gradual, for instance, wedge-shaped transition of a energy-dissipating material in the same manner as for the reduction of the reflection in free space. As a rule a thin dielectric stripe is used, the surface of which, or its interior, is graphitized.

Such a termination with a graphite-wedge works as well in the same range of wave lengths for which the wave guide is laid-out as determined by its geometrical dimensions. If a very accurate match for a given frequency is desired, i.e., a reflection in the order of only a few thousandths, then a tuner with suitable adjustment must be placed in front of the absorber.

Another, however narrow-banded procedure for a nonreflecting termination of a wave guide is the use of a 377-ohms-foil in a distance of $\lambda'/4$ in front of a short circuiting plate where λ' stands for the wave length in the wave guide (see Sec. 3).

At this occasion, the nonreflecting termination of concentric conductors is to be mentioned which has a great practical significance. For instance, one could make

it in such a way that a 377-ohms-foil is pressed against the open end of the coaxial cable, that is against both the inner and outer conductor. Since the line wave impedance of the cable equals the wave impedance in space (377 ohms) times a geometrical factor as pertaining to the cable dimensions, a complete matching is achieved. This method has however, a more theoretical significance than a practical one. For practical purposes another termination is being chosen which can be seen in Fig. 5.2, especially if the absorption of greater power is concerned. The inner conductor of a coaxial cable with the diameter d is continued by a layer resistance of the value R = Z, where Z stands for the wave impedance while at the same time the outer cylindrical mantle narrows according to an exponential law $D = d \exp \left[(Z/60) \cdot x/1 \right]$. D stands for the respective diameter of the transition at the spot x at a total length L of the contraction. The curves in Fig. 5.2 show the variation of the outer-conductor-diameter with increasing distance from the end of the line for the various wave impedances, a complete matching provided.[32]

5.2 The Reverberation Room

In the preceding chapter methods for the measurement of reflections on absorbers have been discussed by which the reflection factor can be determined of a test piece for every given polarization direction and for each given incidence angle. Consequently, the question arises, to measure the reflection factor in a diffuse field, that is, to find an average value for all polarization directions and all incidence angles.

If ψ is the polarization angle and ϑ the incidence angle of the radiation, the reflection factor $| r (\vartheta, \psi) |$ at a randomly selected polarization for the incidence angle ϑ becomes

$$| r (\vartheta, \psi) |^2 = | r_{||} (\vartheta) |^2 \cos^2 \psi + | r_{\perp} (\vartheta) |^2 \sin^2 \psi$$

where $r_{||}$ and $r_{\perp}$ are the corresponding reflection factors for parallel and normal polarization. One divides the electrical or magnetic vector into its components, parallel and normal to the plane of incidence.

The average value across all polarization directions is

$$\langle |r(\vartheta)|^2 \rangle_\psi = \frac{1}{2} \left[|r_{\parallel}(\vartheta)|^2 + |r_{\perp}(\vartheta)|^2 \right] .$$

In order to obtain the average value for all angles of incidence $A = 1 - |r|^2$ is introduced as absorption degree. Then, according to Paris[33] the average value $\bar{A}$ becomes

$$\bar{A} = 2 \int_0^{\pi/2} A(\vartheta) \cos\vartheta \sin\vartheta \, d\vartheta = - \int_0^{\pi/2} A(\vartheta) \, d(\cos^2\vartheta).$$

The average value $\bar{A}$ can be determined somewhat laborously by measurement of the reflection factors $r_{\perp}$ and $r_{\parallel}$, or the corresponding absorption degrees for each angle of incidence; $\bar{A}$ is then to be calculated according to the aforementioned formulas. Then one obtains the absorption or the reflection of the test piece, respectively, in a diffuse wave field.

It is much simpler to determine this value by a single measurement in the diffuse field of a reverberation room.[35] Here, a large empty room with extremely well reflecting walls can be used; in this room many resonant frequencies are excited by a transmitted frequency band, for instance by means of a pulsed magnetron. The measurements are taken according to the acoustical reverberation room by measuring either the stationary energy density with permanent excitement or the decay of the energy density with pulse excitement. In both measuring values the amount of energy losses at the walls is involved when the losses in the medium can be assumed to be negligibly small. The formula for the reverberation time contains also the room volume.

A diffuse wave field assumed, the employment of the Jaeger-Sabine reverberation theory to the electrical process yields as formula for the reverberation time τ (τ equals the duration of the reverberation for a level difference of 60 db, that is, for a energy density ratio if $1 : 10^{-6}$):

$$\tau = \frac{1.84 \cdot 10^{-7} V}{F_o}$$

where V is the volume in m^3 and F_o the absorption area in m^2. The latter area indicates how many m^2 open window space with the absorption degree 1, the room would have provided that all other surfaces would reflect 100 percent. F_o is combined from the sum of the absorptions of the individual surface elements F_i, namely $\sum A_i F_i$.

The quality Q, normally given in radio-frequency applications for a resonator, is connected with the reverberation time in the form $\tau = 2.2\,Q/\nu$ where ν stands for the test frequency. In the same manner follows for Q the formula $Q = \frac{8\,\pi V}{\lambda \cdot F_o}$ as the relation between quality and absorption area with λ as wave length.

In a stationary state the resulting energy density is directly proportional to the power supplied by the transmitter, and inverse proportional to the absorption area. Both procedures, the measurement of reverberation and the measurement of the stationary energy density, permit the determination of the absorption area of additional absorbers, which are brought into room, being located either within the room or on the surface of the room.

The measurement of the reverberation time τ of the empty room gives its self-absorption when the volume is known. Each additional absorption causes a decrease of the reverberation time and can be determined directly from it. In case of the measurement of the stationary energy density, a known additional absorption is required in order to calculate the self-absorption of the empty room. For instance, the additional absorption is, according to the procedure introduced by W. C. Sabine into the room acoustics, an "open window" in one wall of the reverberation room, assumed that the radiation going out through the window does not re-enter the room (absorption degree of the open window equals 100 percent).

The determining assumption of the reverberation method is the diffuse field. In the sense of the wave concept of the reverberation as a superposition of the decay processes of the various modes, it can be expected that this requirement is better fulfilled the larger the number of modes, since to each of them is attributed a certain wave direction.

The number of acoustical eigen-frequencies in a square room is for a frequency interval $d\nu$

$$N_{ak} = \left(\frac{4\pi V}{\lambda^3} + \frac{\pi F}{2\lambda^2} + \frac{L_K}{8\lambda} \right) \frac{d\nu}{\nu}$$

where V stands for volume, F for the total surfaces, and L_K as the total length of the edges of a rectangular parallelepiped room. For high frequencies, only the first term, the volume term $\frac{4\pi V}{\lambda^3}$ is determining, and the number of eigen-frequencies does not depend any more from the shape of the room. M. Schroeder[34] has demonstrated that the corresponding formula for the electrical case is

$$N_{el} = \left(\frac{8\pi V}{\lambda^3} - \frac{L_K}{4\lambda} \right) \frac{d\nu}{\nu}$$

In the case of high frequencies and also in the case of restriction to the first term, it follows that the number of eigen-frequencies is twice as high in the electrical case as in the acoustical case (there are H- and E-waves).

For experiments of the aforementioned type[35] at a wave length of 3 cm, a wooden box covered with thin copper sheets of about 2 m^3 volume has been used; two sliding windows made of metal were planned. The room had been excited by oscillation impulses with a length of 0.45; 0.8 and 1.4 usec. Analogous to the original acoustical experiments by W. C. Sabine, an adjustable metallic propeller had been installed in the room as a "mode mixer."

The calculated number of the excited natural vibrations for the aforementioned impulse lengths is 700, 390, and 220.

Turning the energy on and off was accomplished at several spots through small openings in the wall which were connected to wave guides.

First an example for the stationary measurements. With a constant supply of electrical power, one of the aforementioned openings was opened to different degrees by means of a sliding window. The reciprocal value of the respective energy density is plotted as ordinate in Fig. 5.3, as related to the energy density of the closed

reverberation room while the abcissa denotes the order of the opened area in cm^2. The curve must be a straight line. From it follows that the absorption area of the closed, empty room amounts to 85 cm^2.

The reverberation time has been measured, too. In doing so, the output exciting frequency band is modulated by a fixed frequency in its vicinity. The resulting difference-oscillations are being amplified by a so-called momentary logarithmic amplifier (limiting frequency 5 Mc, dynamic range 60 db); the "reverberation process" can be made visible in such a way on the screen of an oscilloscope with a logarithmic scale. (Fig. 5.4). The resulting reverberation time τ in this case is about 50 usec, which corresponds, by the way, of Q about 200,000.

In order to give an example for the achievable accuracy of the measurement of the "statistical" absorption degree: Two materials, a 370-ohms and a 150-ohms foil, respectively, on a 4 mm thin Pertinax* plate made conducting in the rear, has been measured in the reverberation room relative to their average absorption. By measurements of the propagating planar waves in free space first the average values for the two absorbers for all polarization and incidence directions had been noted (the latter ones only up to 75°); they amounted to 88 percent and 70 percent, respectively. The measured values according to the method of the stationary energy density were 103 percent and 81 percent, respectively; according to the reverberation methods 87 percent and 69 percent resulted, which can be considered as relatively good coincidence for the first attempts of this kind, especially when considering the difficulties in the construction of a real diffuse field in a reverberation room with additional absorption as known from the acoustics.

The absorption has been measured by the reverberation method also for wall openings of different areas (λ). The results showed good agreement between the geometrically and the electrically determined opening areas; only with larger openings, of the order of 4 percent of the total room surface, deviations of 10 percent occured.

---

* - commercial material

Walther[12] gives theoretical data about the average reflection factor of absorbers with incidence of planar waves with statistically distributed incidence angles ϑ and polarization directions ψ as found by reverberation measurements. He confines himself to the class of very thin-layer absorbers whose input impedance is almost independent from the incidence angle and from the polarization direction (for example 377-ohms-foil absorbers with a very high dielectric constant ($\varepsilon' >> 1$) of the loss-free dielectric intermediate layer or $\lambda/4$-layer absorber with $|\varepsilon \mu| >> 1$). For absorbers, matched completely for vertical incidence, i.e., with oblique incidence equally well matched for both polarization directions, Walther obtains the value 0.3 as an average reflection factor. This value is derived also, when the absorber is not matched for vertical incidence but for a desired incidence angle $\vartheta_0 < 35^\circ$ with vertical or parallel position of the electrical field strength vector to the incidence plane.

A very large electric reverberation room has been built in the III. Physikalischen Institut der Universitat Gottingen by covering the walls of the 350 m^3 acoustic reverberation room with copper foil. The reverberation time of the empty room amounts to 400 µsec for electromagnetic waves of the frequency 10 kmc/s. This value corresponds to a quality of $1.7 \cdot 10^6$. It agrees well with the value calculated from volume, surface and skin depth data.[35]

The reverberation room is suitable especially to determine the absorption on big surfaces with relatively weak absorbing faces, for example, painted metal surfaces, objects made of plastic, metal wires and the like, for a diffuse wave incidence. The measurement of the absorption area of persons in the large Goettinger reverberation room gave about 1 m^2 per person.

5.3 The Nonreflecting Room

The most frequent use of weakly-reflecting absorbers for electromagnetic waves are to be found in the construction of nonreflecting rooms. Such a room must meet the following requirements. The reflection factor of the absorbing arrangement must be, of course, as small as possible, it should be in the order of several percent only.

Besides, the absorber must be effective over a wide range of frequencies which requires a certain layer thickness. Finally, a certain size of the room is required in order to conduct the investigations in the far field of the transmitter and receiver as well as of the test piece.

Because of the wide-band requirement, only wedge or rib absorbers will have to be considered. As an example of a non-reflecting room the large Goettinger room should be mentioned (light volume 5.5 x 10 x 14 m^3).[7] Since the room serves at the same time acoustical purposes, it has therefore wedges of porous glass-wool being 1 m long. Into these wedges, graphite powder had been inserted with 6.7 weight percent, that is, with only 1 volume percent (see Sec. 2). For reasons of traversing, it contains in the lower third a widely meshed wire net consisting of thin steel ropes (5 cm width of mesh) which for acoustical purposes does not hinder but electrically represents a reflecting plane. The electrical measurement area contains therefore only 5 nonreflecting planes; the floor is reflecting but can be made nonreflecting by covering with absorbers. In case this is not done, then one obtains a nonreflecting half-room and the transmitter or the receiver of the respective measuring arrangement has to be brought into the plane of the net in order to eliminate its reflection.

Nonreflecting rooms are tested for their quality acoustically as well as electrically by measuring the deviation from the distance law (1/S) in the wave propagation by the use of a small transmitter and a small receiver. The wave lengths in the aforementioned case were 3, 10, 20 and 46 cm. Figure 5.5 shows examples of level recorder diagrams. The first curve is recorded along the diagonal of the basic plane, the other curves are measured in the direction of the room diagonal. The electrical polarization was vertical to the wire net. One recognizes in Fig. 5.5 that only at larger distances considerable variations in the intensity occur caused by the wall reflection.

Figure 5.6 gives a summary of all measurements with the distance-ranges 1-4m, 4-8 m, and 8-12 m. The ordinate designates the maximum deviation from the 1/S law, the abscissa designates the test frequency or the wave lengths, respectively. Part a of the illustration is related to the vertical polarization, part b to the horizontal polarization.

The first one provides somewhat better results than the second one (influence of the net). The level variations in the vicinity of the transmitter are very low. With vertical polarization they remain up to 20 cm wave length still under 1.5 db, even with the highest possible distances in the room. The graphite concentration used in the Goettinger room (see above) is very low since the main interest was accorded to the absorption of the dm- and cm-waves. With the large wedge length one can obtain without difficulties considerable lower reflection factors likewise for higher wave lengths by a higher graphite filling.

Another room, acoustically and electrically effective, has been built in Bern[36] namely by use of glass-wool wedges with thin iron wires. In this room, instead of the wire nets which cause electrical disturbances, a plastic net made of 4 mm strong perlon ropes has been used.

Besides a great frequency bandwidth and low reflection also the incidence angle dependence of the reflection factor is of importance with absorbers used in measuring rooms. It plays a noteworthy role in the case of multiple reflections. They are especially troublesome if they run back into the main incidence direction.

As is shown in Fig. 5.7, this is the case with radiating into an edge or a corner at which two or three walls meet resp. Such an edge or corner of a room is reflecting with respect to the direction like an angle mirror. The "edge reflection factor" $|r_{\measuredangle}| = |r(\vartheta)| \cdot |r(\frac{\pi}{2} - \vartheta)|$ of a rectangular edge in dependence of the incidence angle ϑ is plotted in Fig. 5.7 for a wedge-type absorber (see 2.3) and for a single dipole absorber (see 3.3). The angular dependence $|r(\vartheta)|$ of the single dipole absorber is less favorable then that of the wedge absorber (compare Figs. 2.15 and 3.18). This is also evident from $|r_{\measuredangle}|$ in Fig. 5.7 and makes the wedge absorber more appropriate for lining room walls.

Besides the wedge and rib absorbers, the chimney absorbers also mentioned in 3.2 are practically used for poorly reflection test rooms. The incidence angle dependence of their reflection factor does not strongly differ from that of the wedge and rib absorbers.

REFERENCES

1. SMITH, P. H., Electronics 12, 29, January 1939.
2. MEYER, E., BUCHMANN, G., SCHOCH, A., Akust. Z. 5, 352 (1940).
3. MEYER, E., SCHMITT, H. J., SEVERIN, H., Z. angew, Phys. 8, 257 (1956).
4. LEWIN, L., Jour. I.E.E., 94, Pt. III, 65 (1947).
5. LENZ, K. L., Z. angew. Phys. 10, 17 (1958).
6. HADDENHORST, H. G., Z. angew. Phys. 8 , 264 (1956).
7. MEYER, E., KURTZE, G., SEVERIN, H., TAMM, K., Acustica 3, 409 (1953).
8. SIMMONS, A. J., EMERSON, W. H., Tele-Tech. u. Electronic Industries, 47, July 1953.
9. MEYER, E., TAMM, K., Akustische Beihefte (Acustica) Heft 2, 91 (1952).
10. MORSE, PH. M., J. acoust. Soc. Amer. 11, 205 (1939).
11. MEYER, E., SEVERIN, H., Z. agnew. Phys. 8, 105 (1956).
12. WALTHER, K., Z. agnew. Phys. 10, 285 (1958).
13. WALTHER, K., Reflection Factor of Gradual-Transistion Absorbers for Electromagnetic and Acoustic Waves. Report of the Bendix Aviation Corporation, Res. Lab. Div., Detroit, Michigan.
14. MULLER, R., Arch. f. Elektr. Ubertr. 7, 223 (1953).
15. V. TRENTINI, G., Z. angew. Phys. 5, 221 (1953).
16. FRANZ, W., Z. angew. Phys. 6, 449 (1954).
17. SCHMITT, H. J., Z. angew. Phys. 11, 335 (1959).
18. MONTGOMERY, C. G., DICKE, R. H., PURCELL, E.M., Rad. Lab. Ser., Vol. 8, S. 396, McGraw Hill Book Co., New York, 1948.
19. MALJUSHINEZ, G. D. Inf. tech. bull, uber d. Bau d. Sowjetpalastes 5-6, 32 (1941).
20. DALLENBACH, W., KLEINSTEUBER, W., Hochfrequenztechn. u. Elektroak. 51, 152 (1938).
21. SCHMITT, H. J., Z. angew. Phys. 8, 372 (1956), see also Deutsches Patent No. 1004248.

22. KURTZE, G., NEUMANN, E. G., Ein Dipolabsorber fur elektromagnetische Zentimeterwellen mit verminderter Reflexion bei schrager Inzidenze Z. angew. Phys. 12 (1960).

23. SCHMITT, H. J., FUTTERMENGER, W., Z. angew. Phys. 10, 1 (1958).

24. WIEKHORST, F., Z. angew. Phys. 10, 173 (1958).

25. MEYER, E., SEVERIN, H., UMLAUFT, G., Z. f. Physik, 138, 465 (1954).

26. POTTEL, R., Z. angew. Phys. 11, 46 (1959).

27. FROHLICH, H., Theory of Dielectrics, S. 4, Oxford, Clarendon Press (1949).

28. LIPPERT, W., Hf.-Tech u. Elektroakustik 60, 11 (1942).

29. DEUTSCH, J., THUST, P., Z. angew. Phys. 11, 453 (1959).

30. PARK, D., Phys. Rev. 97, 60 (1955).

31. POTTEL, R., Z. angew, Phys. 10, 8 (1958).

32. NEINKE, H., GUNDLACH, F. W., Taschenbush d. HF.-Tech., Springer-Verlag, Berlin, S. 87 (1956).

33. PARIS, E. T., Philosoph. Mag. 5, 489 (1928).

34. SCHRODER, M., Acustica 4, 456 (1954).

35. HELBERG, H. W., MEYER, E., VOGEL, S., Hallraum-Mebtechnik und Bau eines groben, Hallraums fur elektromagnetische wellen, Z. angew. Phys. 12, (1960).

36. EPPRECHT, G. W., KURTZE, G., LAUBER, A., Acustica 4, 568 (1954).

FIGURE CAPTIONS

Fig. 2.1 Amount of the dielectric constant ($|\epsilon|$) and the permeability ($|\mu|$) as well as the electric and magnetic loss factors of mixtures made from graphite and paraffin dependent upon the volume concentration at a wave length of 3 cm (from Ref. 3).

Fig. 2.2 The amount of the dielectric constant and the permeability as well as magnetic loss factor of mixtures made of paraffin and iron powder depending upon the volume concentration at 3 cm wave lengths. a, b, c: curves for different iron grain diameters (from Ref. 3).

Fig. 2.3 a, b Circle diagrams of the input impedance of a parellel damped network as related to the wave impedance with two different steep linear damping courses x = plane coordinate; L = length of line; α_{x} = attenuation constant; a_{α} = total attenuation. (from Ref. 5).

Fig. 2.4 Circle diagram of the input impedance of a damped network related to the wave impedance with exponentially increasing attenuation. (from Ref. 5).

Fig. 2.5 Test pieces for wave guide measurements with wedge and pyramid absorbers. (from Ref. 6).

Fig. 2.6 Attenuation constant α of paraffin-graphite mixtures with respect to graphite content in volume percent measured in the TE_{10} wave guide at a frequency of 3.4 kmc/s (wave length in space 8.75 cm). (from Ref. 6).

Fig. 2.7 Reflection factor of pyramid-shaped absorbers made of paraffin-graphite mixtures with different graphite content (volume percent) c depending upon the length of the pyramid, measured in the TE_{10} wave guide with a wave length in space of 8.75 cm. (from Ref. 11).

Fig. 2.8 Reflection factor depending upon the total length d = T + S of pyramid-shaped absorbers made of paraffin-graphite mixtures with different graphite content c measured in the TE_{10} wave guide at a wave free space length of 8.75 cm. The pyramid length T is according to Fig. 2.7 selected in such a way that $|r| = 0.1$ for $d \to \infty$. (from Ref. 6).

Fig. 2.9 The smallest overall length of pyramid-shaped absorber, made of paraffin-graphite mixtures for a given reflection factor $|r| = 0.1$ with respect to the graphite content in volume percent. The pyramid length T is selected in such a way that $|r| = 0.1$ for $d \to \infty$ according to Fig. 2.7. (from Ref. 6).

Fig. 2.10 Reflection factor of an absorber configuration made of Oppanol-ribs with respect to the frequency with different termination. (from Ref. 11).

Fig. 2.11 Square of amplitude of electrical field strength in front of and in parallel plate media, made of poorly conducting foils with the distances d from each other and the surface resistivities $R_{\square}$, measured at 3.2 cm wave length. Electric field strength vector and wave propagation direction parallel to the plates. (from Ref. 11).

Fig. 2.12 Attenuation constant of a medium of conducting plates with respect to their surface resistivities at different plate distances. Wave length $\lambda = 3.2$ cm. Electric field strength vector and wave propagation direction parallel to the plates. (from Ref. 11).

Fig. 2.13 Reflection factor of a rib absorber with different rear terminations with respect to the wave length of the normal incident wave. Surface resistivity of the ribs 200 ohms.

Fig. 2.14 Wide-band absorber made of foam material with rib-shaped cavities, the walls of which being graphitized. (from Ref. 11).

Fig. 2.15 Reflection factor of a rib absorber with respect to the incidence angle at different polarization directions ($E_{\parallel}$, $E_{\perp}$) of the incident wave and different absorber positions.

--o--o-- Ribs parallel and normal to the incident plane

__o__o__ Ribs included by 45° against the incidence plane (from Ref. 12).

Fig. 3.1 The 377-ohms-foil absorber and its substitute circuit.

Fig. 3.2 Reflection factor of 377-ohms-foil absorbers with different intermediate layer dielectric constants with respect to the frequency. (from Ref. 17).

Fig. 3.3 Reflection factor of very thin ($\varepsilon' \geq 1$) single foil absorbers with respect to the incidence angle at complete matching for one polarization direction ($r_1(\vartheta_1)$) and equal matching for both polarization directions ($r_2(\vartheta)$). (from Ref. 12).

Fig. 3.4 Reflection factor of 377-ohms-foil absorbers for different polarization directions with respect to the incidence angle; (from Ref. 12) dielectric constant of the intermediate layer $\varepsilon' = 1$ and $\varepsilon = \infty$.

Fig. 3.5 a, b Reflection factor of single-foil absorbers with two resonant layers with respect to the frequency. (from Ref. 17).

Fig. 3.6 Reflection factor of a dual-foil absorber with three resonant layers with respect to the frequency; G = foil surface conductance. (from Ref. 17).

Fig. 3.7 Reflection factor of a three-foil absorber with four resonant layers with respect to the frequency. (from Ref. 17).

Fig. 3.8 Measured reflection factor of the three-foil absorber with four resonant layers (see also Fig. 3.7) with respect to the frequency for oblique incidence (15° and 45°); electric field strength vector in the incidence plane. (from Ref. 17).

Fig. 3.9 Dielectric constant of like, loss-free dielectric intermediate layers of multi-foil absorbers, and total thickness of these absorbers depending upon the number n of the resonant layers when matching is required for the harmonic frequencies $K\nu_0$ ($K = 1, 2 \ldots n$); λ_0 greatest absorption wave length. (from Ref. 17).

Fig. 3.10 Reflection factor of a multi-foil absorber ("electrical swamp") with respect to the frequency. (from Ref. 18).

Fig. 3.11 Schematic of a $\lambda/4$-layer absorber. Real and imaginary part of the dielectric constant of the layer material of $\lambda/4$-layer absorbers with pure dielectric losses as function of the ratio layer thickness to wave length. (from Ref. 26).

Fig. 3.12 Real and imaginary part of the permeability of the layer material for $\lambda/4$-layer absorbers with pure magnetic losses as function of the ratio $\varepsilon' d/\lambda$. (from Ref. 26).

Fig. 3.13 Reflection factor of a $\lambda/4$-layer absorber depending upon frequency (wave length). Data of the layer: Thickness d = 1.15 mm; material values $\varepsilon' = 14.4$; $\varepsilon'' = 1.15$; $\mu' = 2.41$, $\mu'' = 1.41$. (from Ref. 26).

Fig. 3.14 Relative frequency bandwidth of $\lambda/4$-layer absorbers with only dielectric losses depending upon the ratio layer thickness to wave length. (from Ref. 26).

Fig. 3.15 Reflection factor of a three-stage shaft-absorber depending upon the frequency. Curve A measured for an angle of incidence of 10^0, electric field strength vector parallel to the plane of incidence. Curve B computed for normal incidence. Drawing of absorber section.

Fig. 3.16 Substitute circuits (a, b) and schematic (c) of a single dipole absorber. Reflection factor of single-dipole absorbers with different surface impedances of the dipole grid depending upon the frequency. Curves are calculated from the substitute circuit (b). Points measured on a dipole absorber at 3 cm wave length. (from Ref. 23).

Fig. 3.17 Input admittance of an energy-dissipating dipole grid depending upon the ratio dipole length to resonant wave length derived from wave guide measurements (oblique incidence) $Z_R = Z_o / \sqrt{1 - (\lambda / \lambda_G)^2}$ = characteristic impedance of the wave guide h and g according to Fig. 3.18. $g/\lambda_1 = 0.36$; $h/\lambda_r = 0.935$; $\lambda_r = 3.2$ cm; $\varepsilon' = 1.08$; incidence angle $\vartheta = 44.4^o$; $R_F = 40\ \Omega$.

Fig. 3.18 Reflection factor of single-dipole absorbers with two different loss-free dielectric intermediate layers with respect to the angle of incidence at normal ($\perp$) and parallel ($\parallel$) position of the electric field strength vector to the incidence plane. (from Ref. 21). Sketch of the dipole grating.

Fig. 3.19 Reflection factor of a dipole absorber with "transversal-dipole-grid" and "longitudinal-dipole-grid" (c) depending upon the incidence angle; (a) reflection factor of the transversal-dipole-grid and (b) the longitudinal-dipole-grid measured individually in front of the metal plate at 3.2 cm wave length. (from Ref. 22).

Fig. 3.20 Calculated frequency dependences of the reflection factor obtained from the a-f substitute circuit of a dual-dipole absorber (c), of a single-dipole absorber (b) and a 377-ohms-foil absorber (a). (from Ref. 23).

Fig. 3.21 Schematic of a dual-dipole absorber (a); curves of the reflection factor obtained by model measurements on the a-f substitute circuit (see Fig. 3.20c) of dual-dipole absorbers with respect to the frequency (b); reflection factor of a dual-dipole absorber measured in free space at cm-waves (——) and reflection factor measured at the substitute circuit (----) with respect to the frequency (c) (l, g see Fig. 3.18). (from Ref. 23).

Fig. 3.22 Input impedance of an energy-dissipating slotted-foil depending upon ratio slot length L to resonant wave length λ_r measured in the wave guide at 3 cm wave length, and substitute circuit valid in the vicinity of the resonance; slot width 1.8 mm; surface resistivity of the foil 15 ohms. (from Ref. 24).

Fig. 3.23 Reflection factor of a slotted-foil absorber with linear slots (a) and a slotted-foil dipole-absorber with circular slots and dipole crosses (b) with respect to the wave length. (from Ref. 24).

Fig. 3.24 Absorption element of a loop absorber for 3 cm wave length and its substitute circuit. (from Ref. 25).

Fig. 3.25 Reflection factor of a loop absorber depending upon the wave length at 15^o incidence angle (a) and with respect to the incidence angle at 3.18 cm wave length for parallel (//) and normal ($\perp$) position of the electric field strength vector to the incidence plane (b); N = number of resonators per 1 cm^2. (from Ref. 25).

Fig. 5.1 Arrangement of absorbers in free space for measuring the reflection factor with respect to the incidence angle and the polarization angle.

Fig. 5.2 Nonreflecting termination of a coaxial cable; inner conductor as layer-resistance with the value R; diameter of the outer conductor depending upon the distance to the end of the cable for different characteristic impedances Z. (from Ref. 32).

Fig. 5.3 Ratio of energy densities in the closed and opened "electrical reverberation room" with respect to the window area. F_0 = absorption area of the closed room. (from Ref. 35).

Fig. 5.4 Decay of the electric field in the electric reverberation room with respect to time. (from Ref. 35).

Fig. 5.5 Strength of the electric field of a small dipole transmitter as related to the wave length with respect to the transmitter distance at different wave lengths, measured in the Goettinger nonreflection room. The electrical field strength vector is vertical upon the traversing wire net. (from Ref. 7).

Fig. 5.6 Maximum deviations of the dependence from the distance "S" of the electric field of a small dipole transmitter from the 1/S law, measured in the Goettinger nonreflecting room for different wave lengths and distance ranges. The electrical field strength vector is vertically ($\perp$) upon or parallel to ($//$) the traversing wire net. (from Ref. 7).

Fig. 5.7 "Edge-reflection" factor $|r_{\not<}| = |r(\vartheta)| \cdot |r(\frac{\pi}{2} - \vartheta)|$ with respect to the incidence angle ϑ for single dipole absorbers at different polarization directions (electric field strength vector parallel ($||$) or normal ($\perp$) to the incidence plane resp.) and for the wedge absorber.

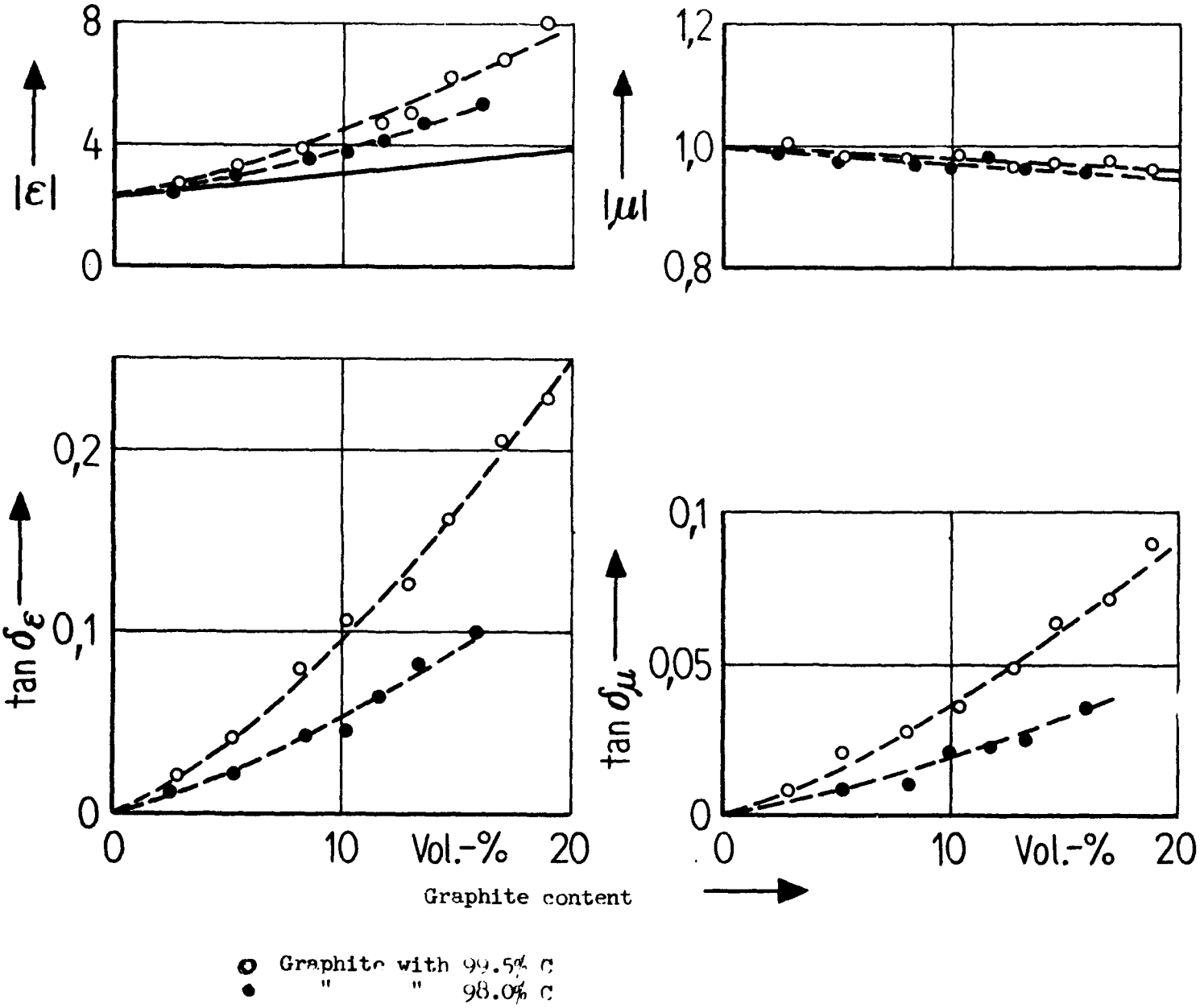
8
4
0
|ε|
1,2
1,0
0,8
|μ|
0,2
0,1
0
tan δε
0,1
0,05
0
tan δμ
0
10
Vol.-%
20
Graphite content
Graphite with 99.5% C
" " 98.0% C

Fig. 2.1

——— Fe, $\sigma \approx 10^5\ \Omega^{-1}\ cm^{-1}$

a, a': Carbonyl iron powder
b, b': grain diameter about 2.10^{-4} cm
c, c': " " " 50.10^{-4} cm
a, b, c measured; a',b',c' calculated 12.21.

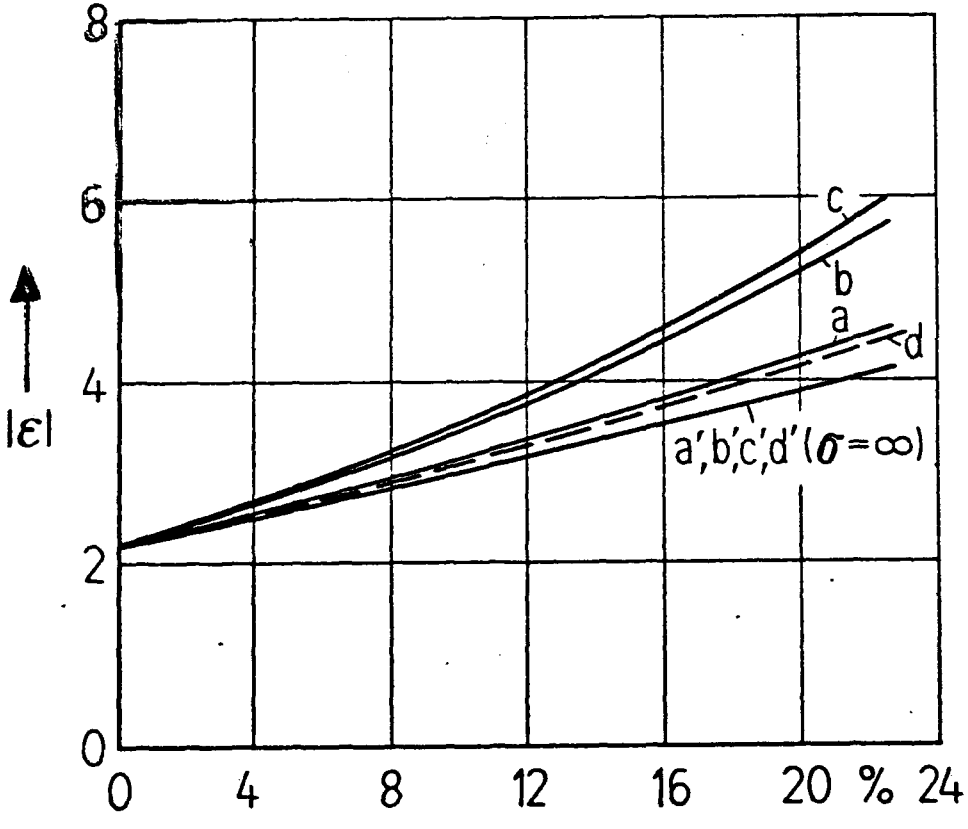

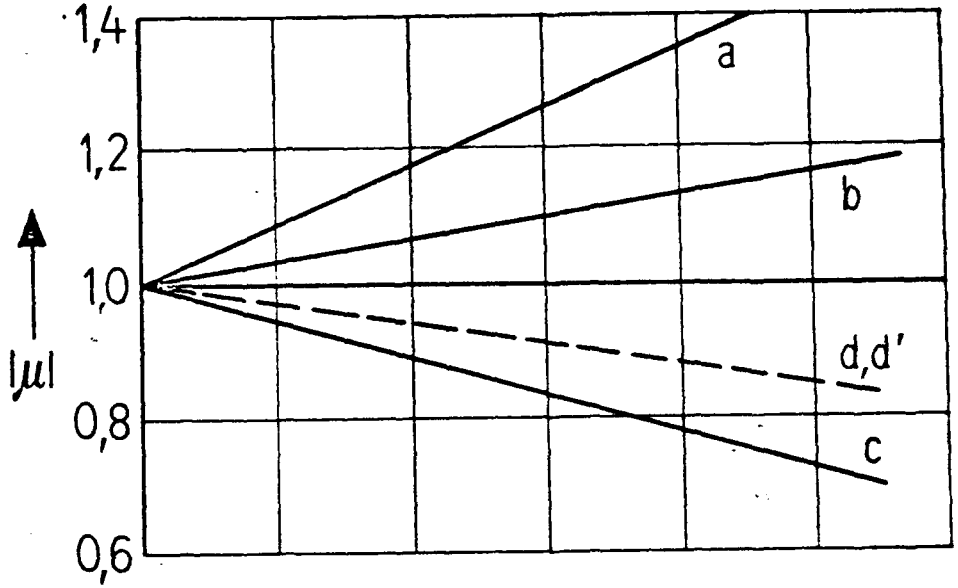

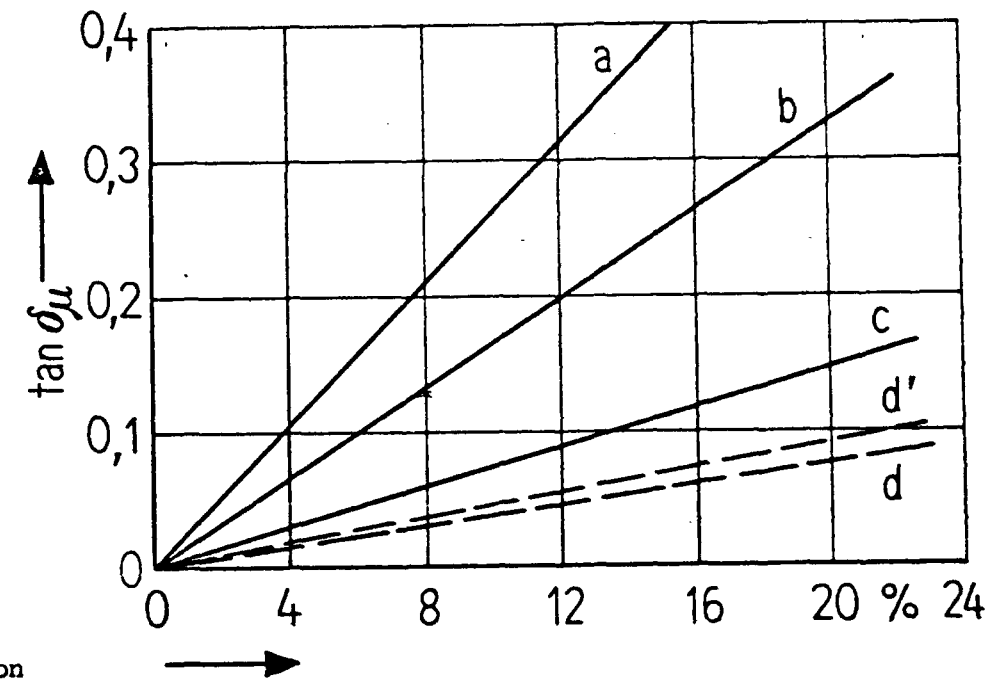

Volume - concentration

Fig. 2.2

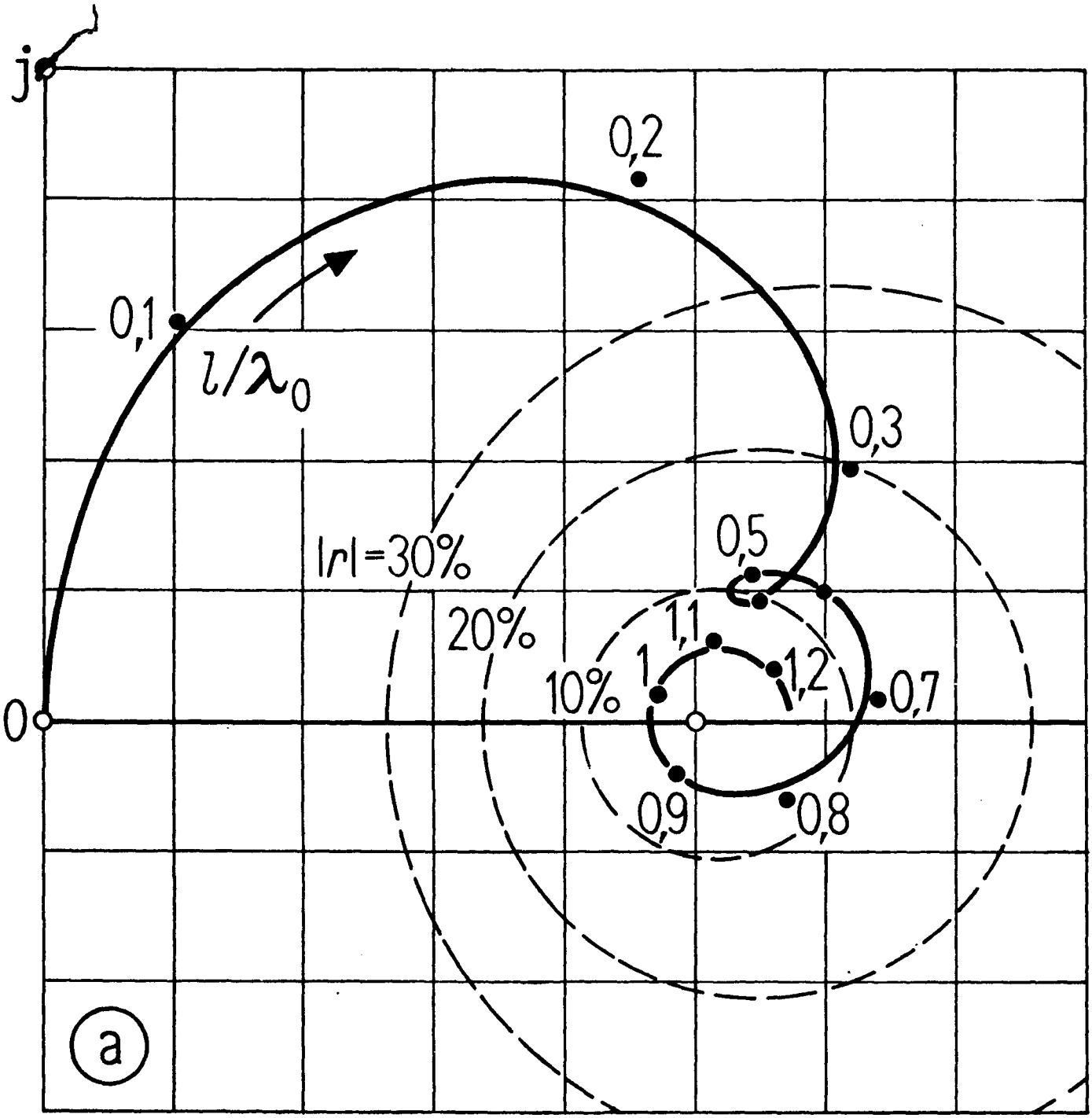

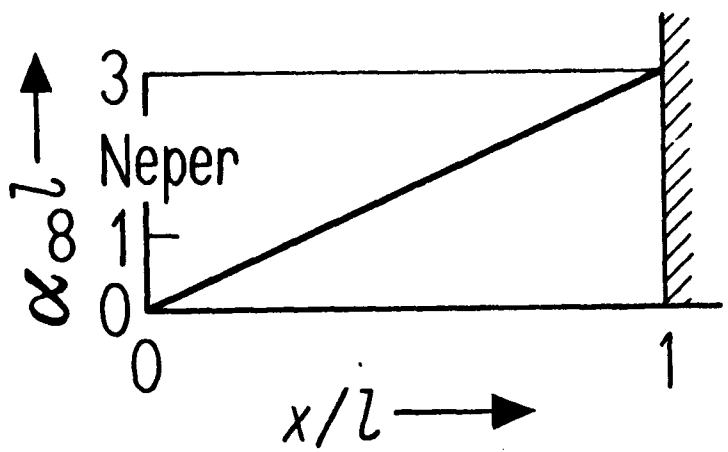

$\alpha(x) = c\,x/l$

$c = 3N$

$n(\infty) = 1.5N$

Fig. 2.3a

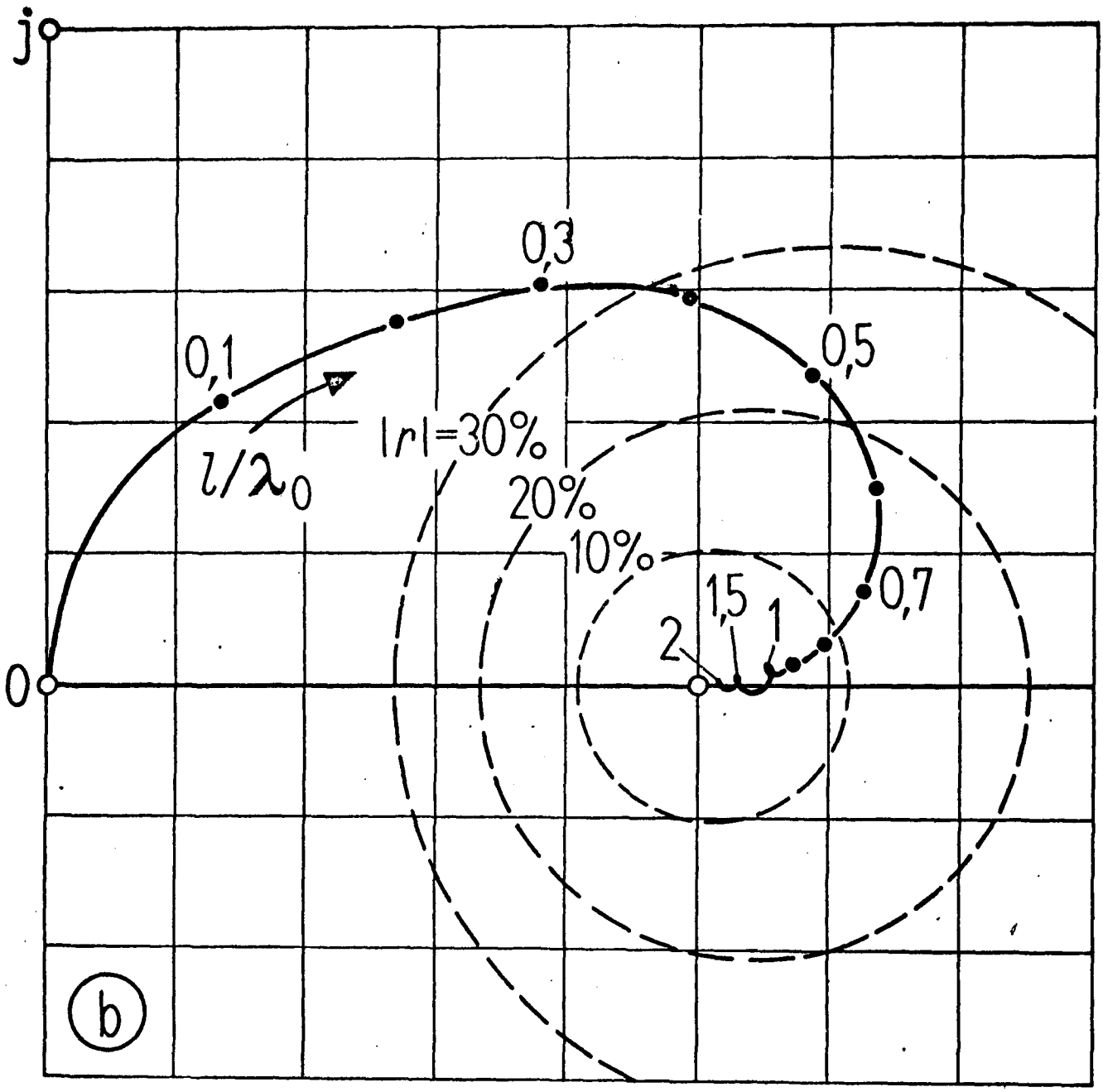

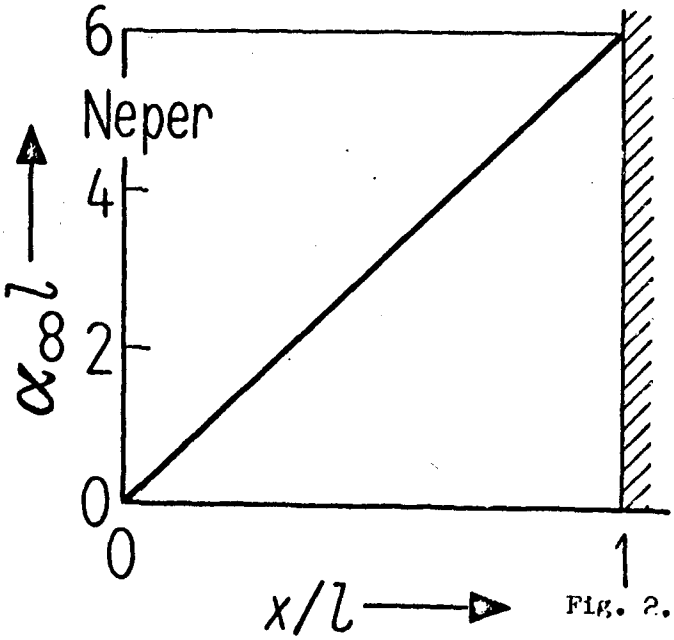

$\alpha_\infty l = c\,x/l$

$c = 6N$

$a_\infty = 3N$

Fig. 2.3b

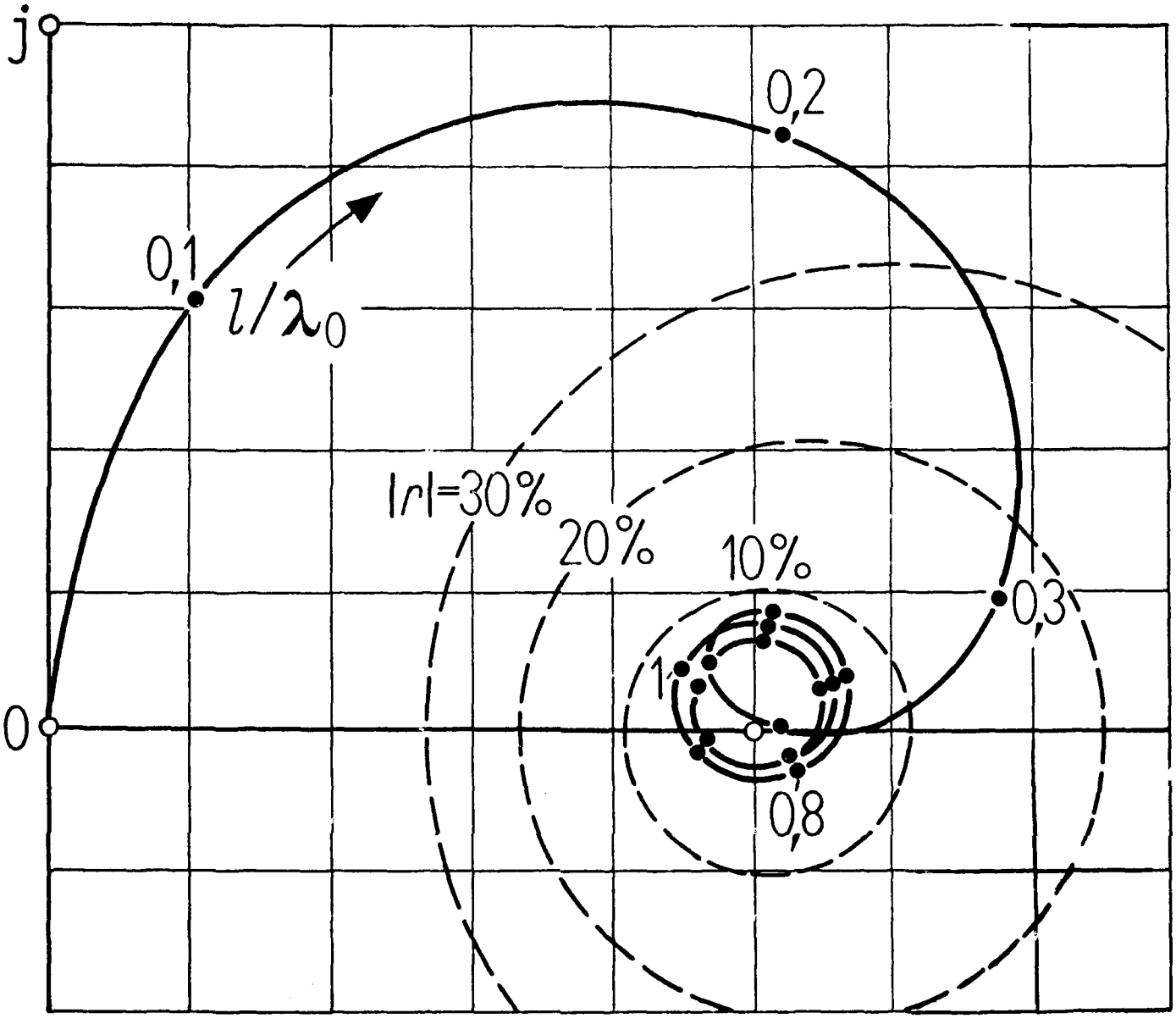

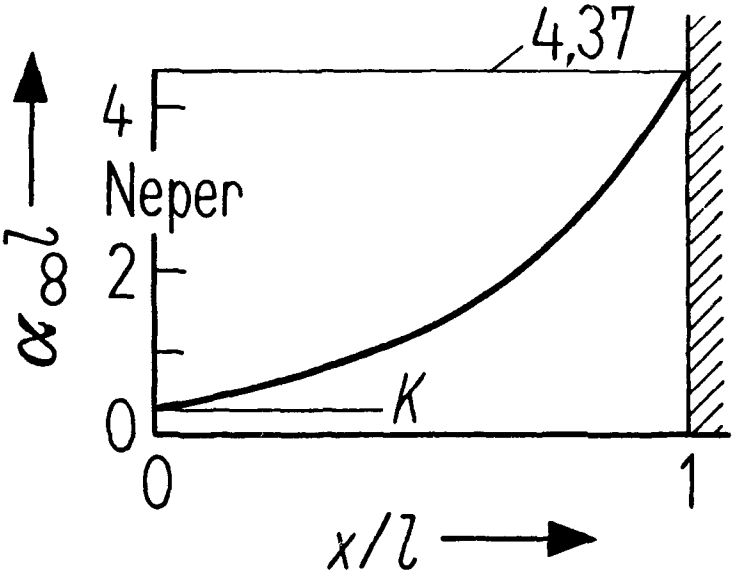

$\alpha(x) = K e^{cx/l}$

K = 0.285N

c = 2.

α_0 = 1.5N

Fig. 2.4

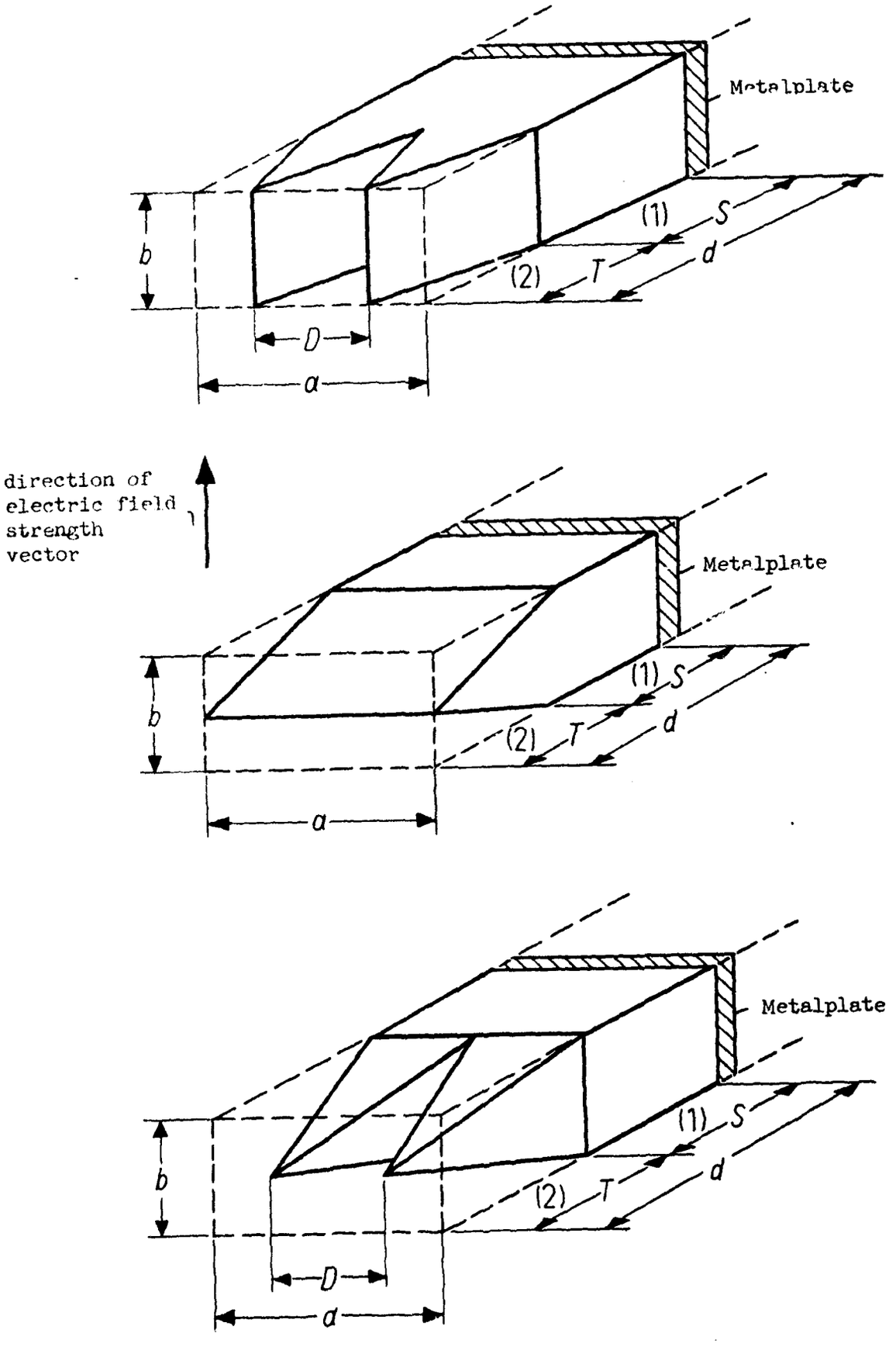
Metalplate
b
(1)
S
d
(2)
T
D
a
direction of
electric field
strength
vector
Metalplate
b
(1)
S
d
(2)
T
a
Metalplate
b
(1)
S
d
(2)
T
D
a

Fig. 2.5

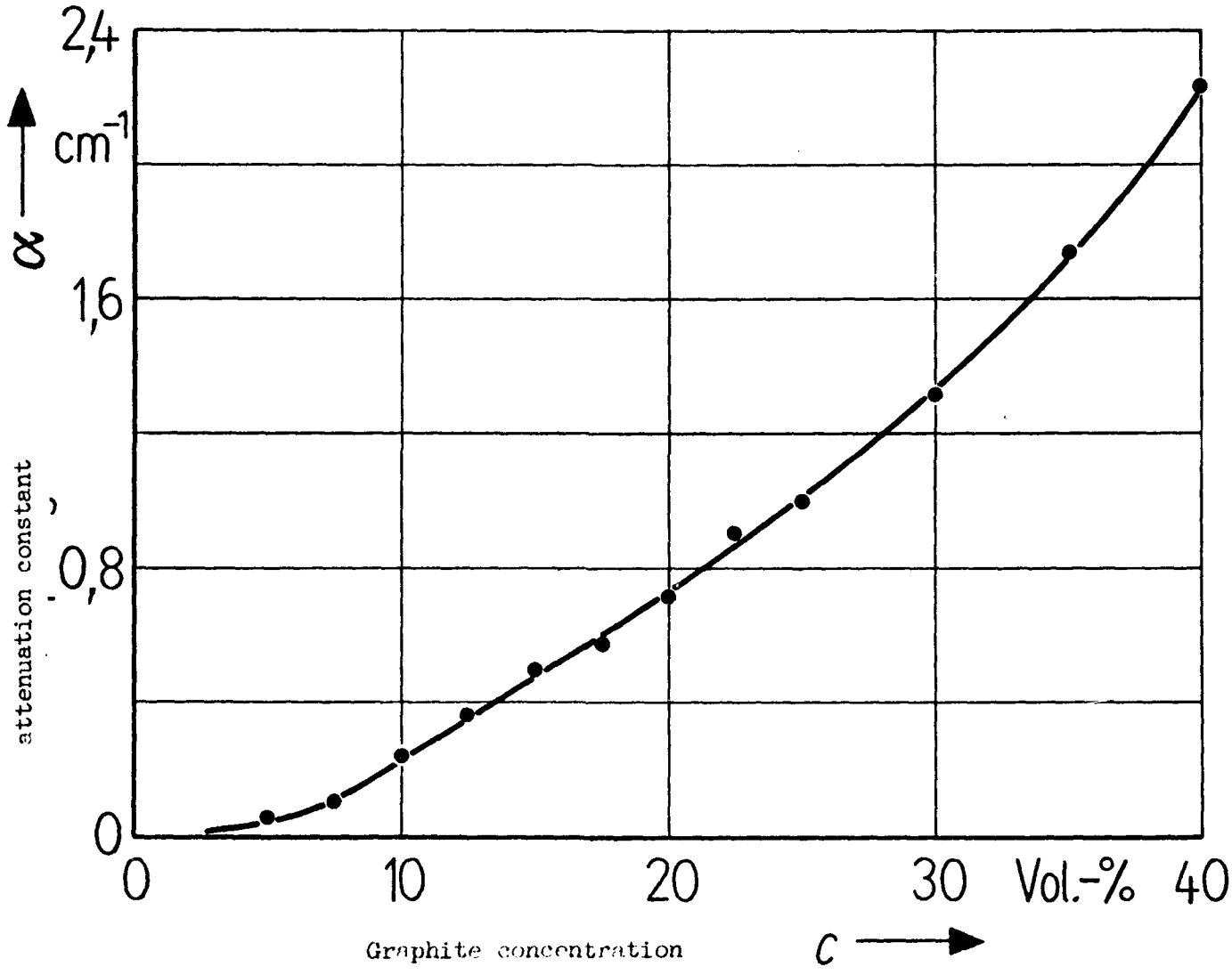
2,4
cm⁻¹
α
1,6
0,8
0
attenuation constant
0
10
20
30
Vol.-%
40
Graphite concentration
C

Fig. 2.6

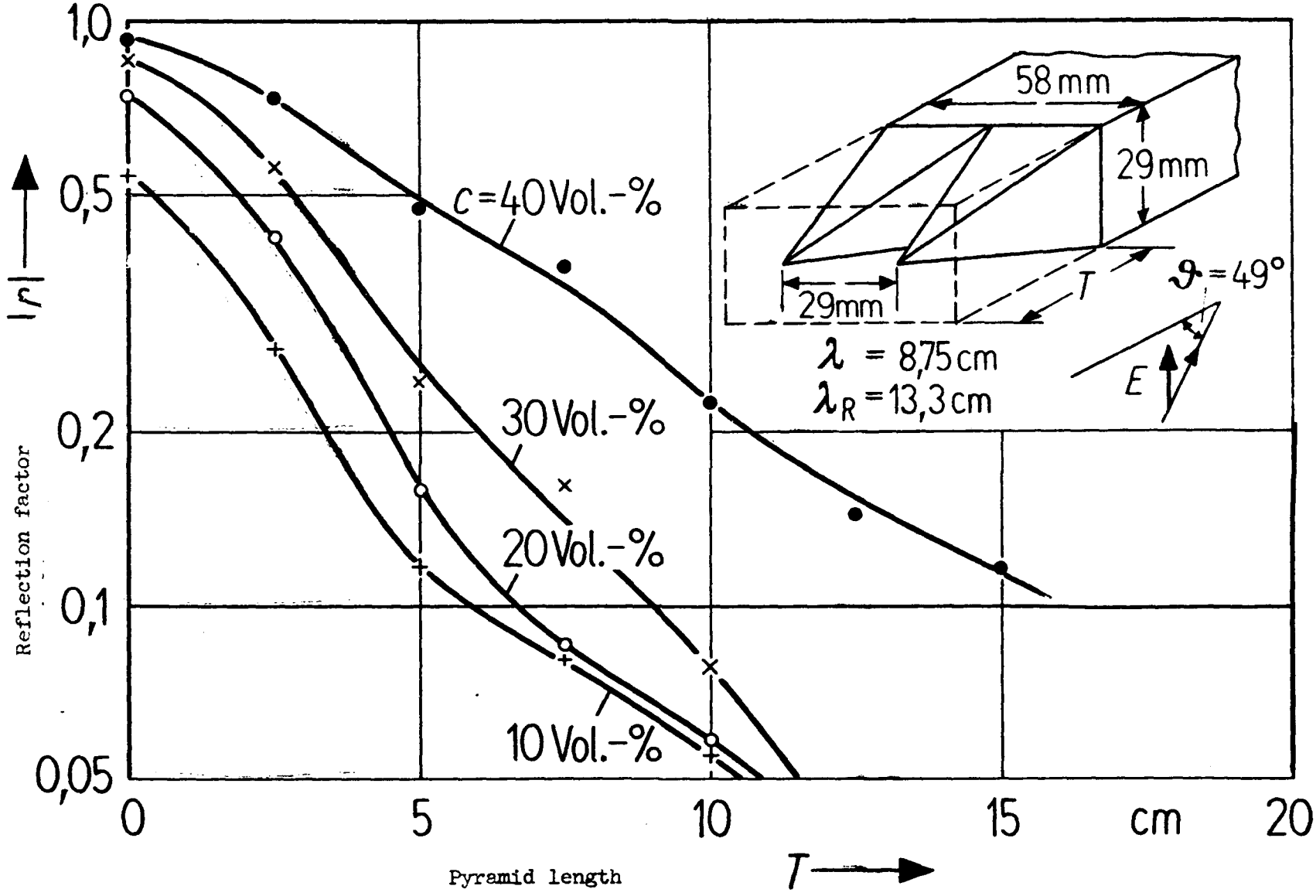
1,0
0,5
0,2
0,1
0,05
|r|
Reflection factor
c=40 Vol.-%
30 Vol.-%
20 Vol.-%
10 Vol.-%
58 mm
29 mm
29mm
T
ϑ=49°
λ = 8,75 cm
λR=13,3 cm
E
0
5
10
15
cm
20
Pyramid length
T

Fig. 2.7

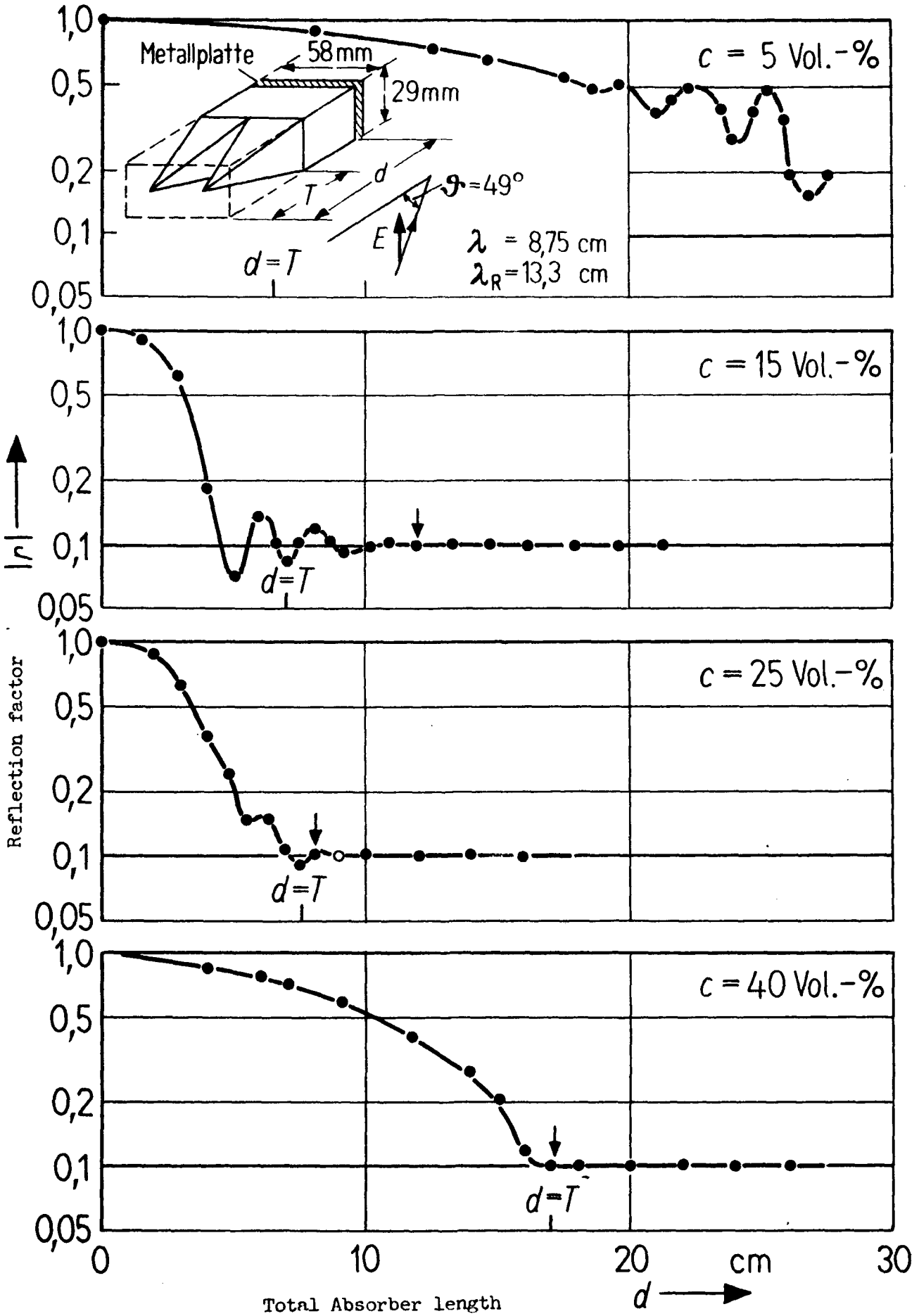
Metallplatte
58mm
29mm
d
T
ϑ=49°
E
λ = 8,75 cm
λR=13,3 cm
d=T
c = 5 Vol.-%
c = 15 Vol.-%
c = 25 Vol.-%
c = 40 Vol.-%
|r|
Reflection factor
1,0
0,5
0,2
0,1
0,05
0
10
20
cm
30
d
Total Absorber length

Fig. 2.8

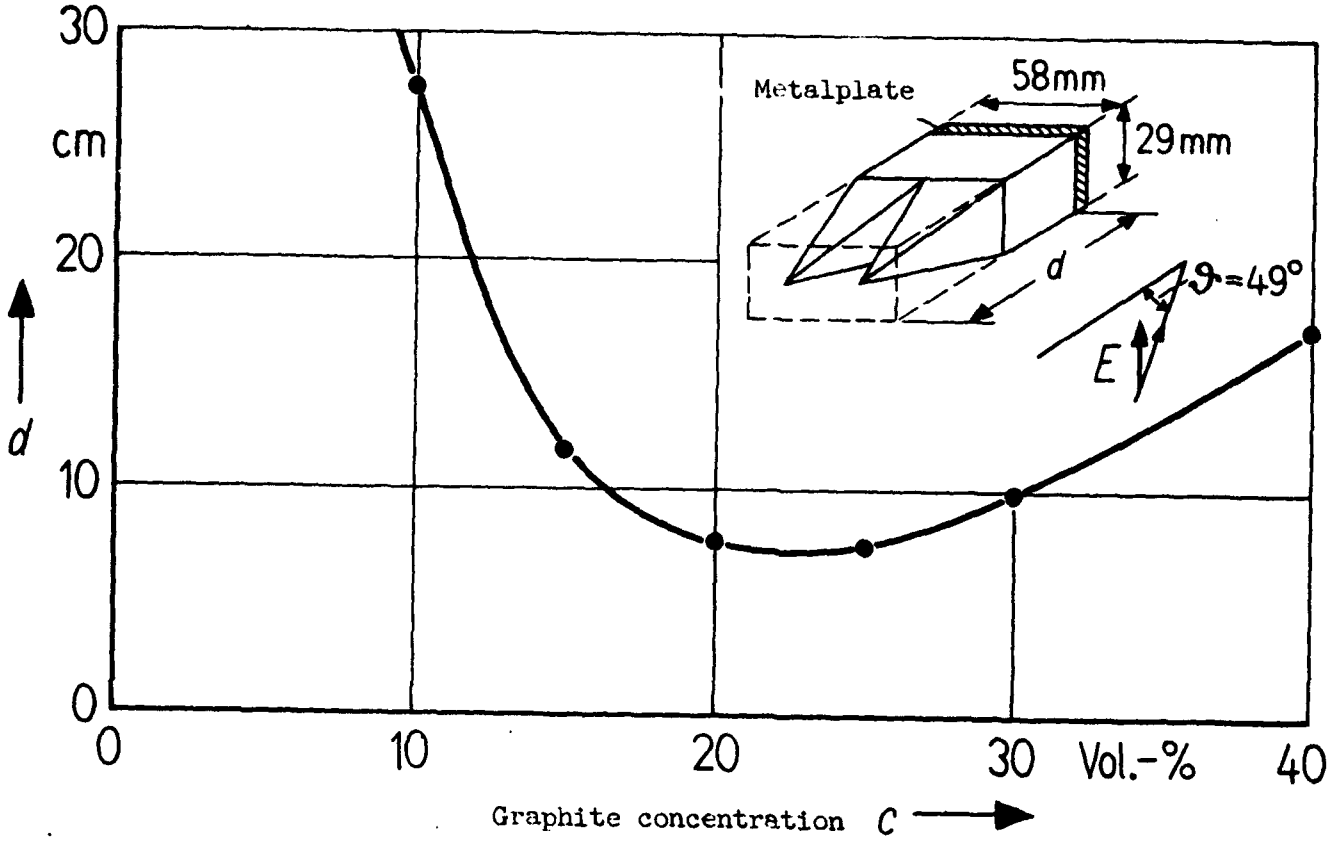

Fig. 2.9

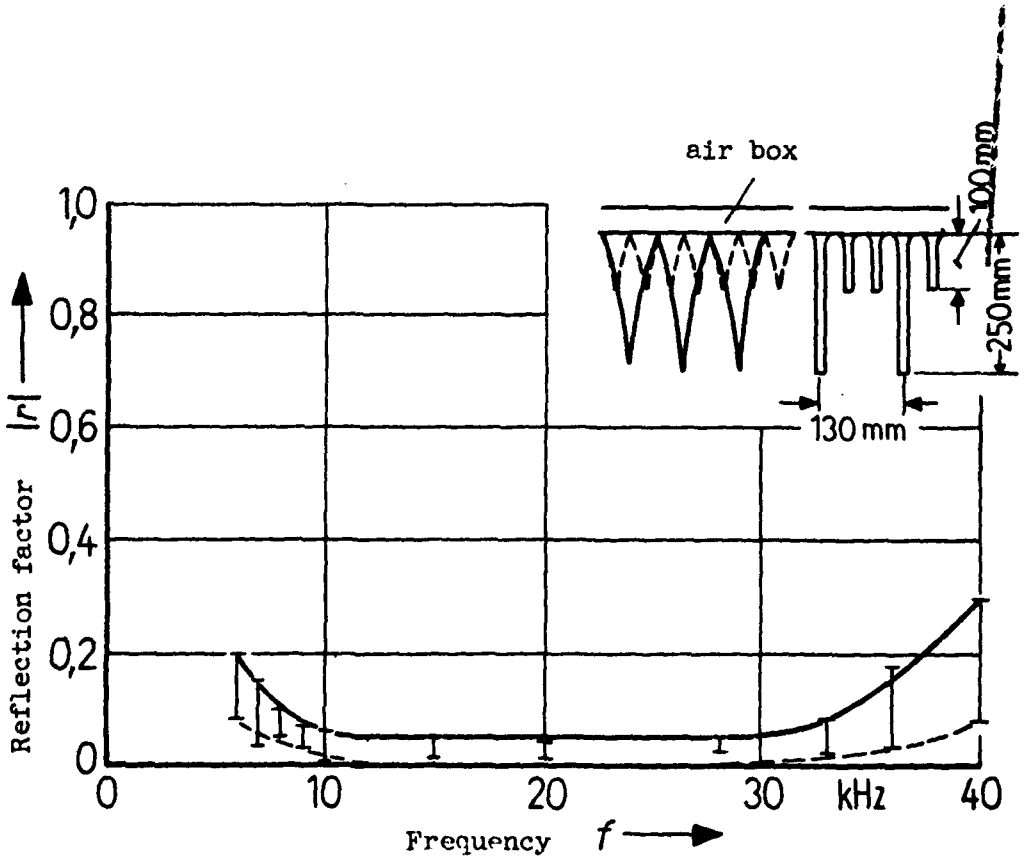

Fig. 2.10

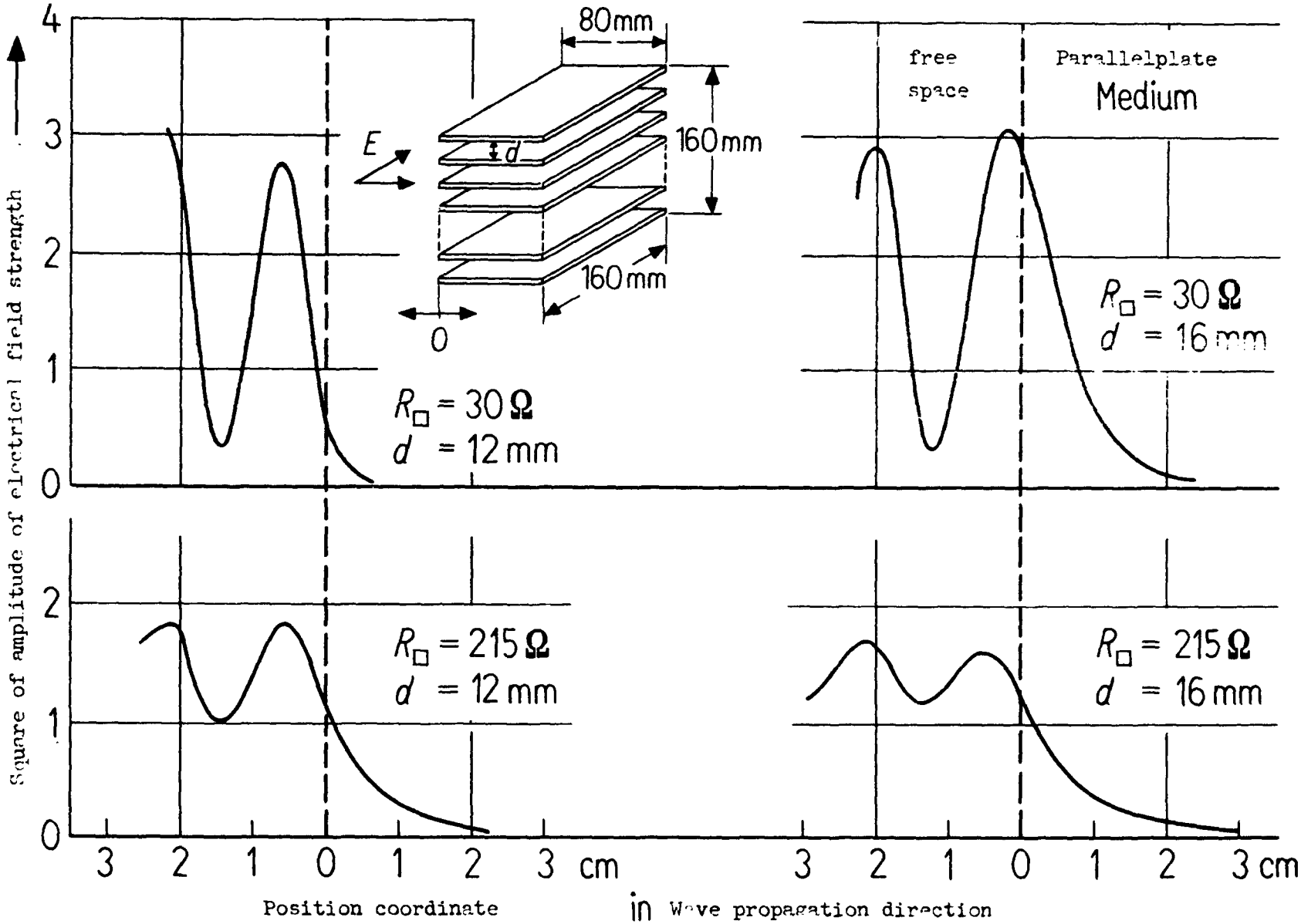
80mm
160mm
160mm
E
d
0
free
space
Parallelplate
Medium
$R_\square = 30\,\Omega$
$d = 12$ mm
$R_\square = 30\,\Omega$
$d = 16$ mm
$R_\square = 215\,\Omega$
$d = 12$ mm
$R_\square = 215\,\Omega$
$d = 16$ mm
Square of amplitude of electrical field strength
4
3
2
1
0
3 2 1 0 1 2 3 cm
3 2 1 0 1 2 3 cm
Position coordinate in Wave propagation direction

Fig. 2.11

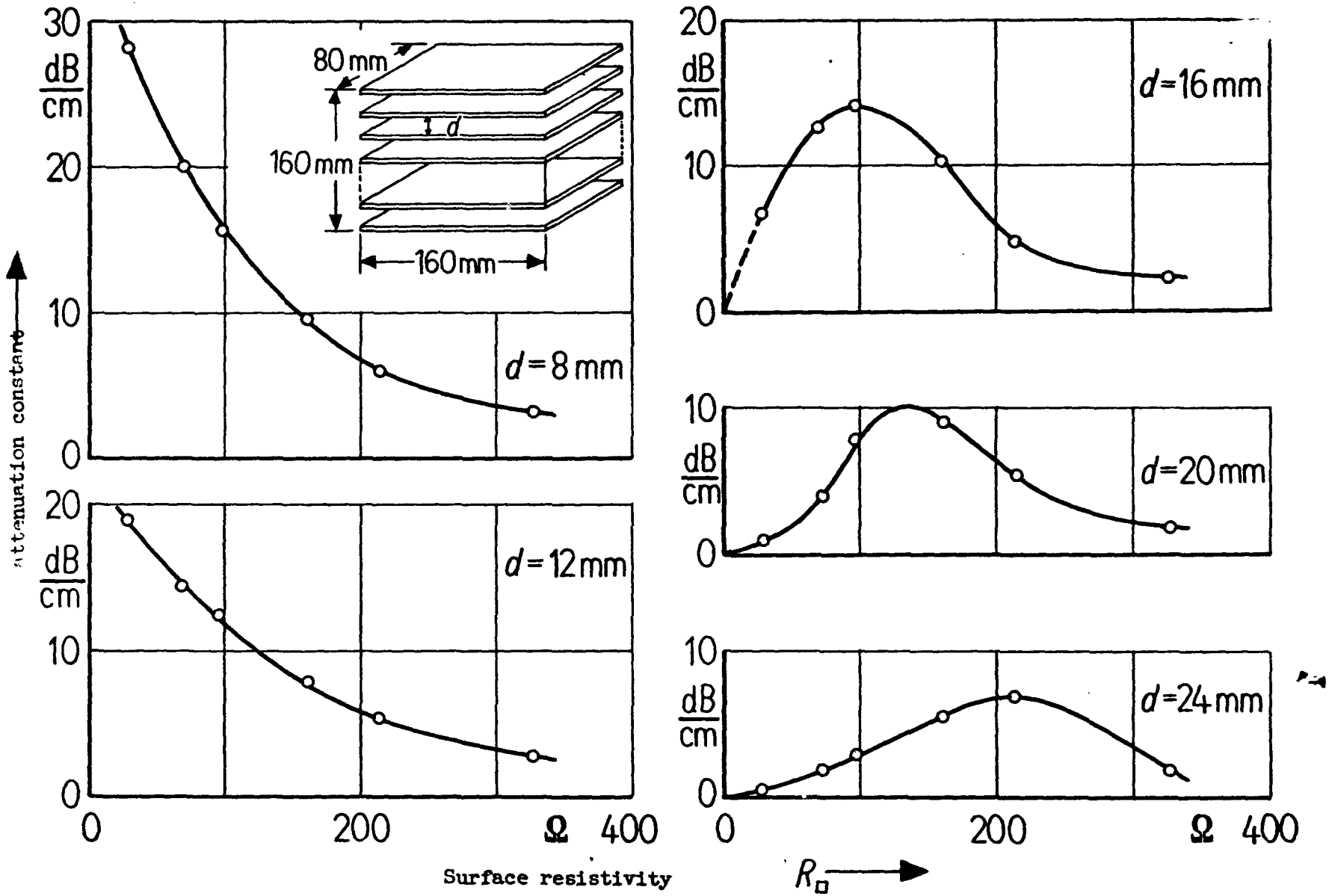
30
dB/cm
20
10
0
80 mm
d
160 mm
160 mm
d=8 mm
20
dB/cm
10
0
d=12 mm
0
200
Ω
400
Surface resistivity
attenuation constant
20
dB/cm
10
0
d=16 mm
10
dB/cm
0
d=20 mm
10
dB/cm
0
d=24 mm
0
200
Ω
400
R□

Fig. 2.12

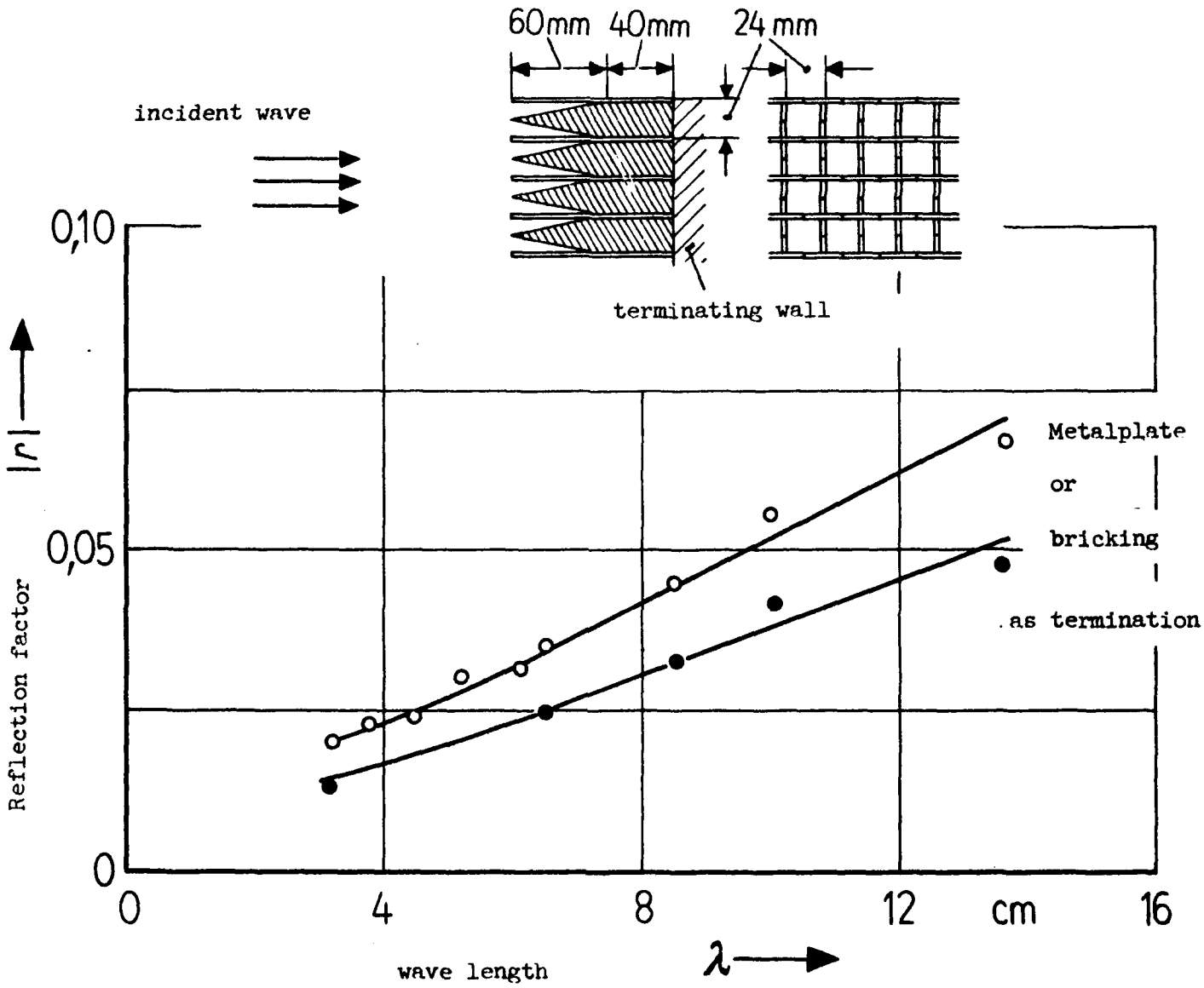
60mm
40mm
24 mm
incident wave
terminating wall
0,10
0,05
0
|r|
Reflection factor
Metalplate
or
bricking
as termination
0
4
8
12
cm
16
λ
wave length

Fig. 2.13

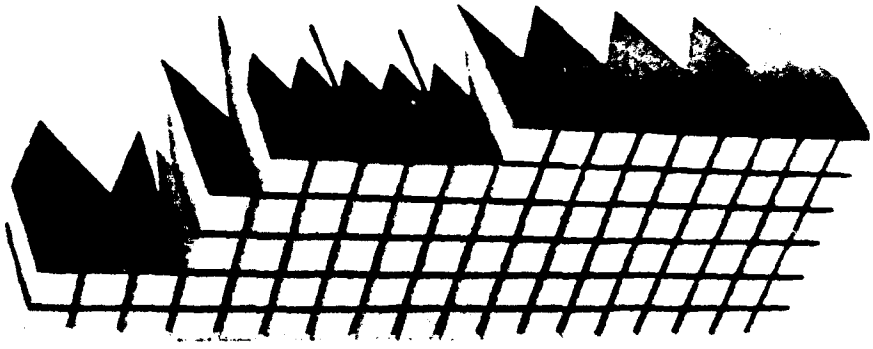

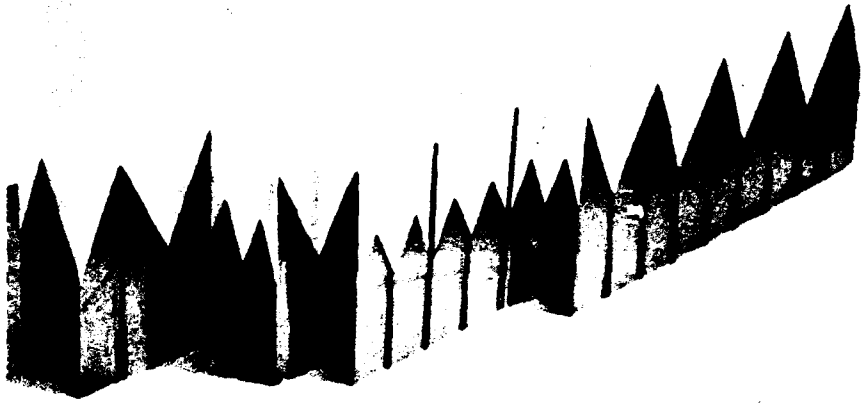

Fig. 2.14

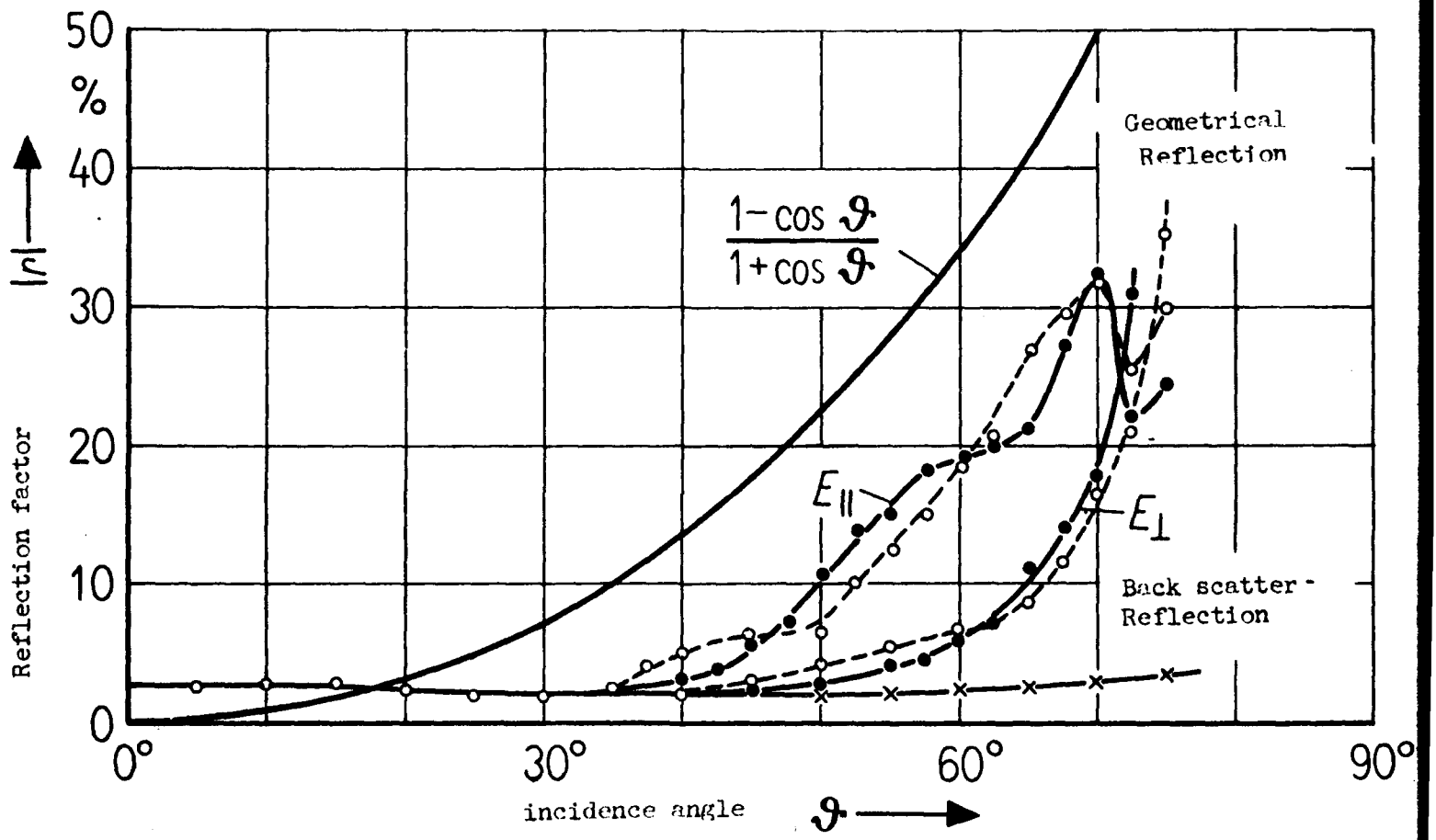
50
%
40
30
20
10
0
|r|
Reflection factor
0°
30°
60°
90°
incidence angle
ϑ
1−cos ϑ / 1+cos ϑ
Geometrical Reflection
E∥
E⊥
Back scatter-Reflection

Fig. 2.15

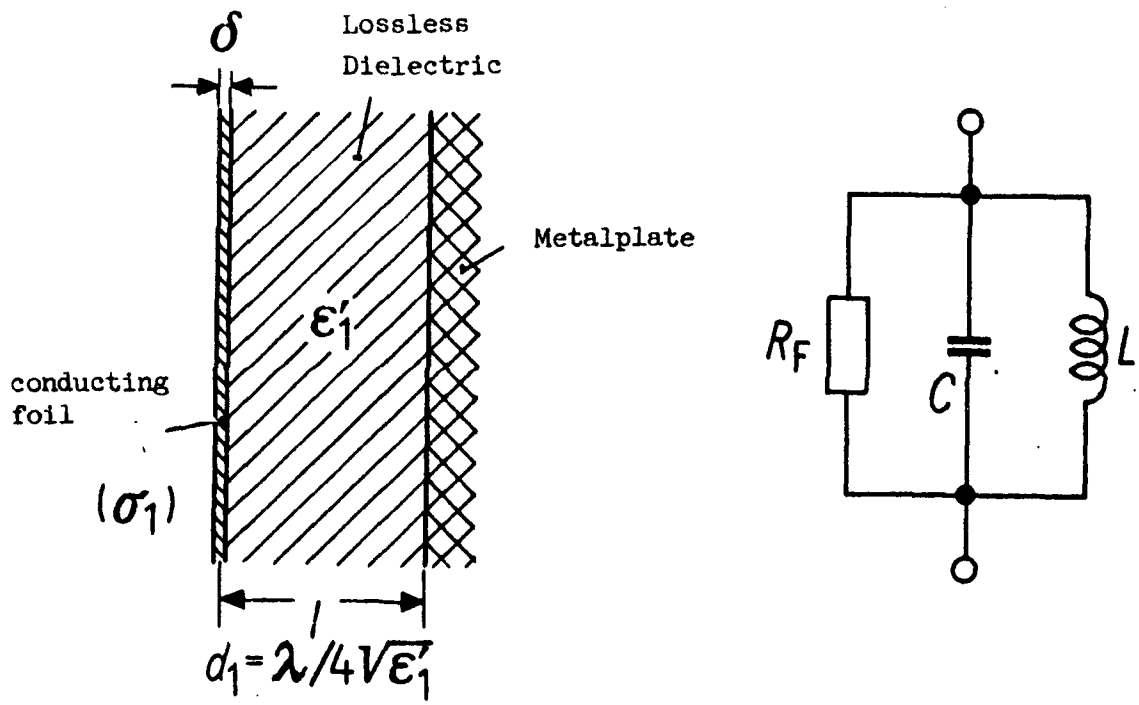
δ
Lossless
Dielectric
Metalplate
ε'1
conducting
foil
(σ1)
l
d1 = λ/4√ε'1
RF
C
L

Fig. 3.1

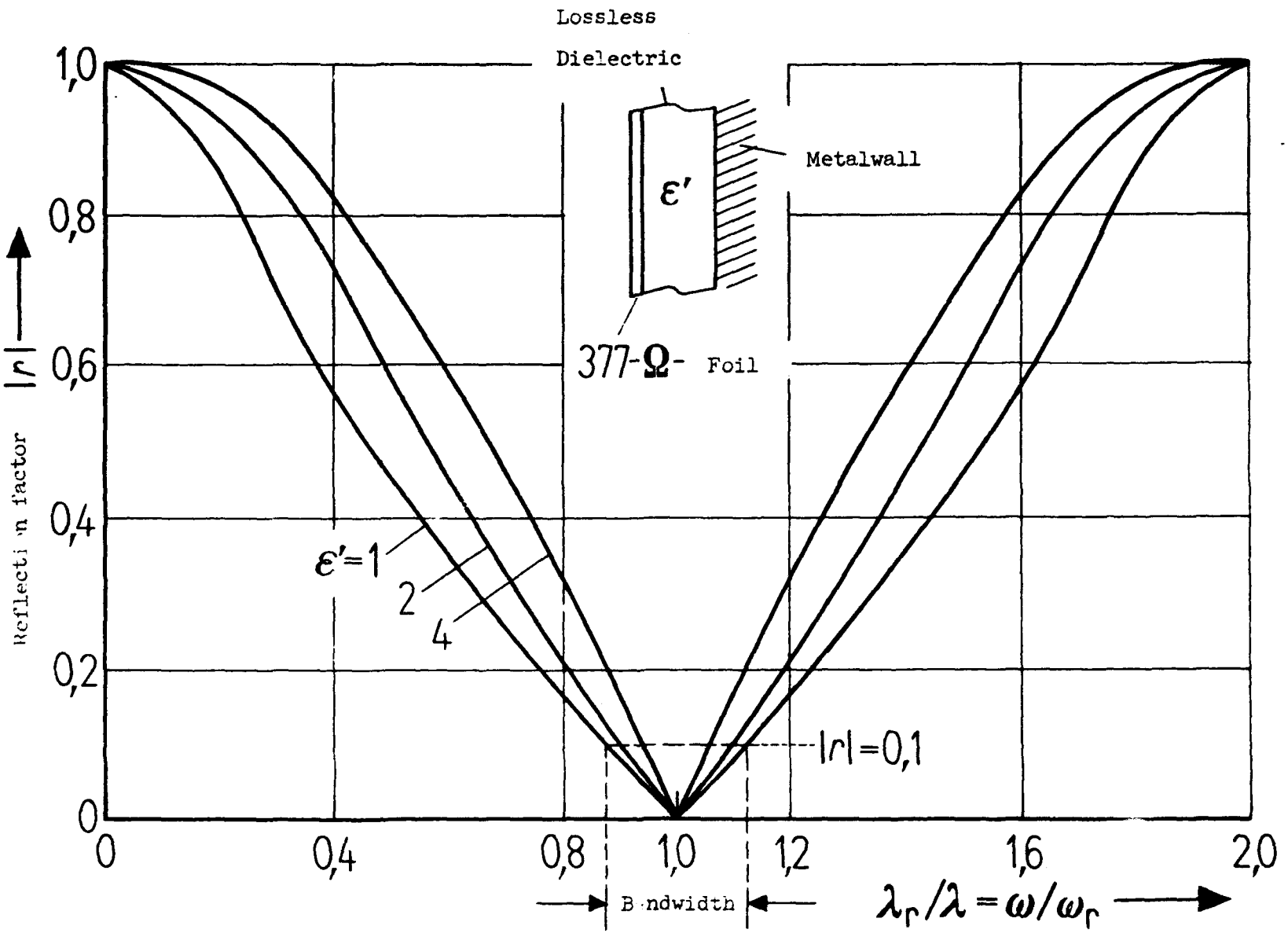
Lossless
Dielectric
Metalwall
ε'
377-Ω- Foil
Reflection factor |r|
1,0
0,8
0,6
0,4
0,2
0
ε'=1
2
4
|r|=0,1
0
0,4
0,8
1,0
1,2
1,6
2,0
Bandwidth
λr/λ = ω/ωr

Fig. 3.2

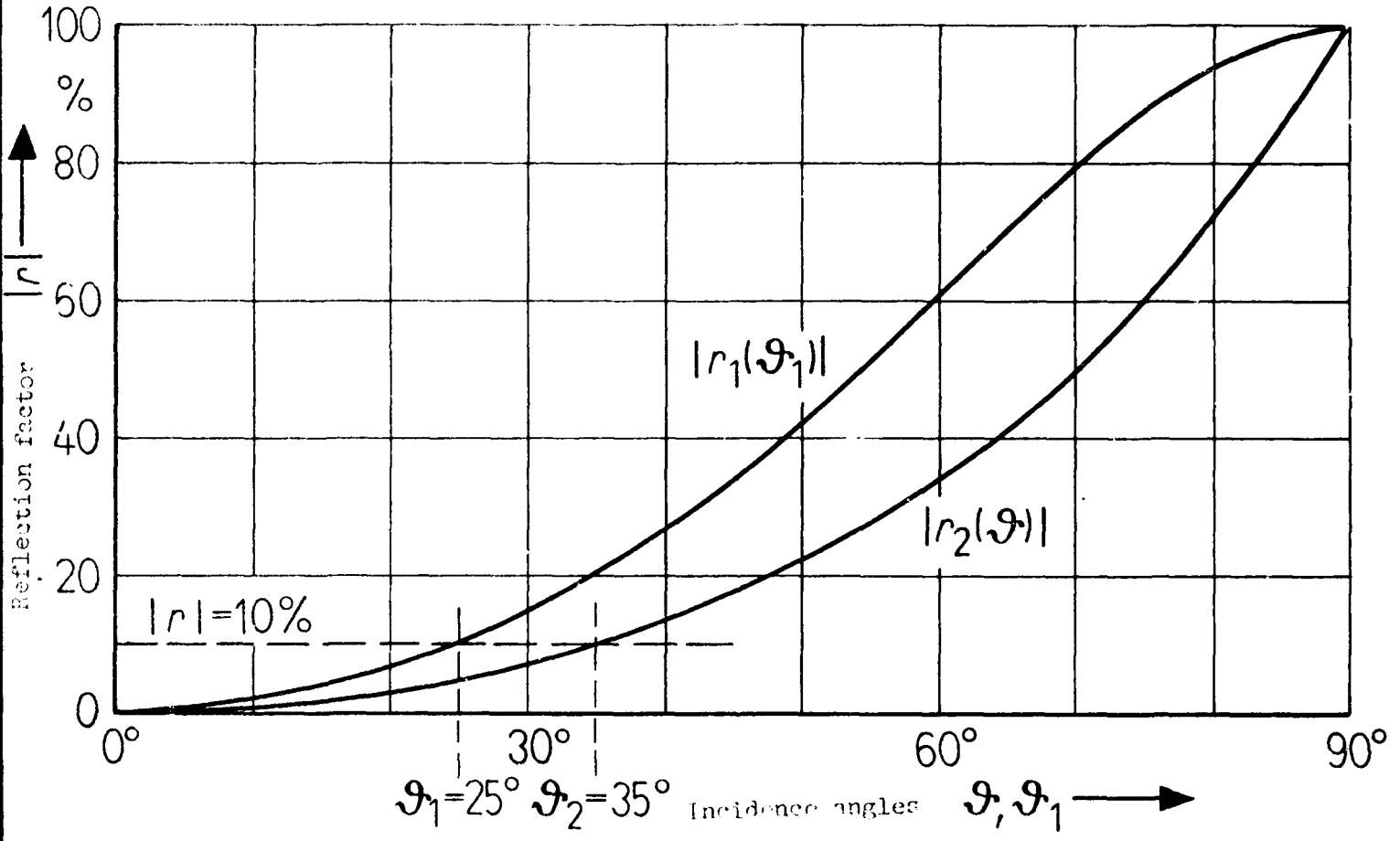
100
%
80
60
40
20
0
Reflection factor |r|
|r1(ϑ1)|
|r2(ϑ)|
|r|=10%
0°
30°
60°
90°
ϑ1=25° ϑ2=35°
Incidence angles
ϑ, ϑ1

Fig. 3.3

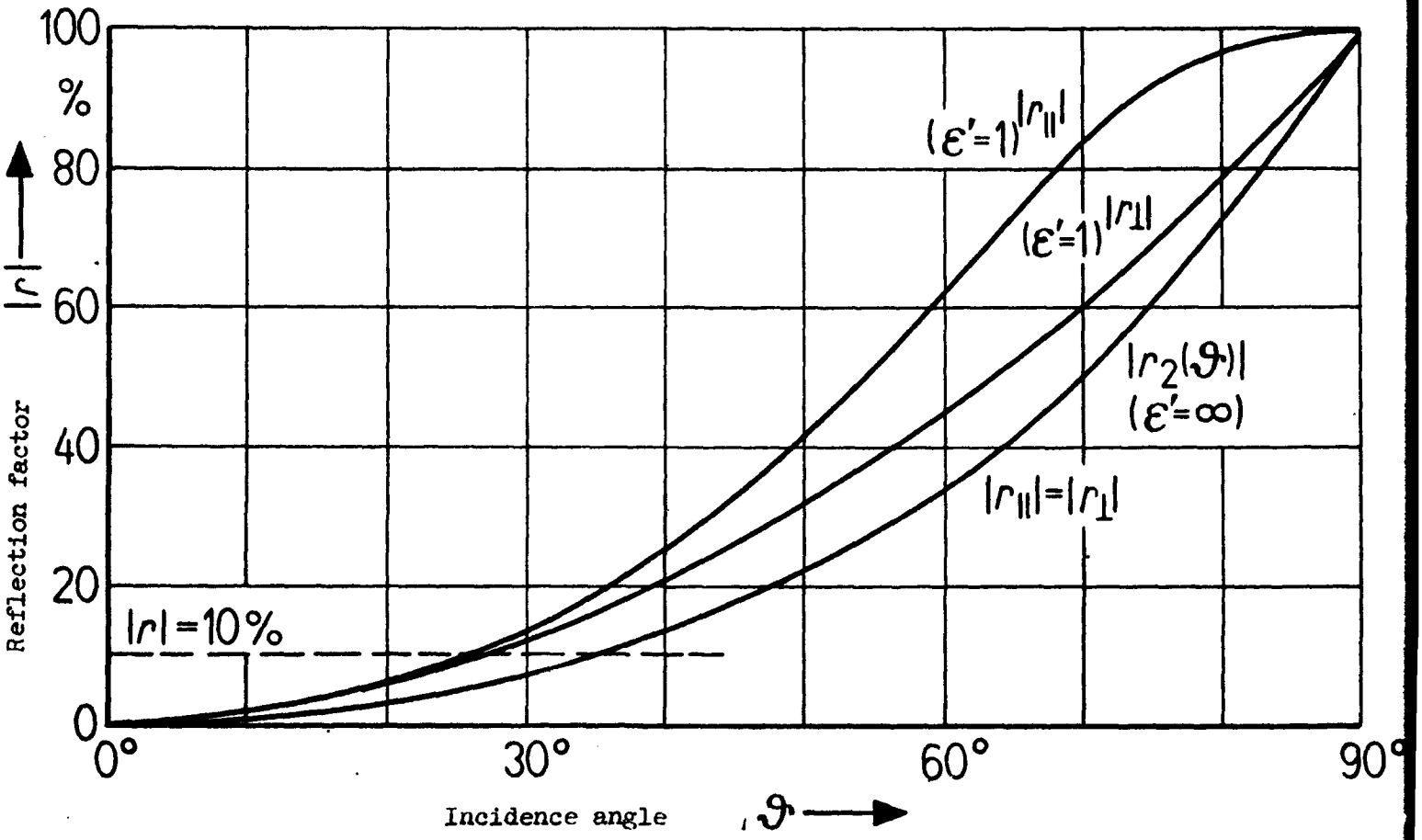
100
%
80
60
40
20
0
|r|
Reflection factor
|r|=10%
(ε'=1) |r∥|
(ε'=1) |r⊥|
|r2(ϑ)|
(ε'=∞)
|r∥|=|r⊥|
0°
30°
60°
90°
Incidence angle ϑ

Fig. 3.4

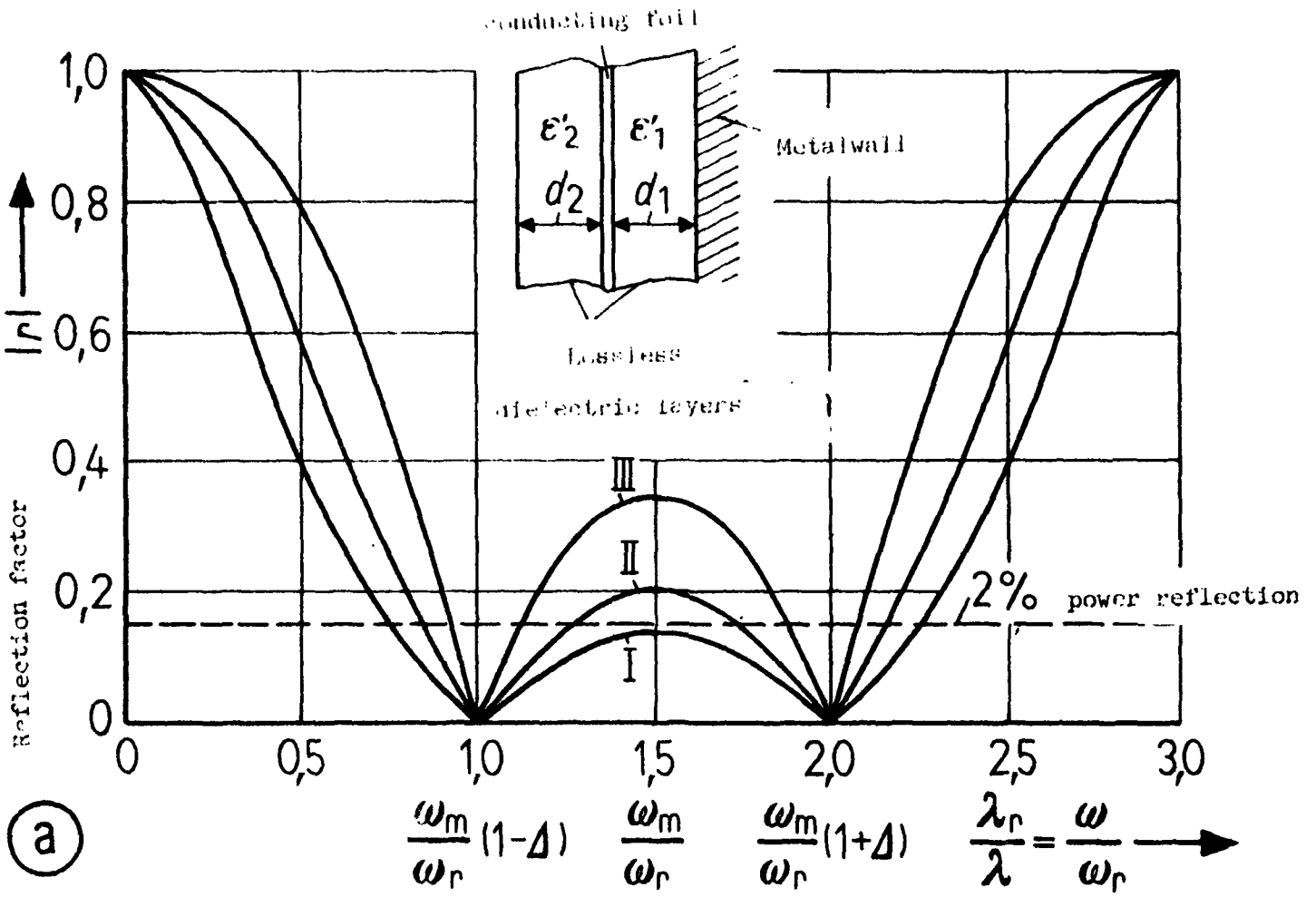

	ε'_2	ε'_1	d_1/λ_r	d_2/λ_r	d_{tot}/λ_r	Z_o/R_F
Curve I	2.14	1	0.169	0.111	0.280	1.68
Curve II	4	4	0.0961	0.0961	0.192	2.00
Curve III	4	11.25	0.0492	0.0742	0.124	2.50

Fig. 3.5a

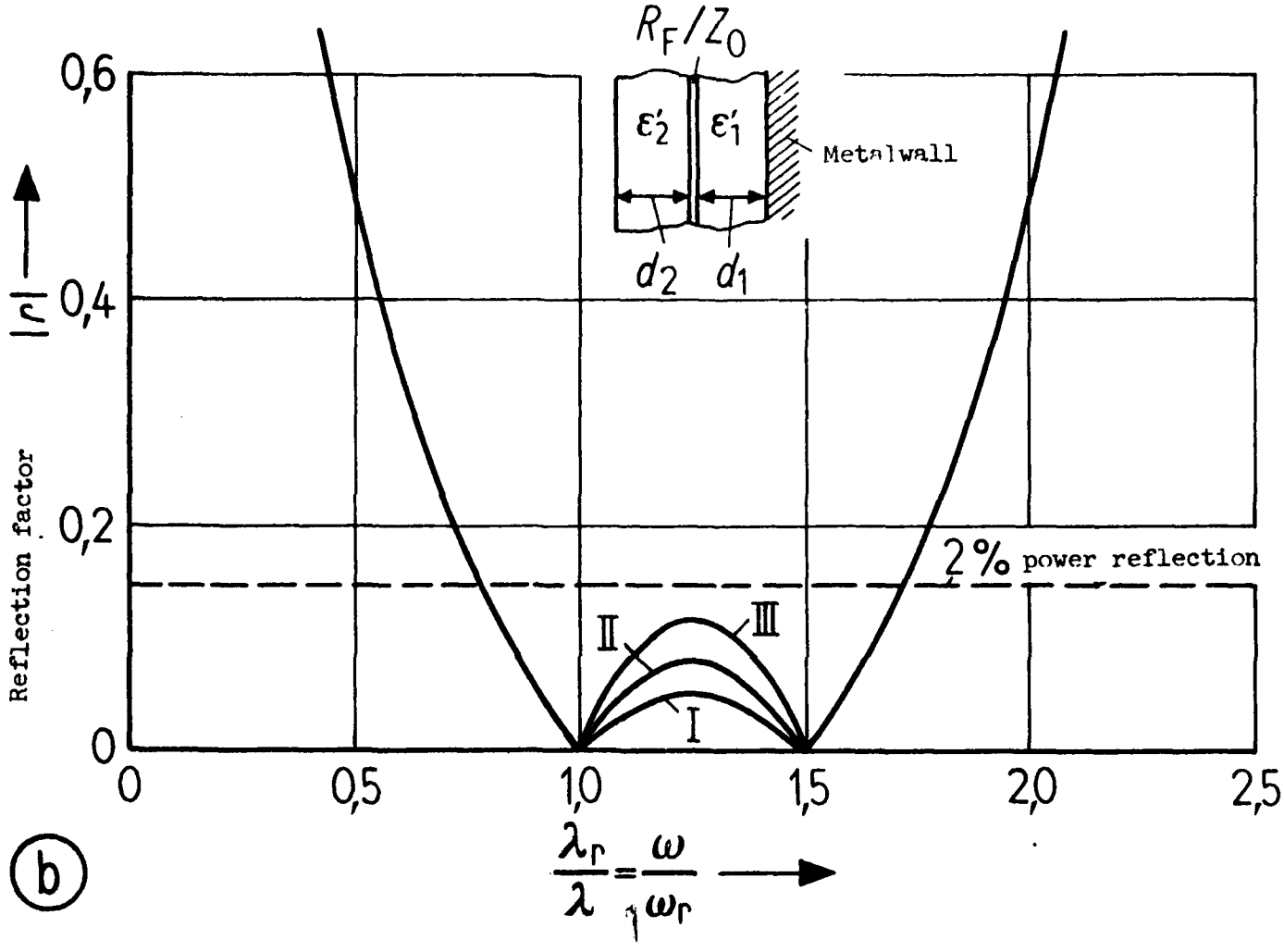

	ε'_2	ε'_1	d_1/λ_r	d_2/λ_r	d_{tot}/λ_r	Z_o/R_F
Curve I	2	2.04	0.14	0.141	0.281	1.83
Curve II	3	6.94	0.076	0.116	0.192	2.52
Curve III	4	12.8	0.0423	0.100	0.1423	3.11

Fig. 3.5b

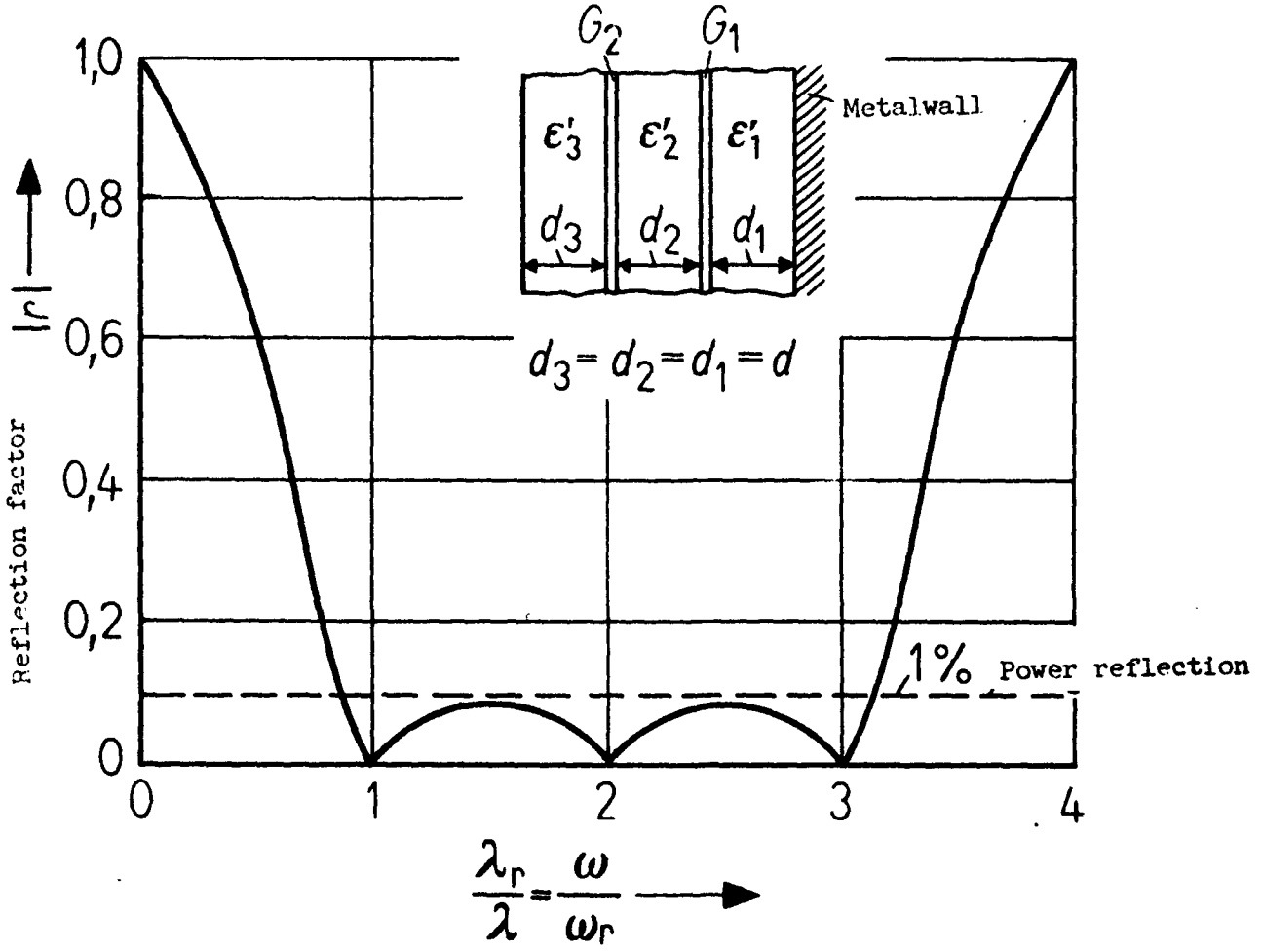

$\varepsilon'_1 = \varepsilon'_2 = \varepsilon'_3$	$G_1 Z_o$	$G_2 Z_o$	d/λ_r	d_{tot}/λ_r
1,76	1.634	0.683	0.0943	0.283

Fig. 3.6

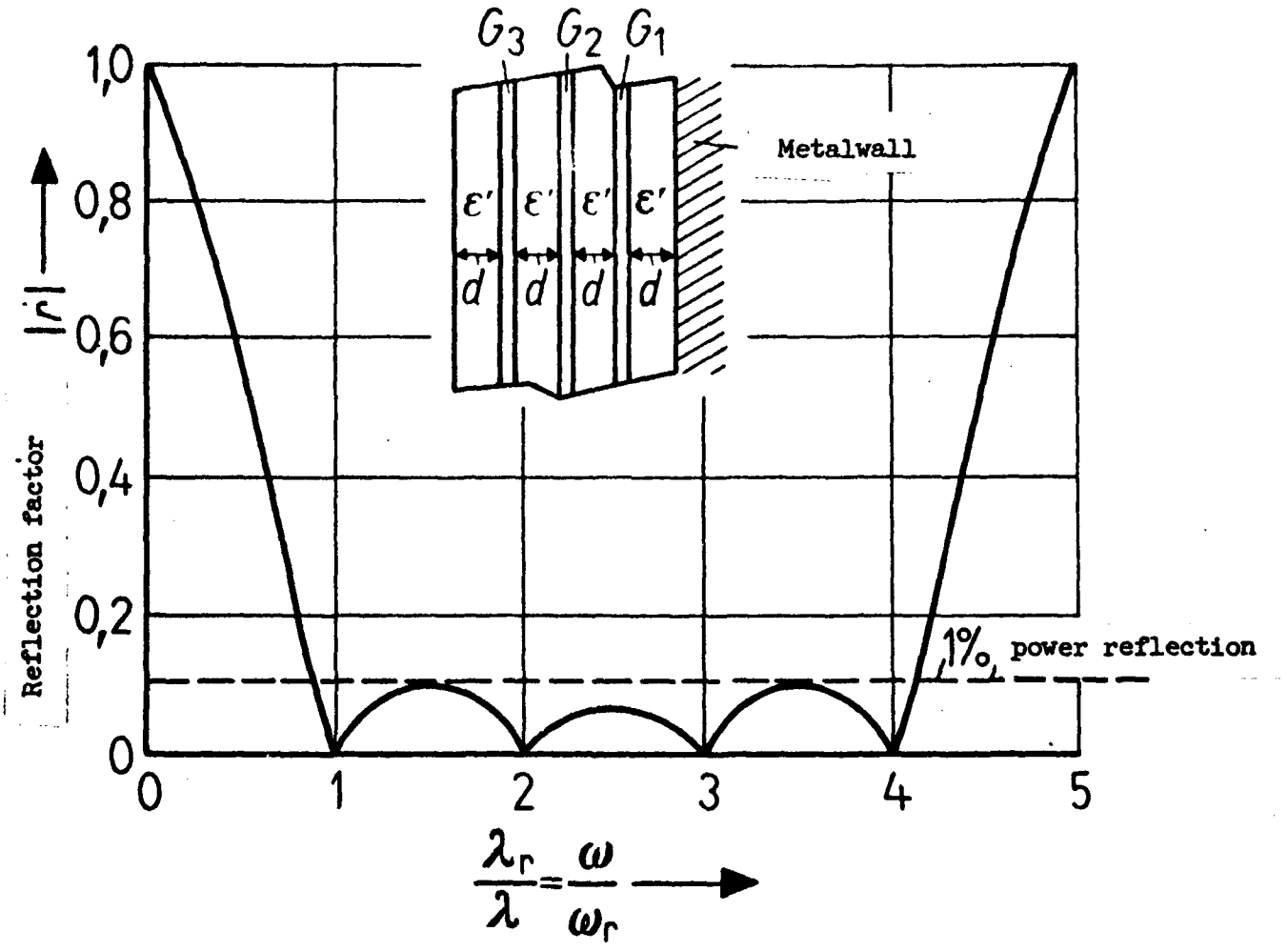

ε'	G_1Z_o	G_2Z_o	G_3Z_o	d/λ_r	d_{tot}/λ_r
1.43	1.534	0.622	0.374	0.0823	0.335

Fig. 3.7

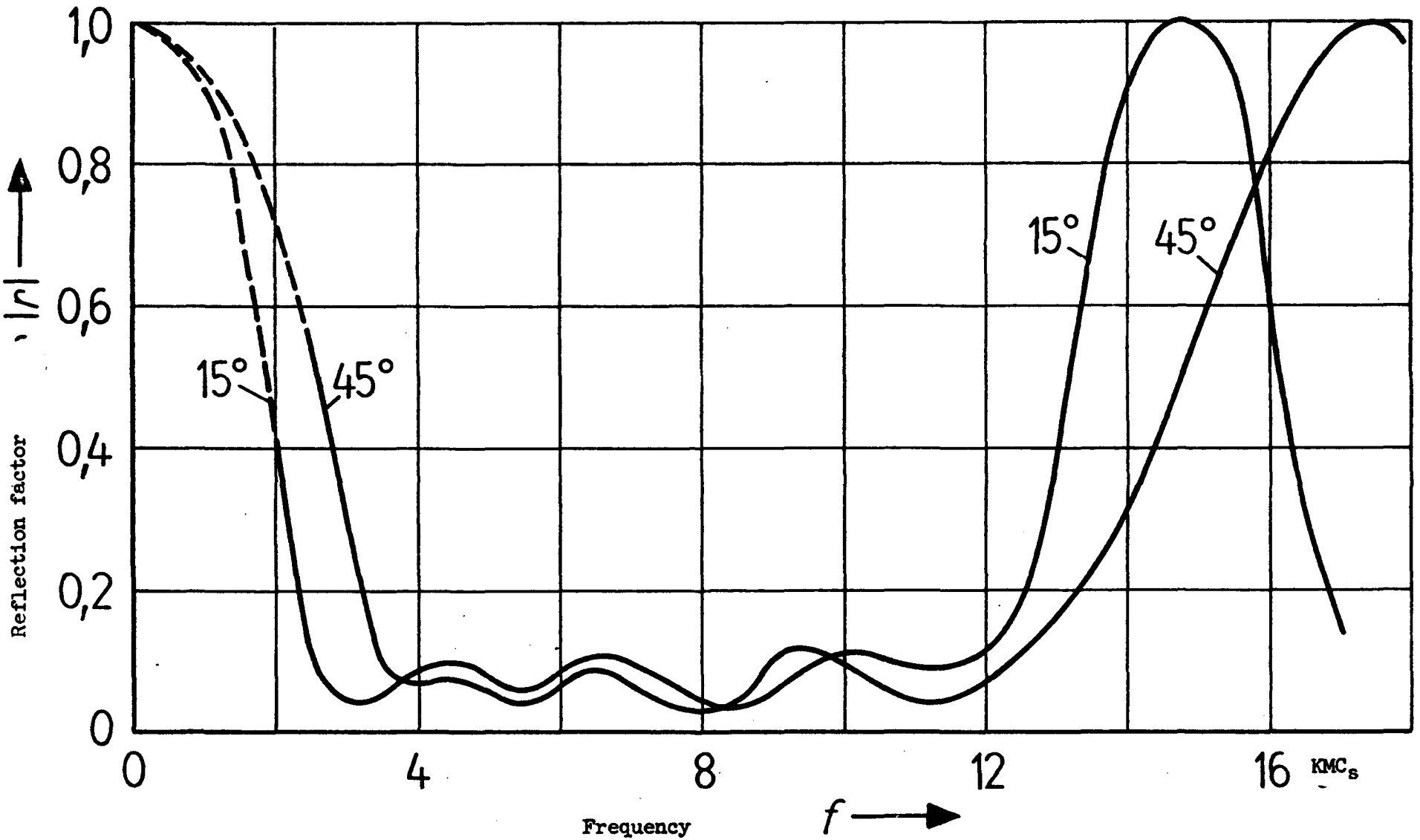
1,0
0,8
0,6
0,4
0,2
0
|r|
Reflection factor
15°
45°
15°
45°
0
4
8
12
16
KMCs
Frequency
f

Fig. 3.8

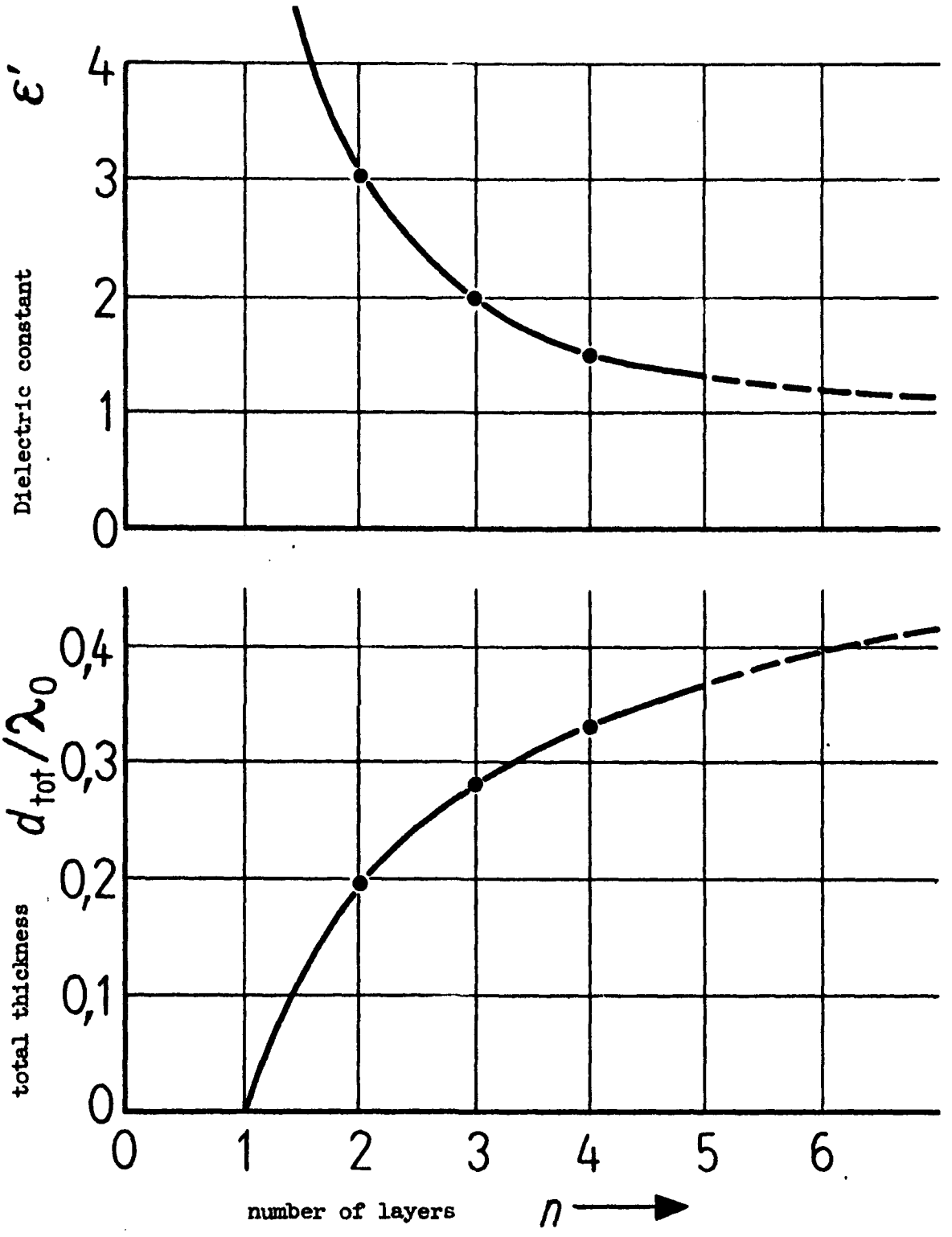
Dielectric constant
ε'
4
3
2
1
0
total thickness
d_{tot}/λ_0
0,4
0,3
0,2
0,1
0
0
1
2
3
4
5
6
number of layers
n

Fig. 3.9

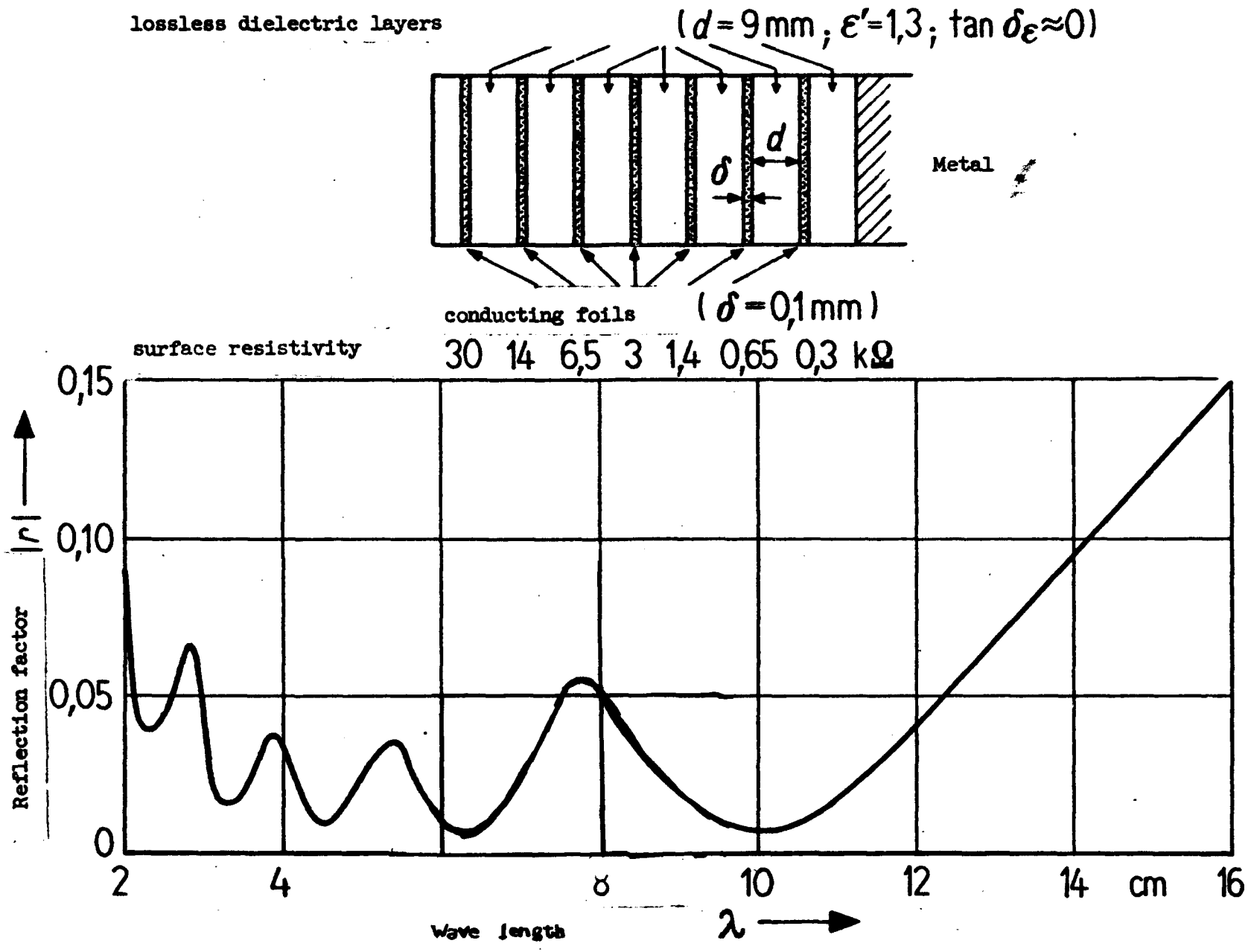
lossless dielectric layers
(d = 9 mm ; ε' = 1,3 ; tan δε ≈ 0)
d
δ
Metal
conducting foils
(δ = 0,1 mm)
surface resistivity
30 14 6,5 3 1,4 0,65 0,3 kΩ
0,15
0,10
0,05
0
|r|
Reflection factor
2
4
8
10
12
14
cm
16
λ
Wave length

Fig. 3.10

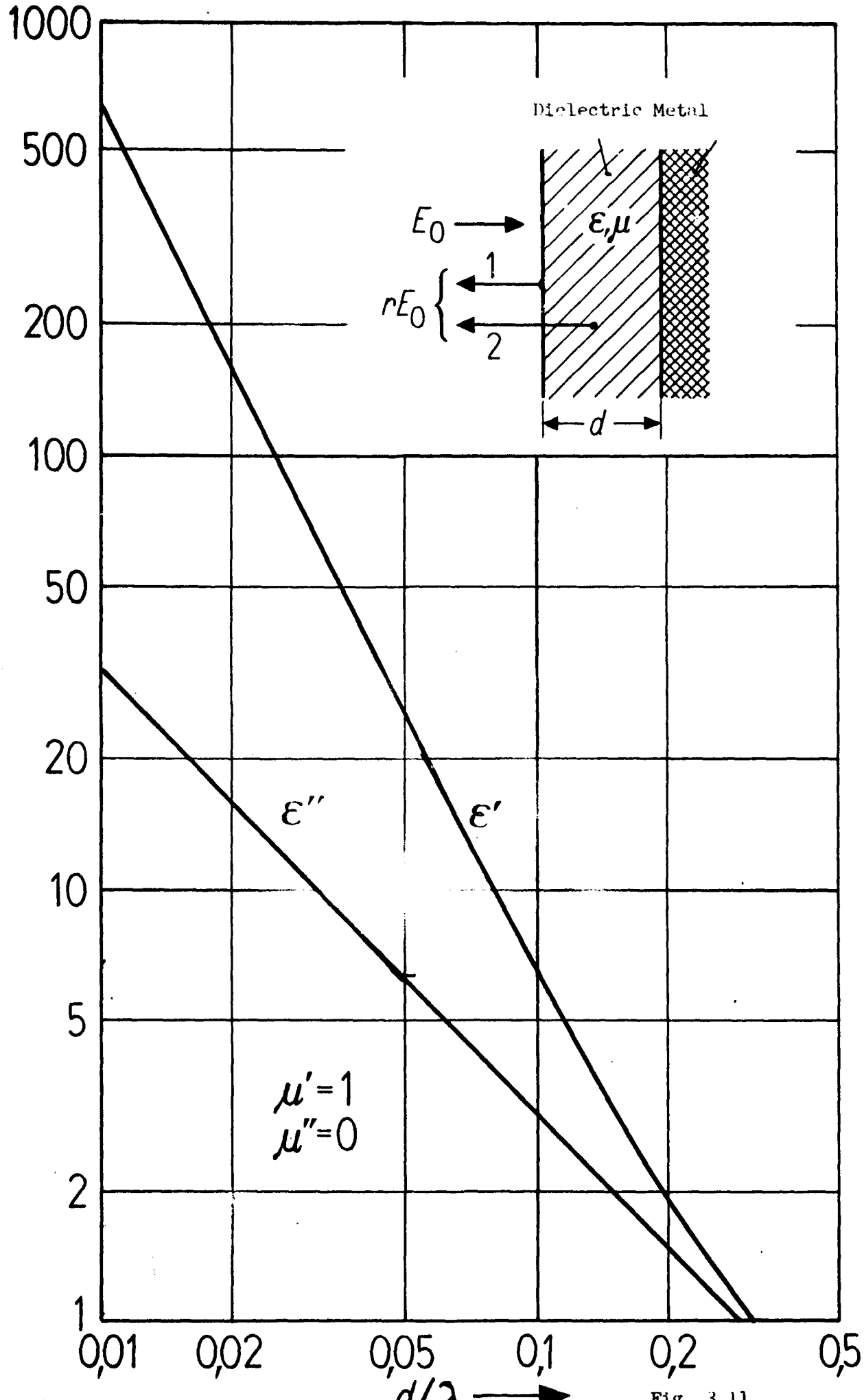
1000
500
200
100
50
20
10
5
2
1
0,01
0,02
0,05
0,1
0,2
0,5
d/λ
Dielectric Metal
E0
ε,μ
1
rE0
2
d
ε''
ε'
μ'=1
μ''=0

Fig. 3.11

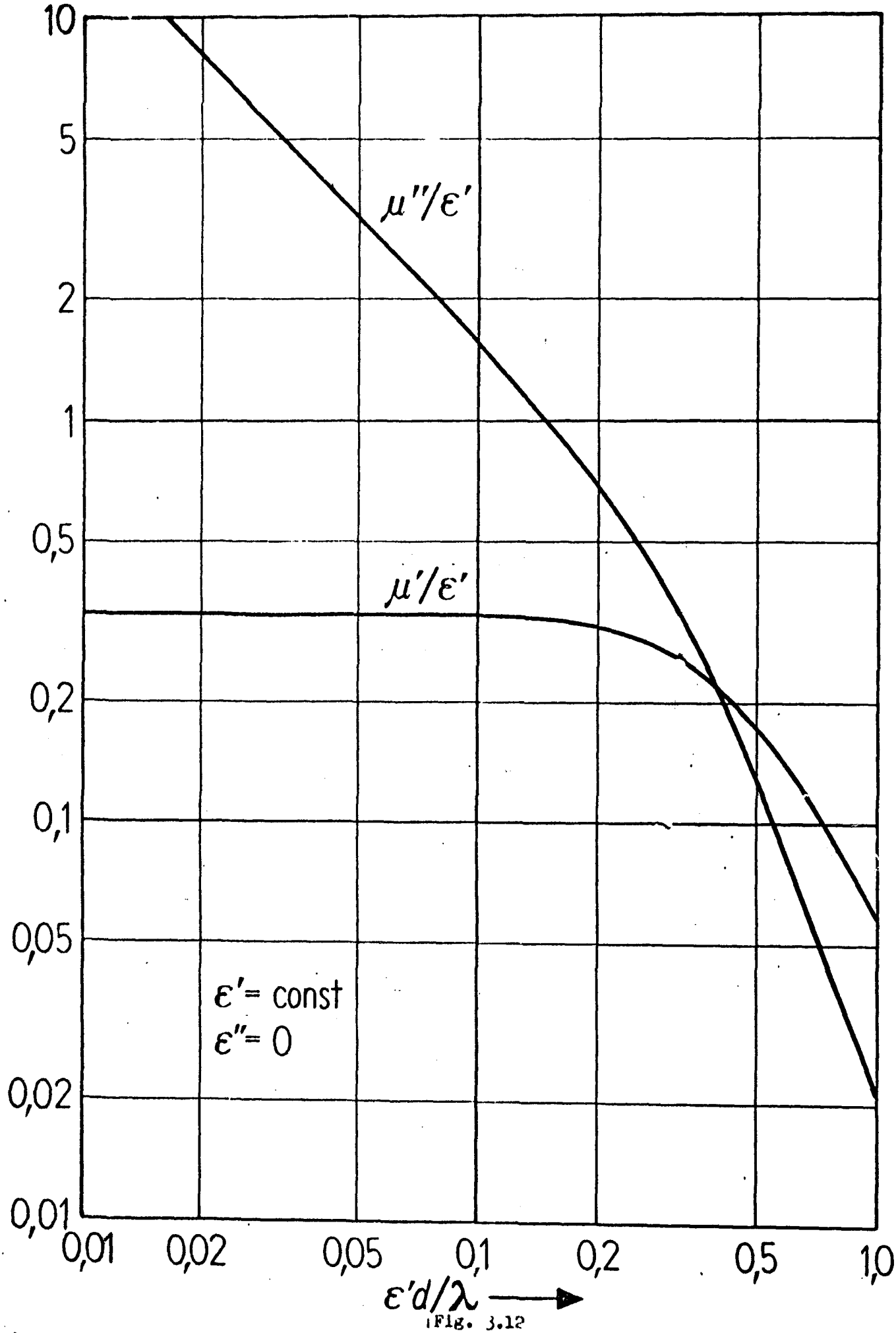
10
5
2
1
0,5
0,2
0,1
0,05
0,02
0,01
μ''/ε'
μ'/ε'
ε'= const
ε''= 0
0,01
0,02
0,05
0,1
0,2
0,5
1,0
ε'd/λ

Fig. 3.12

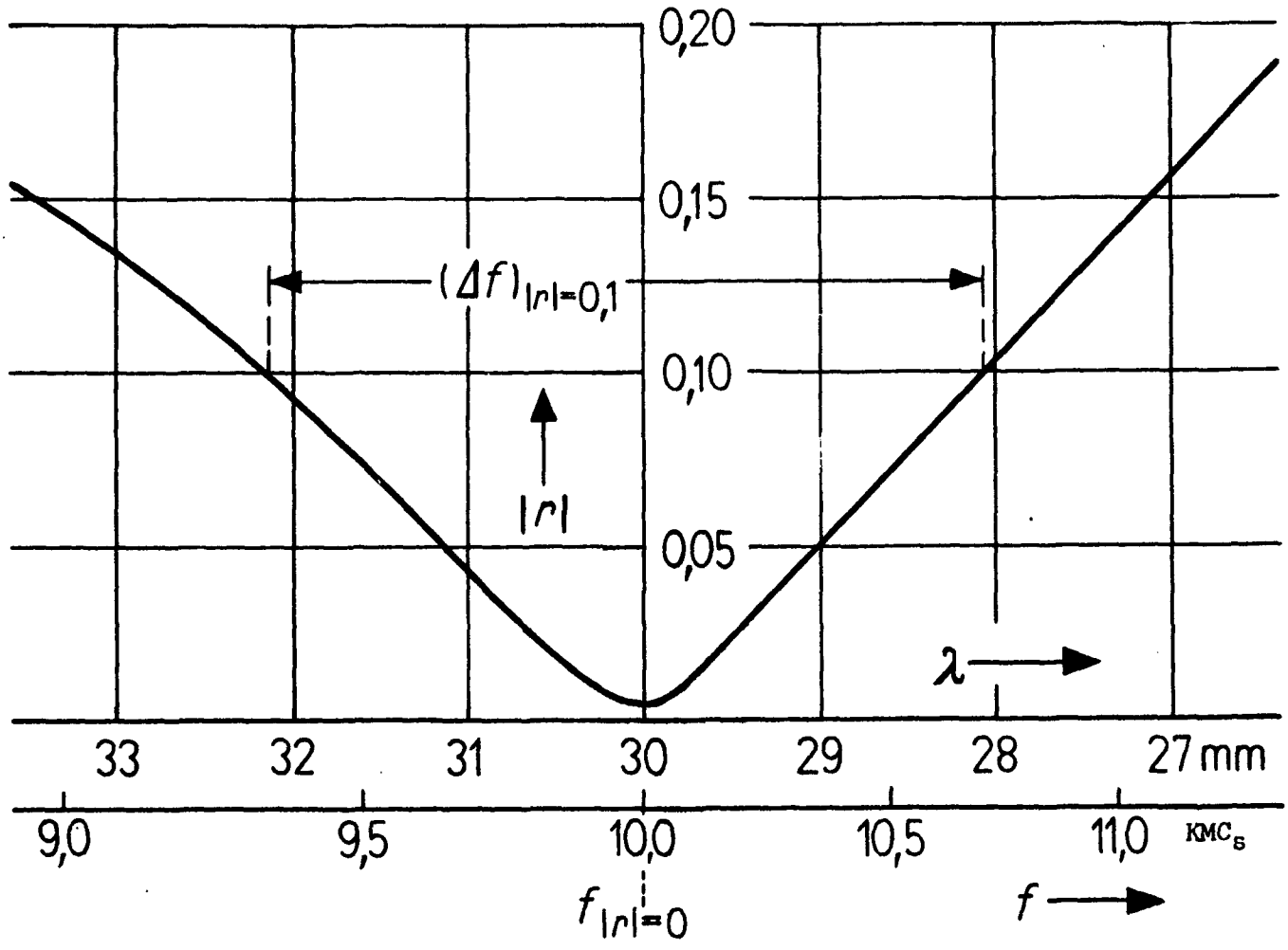
0,20
0,15
0,10
0,05
$(\Delta f)_{|r|=0,1}$
$|r|$
λ
33
32
31
30
29
28
27 mm
9,0
9,5
10,0
10,5
11,0
KMC$_S$
$f_{|r|=0}$
f

Fig. 3.13

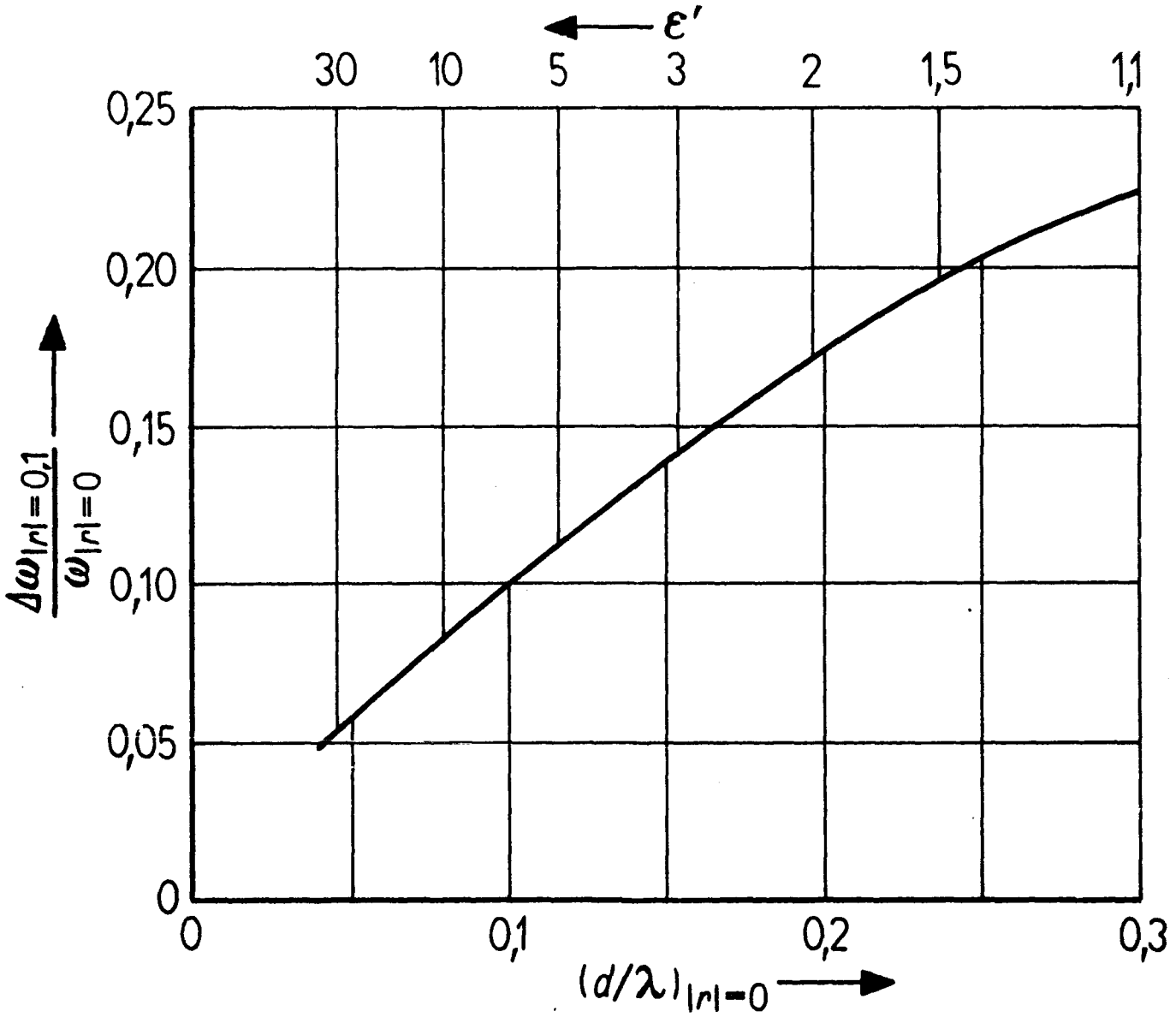

Fig. 3.14

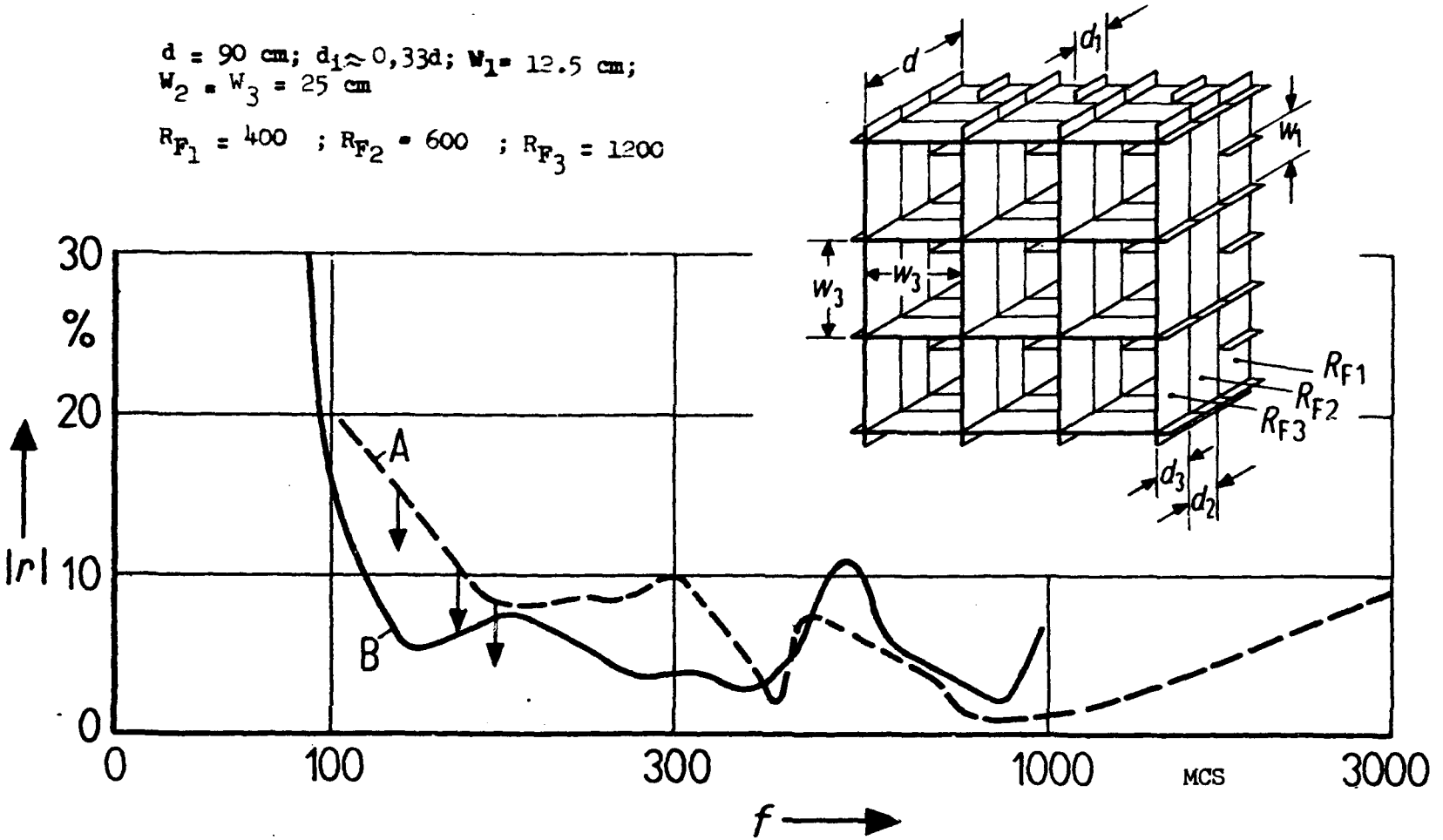
d = 90 cm; $d_1 \approx 0{,}33d$; W_1 = 12.5 cm;
$W_2 = W_3$ = 25 cm
R_{F_1} = 400 ; R_{F_2} = 600 ; R_{F_3} = 1200
30
%
20
|r| 10
0
A
B
0
100
300
1000
MCS
3000
f
d
d_1
W_1
W_3
W_3
R_{F1}
R_{F2}
R_{F3}
d_3
d_2

Fig. 3.15

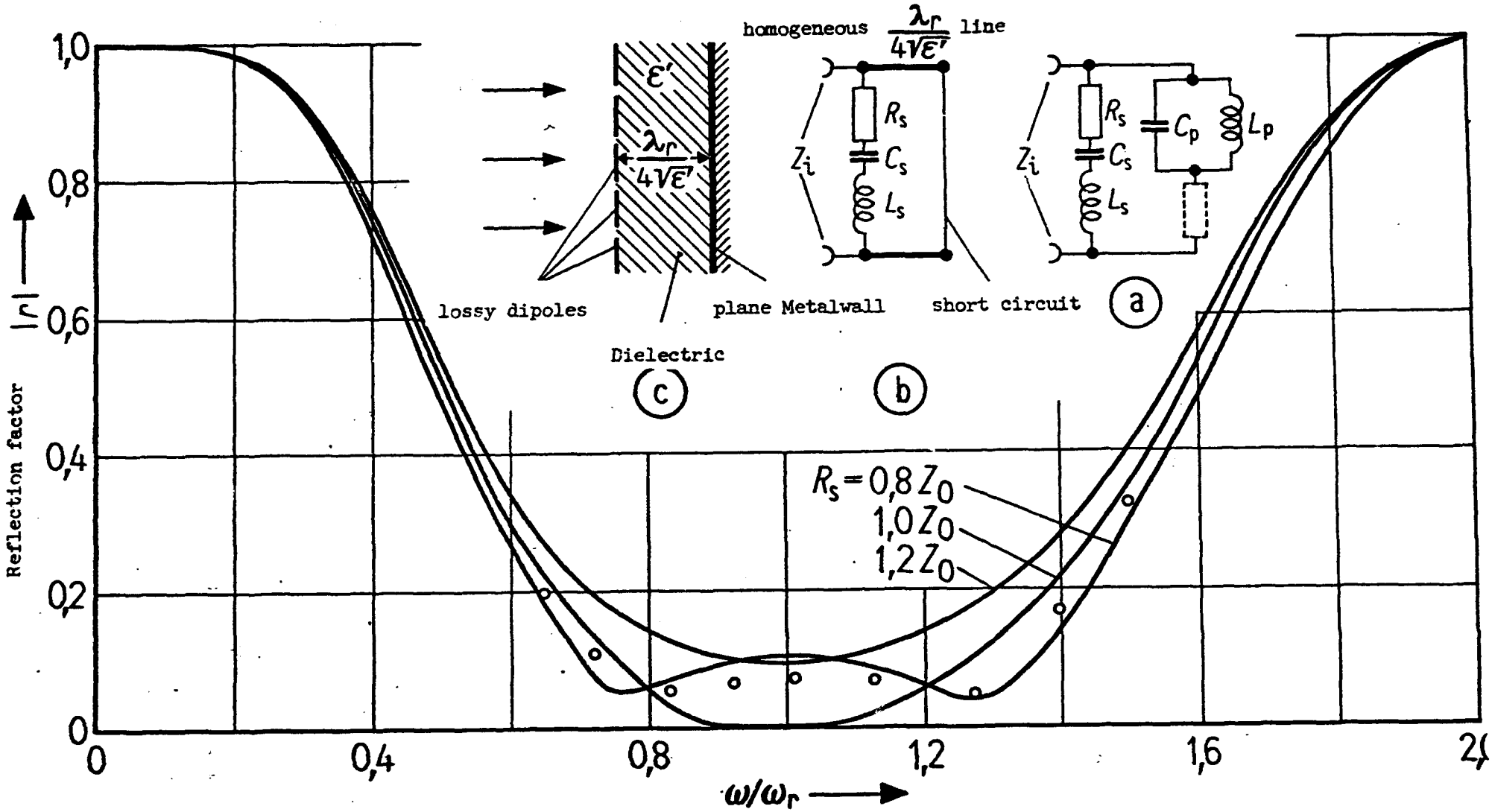
homogeneous $\frac{\lambda_r}{4\sqrt{\varepsilon'}}$ line
ε'
$\frac{\lambda_r}{4\sqrt{\varepsilon'}}$
R_s
C_s
L_s
Z_i
C_p
L_p
lossy dipoles
plane Metalwall
short circuit
Dielectric
a
b
c
$R_s = 0{,}8\,Z_0$
$1{,}0\,Z_0$
$1{,}2\,Z_0$
Reflection factor $|r|$
ω/ω_r
1,0
0,8
0,6
0,4
0,2
0
0,4
0,8
1,2
1,6

Fig. 3.16

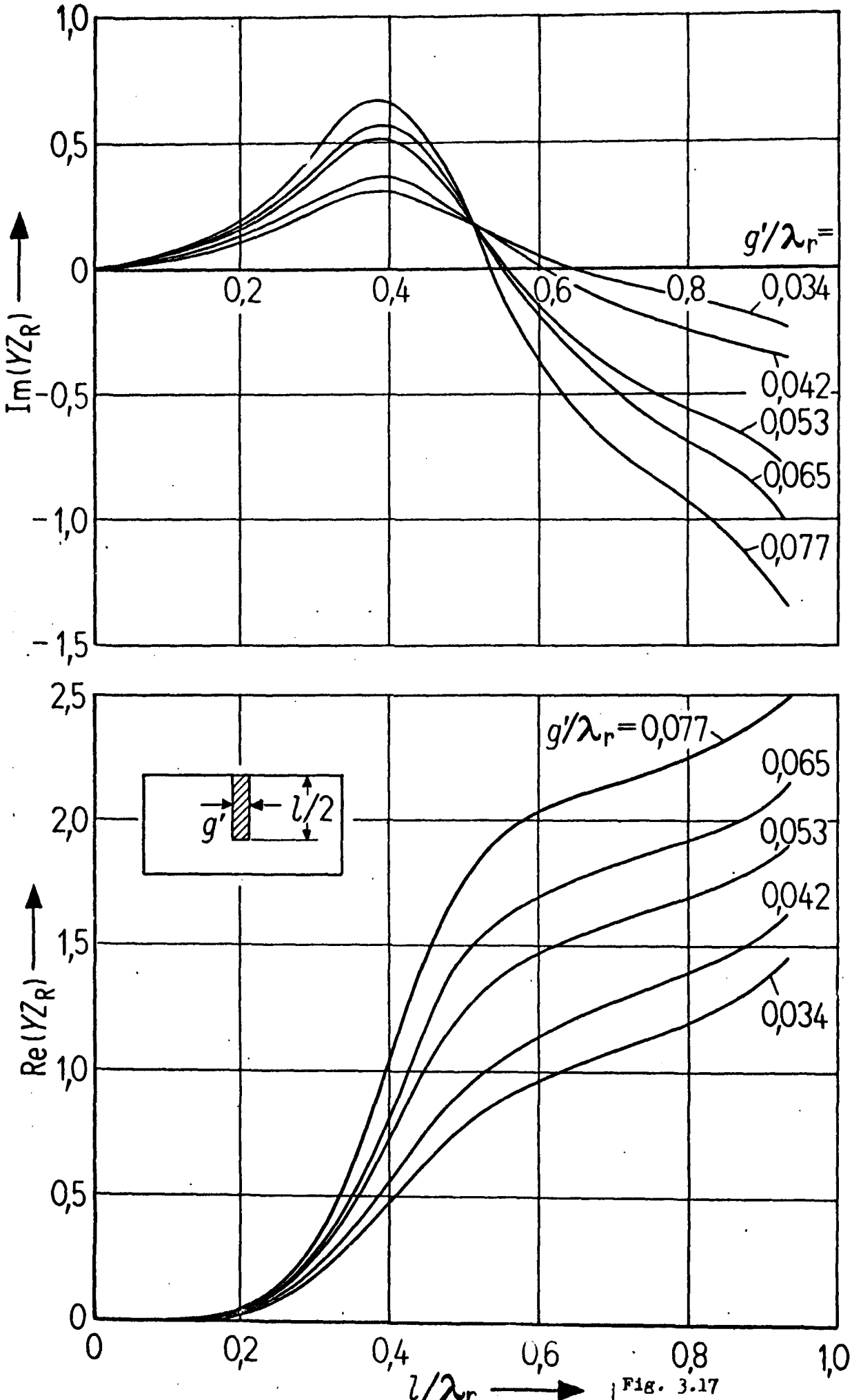
1,0
0,5
0
-0,5
-1,0
-1,5
Im(YZR)
0,2
0,4
0,6
0,8
g'/λr=
0,034
0,042
0,053
0,065
0,077
2,5
2,0
1,5
1,0
0,5
0
Re(YZR)
g'
l'/2
g'/λr=0,077
0,065
0,053
0,042
0,034
0
0,2
0,4
0,6
0,8
1,0
l/λr

Fig. 3.17

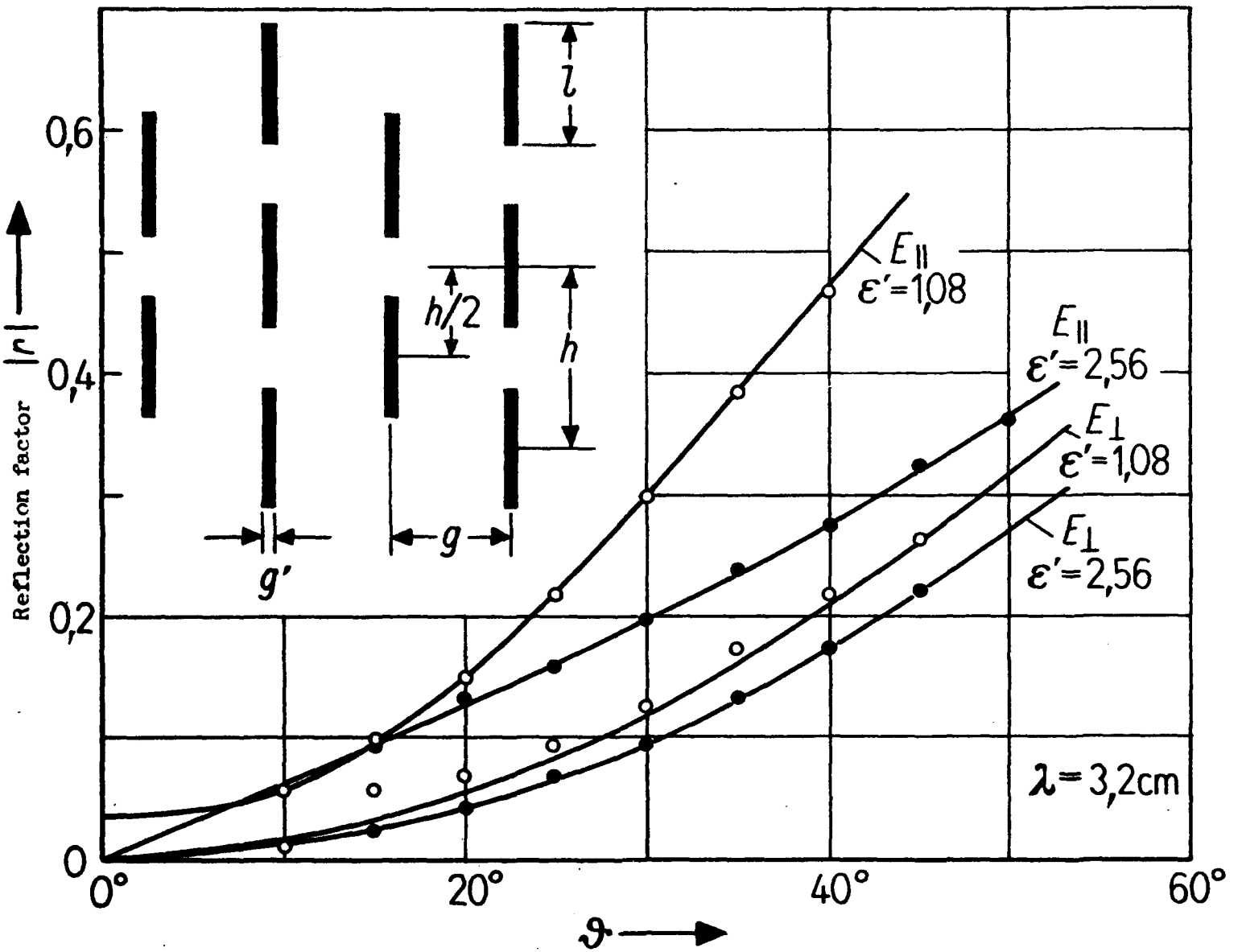
Reflection factor |r|
0,6
0,4
0,2
0
0°
20°
40°
60°
ϑ
l
h/2
h
g
g'
E∥
ε'=1,08
E∥
ε'=2,56
E⊥
ε'=1,08
E⊥
ε'=2,56
λ=3,2cm

Fig. 3.18

transversal, longitudinal grid

l = 22 mm	l = 11.5 mm	dipole width 0.3 mm
g = 15 mm	g = 15 mm	dipole foil surface resistivity 15.0.
h = 25 mm	h = 12.5 mm	(l, g, h see fig. 3.18)

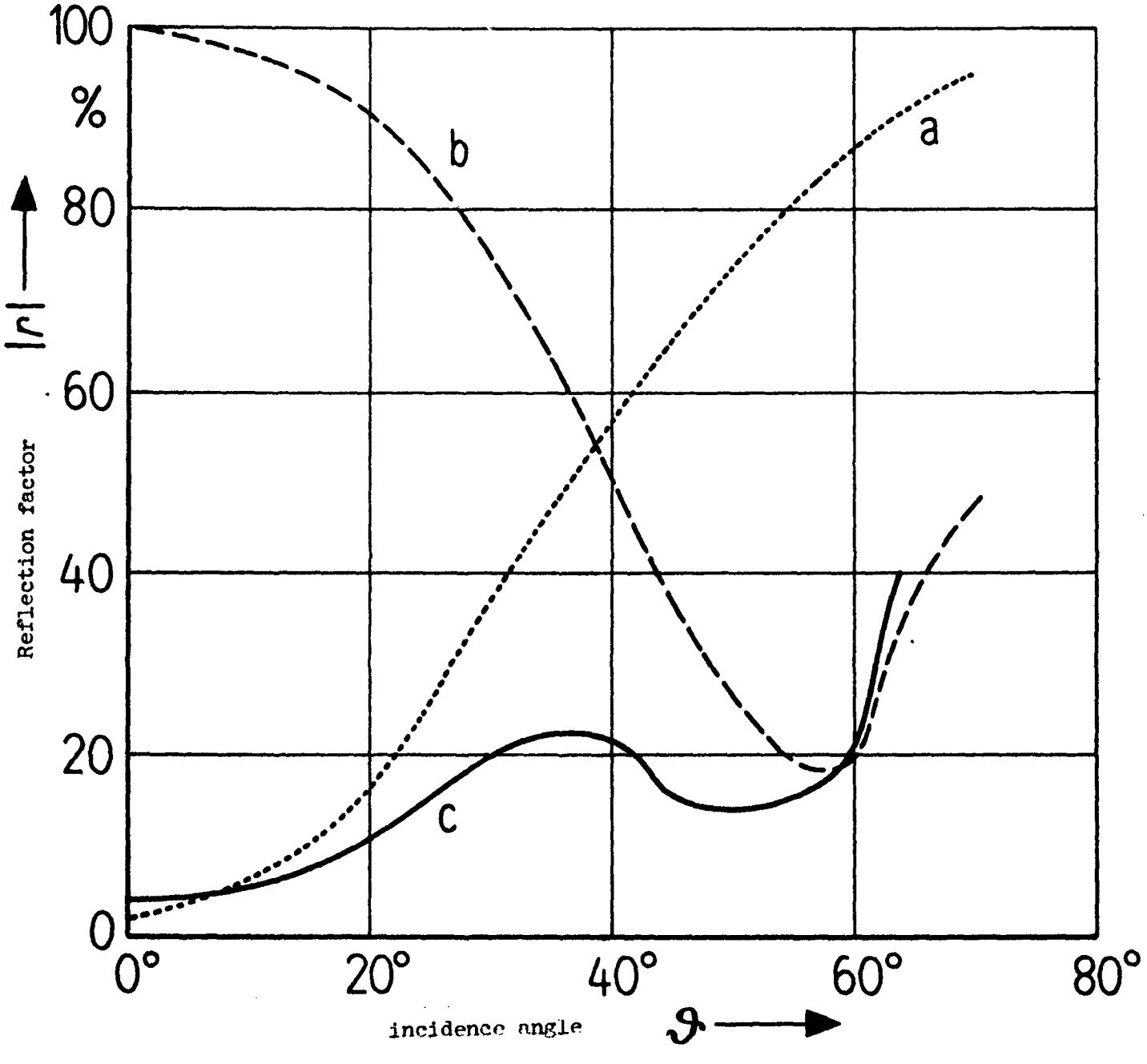

Fig. 3.19

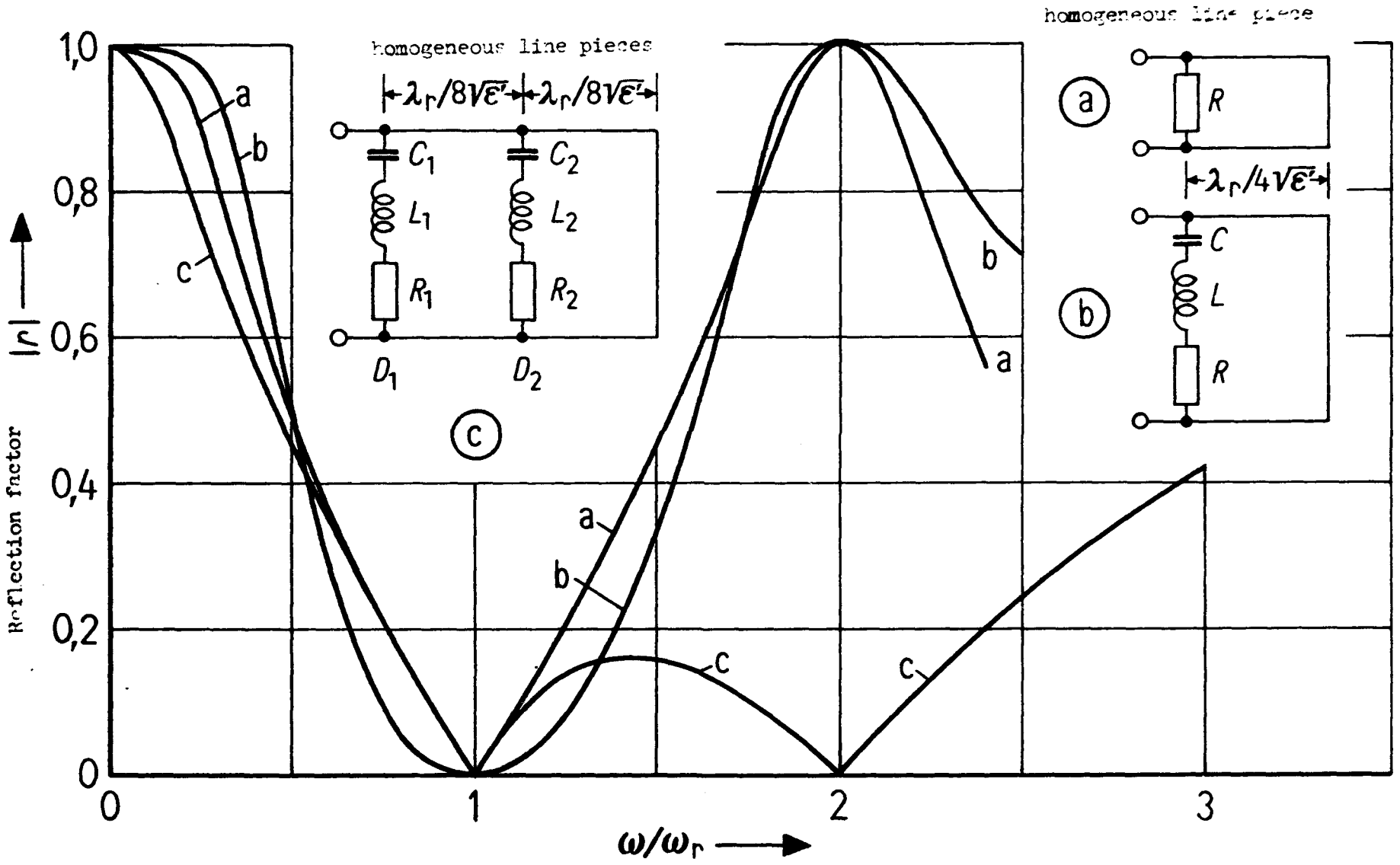
homogeneous line pieces
$\lambda_r/8\sqrt{\varepsilon'}$ $\lambda_r/8\sqrt{\varepsilon'}$
C_1 L_1 R_1
C_2 L_2 R_2
D_1 D_2
c
homogeneous line piece
a
R
$\lambda_r/4\sqrt{\varepsilon'}$
b
C
L
R
Reflection factor |r|
1,0
0,8
0,6
0,4
0,2
0
0
1
2
3
ω/ω_r
a
b
c

Fig. 3.20

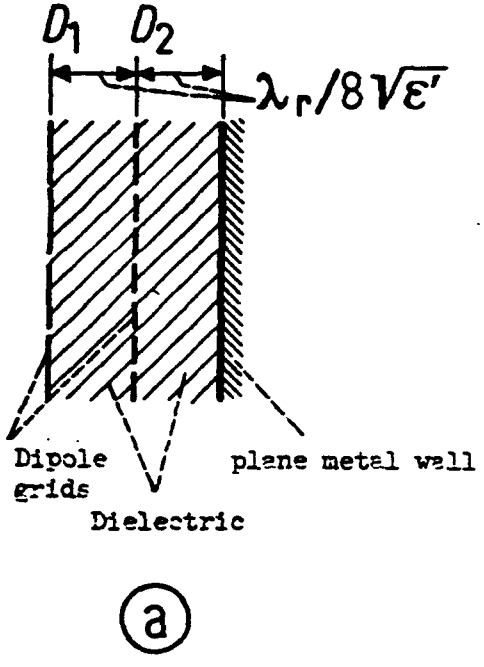
D_1
D_2
$\lambda_r/8\sqrt{\varepsilon'}$
Dipole grids
plane metal wall
Dielectric
a

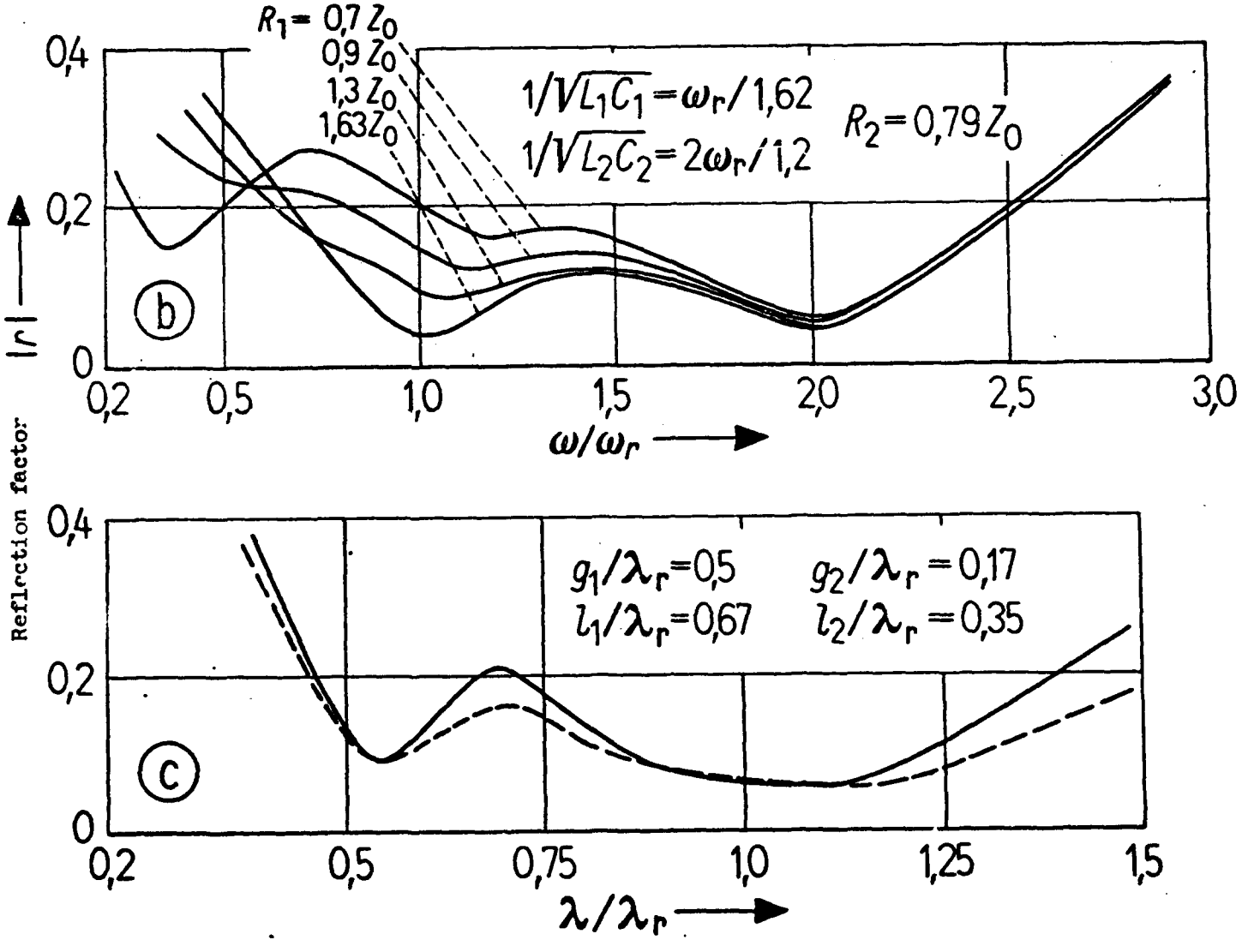
R_1= 0,7 Z_0
0,9 Z_0
1,3 Z_0
1,63 Z_0
$1/\sqrt{L_1C_1}=\omega_r/1,62$
$1/\sqrt{L_2C_2}=2\omega_r/1,2$
$R_2=0,79\,Z_0$
b
|r|
0,4
0,2
0
0,2
0,5
1,0
1,5
2,0
2,5
3,0
ω/ω_r
Reflection factor
$g_1/\lambda_r=0,5$
$g_2/\lambda_r=0,17$
$l_1/\lambda_r=0,67$
$l_2/\lambda_r=0,35$
c
0,4
0,2
0
0,2
0,5
0,75
1,0
1,25
1,5
λ/λ_r

Fig. 3.21

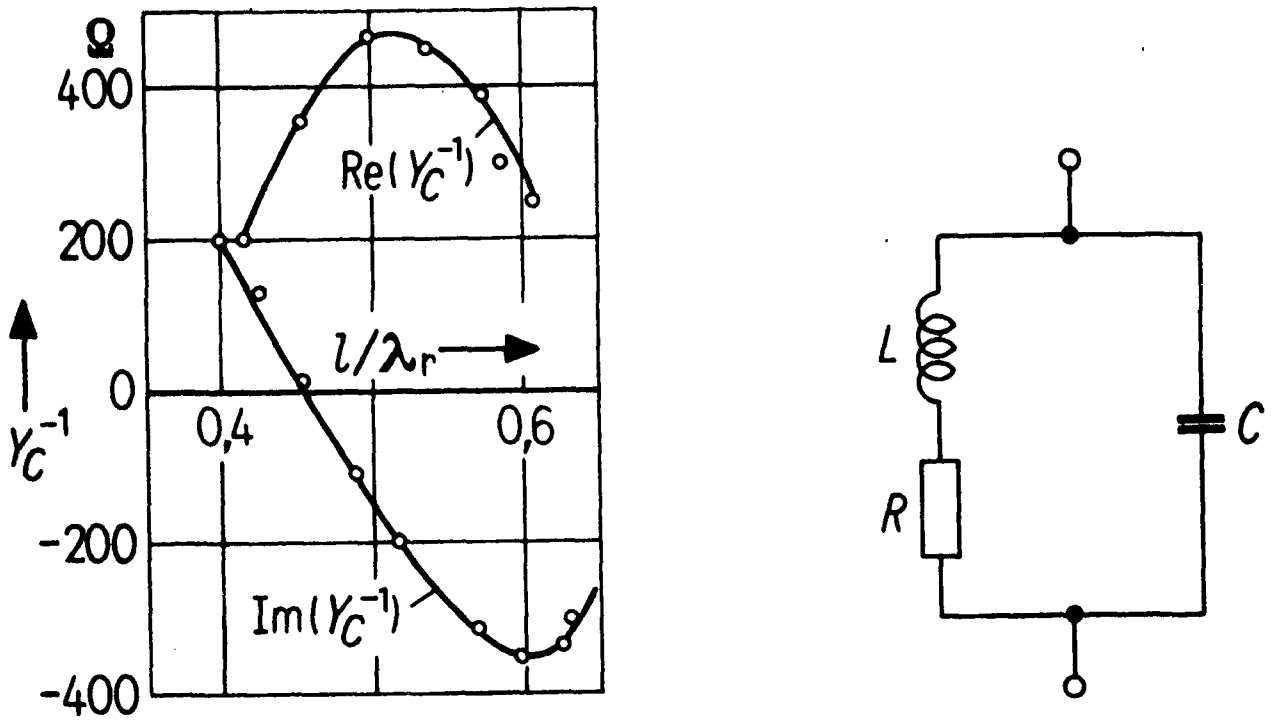

Fig. 3.22

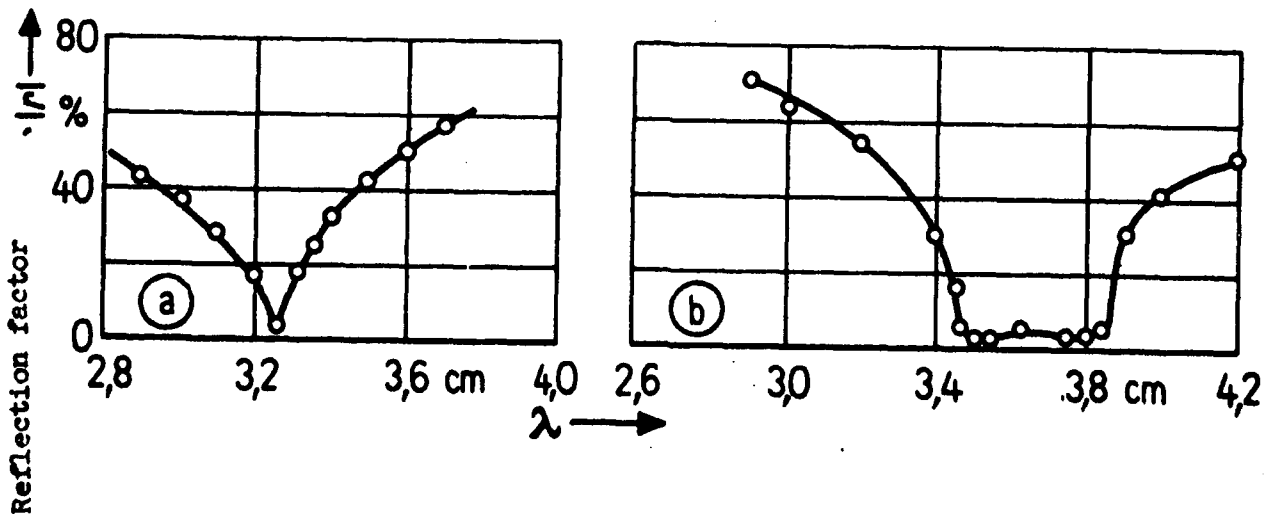

Fig. 3.23

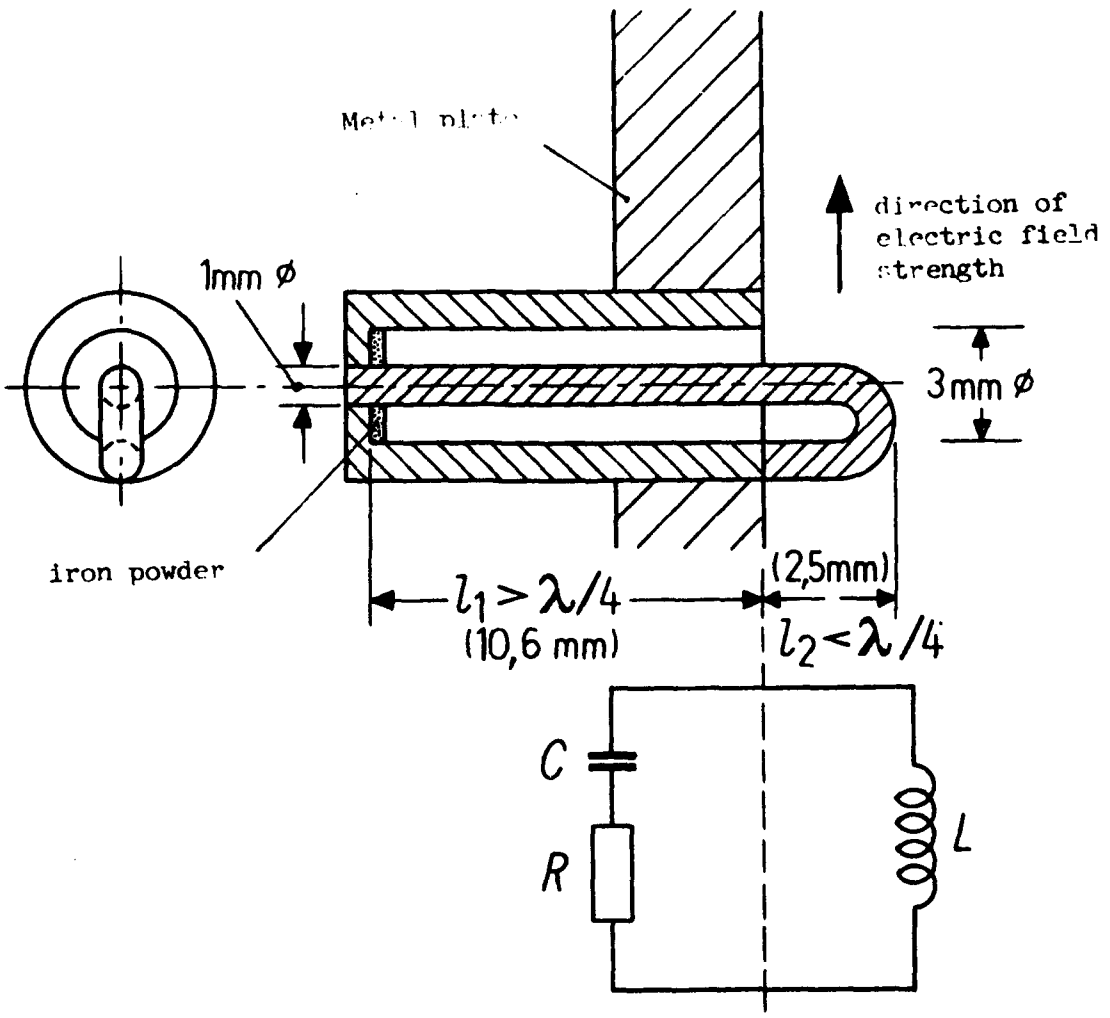
Metal plate
direction of
electric field
strength
1mm ø
3mm ø
iron powder
$l_1 > \lambda/4$
(10,6 mm)
(2,5mm)
$l_2 < \lambda/4$
C
R
L

Fig. 3.24

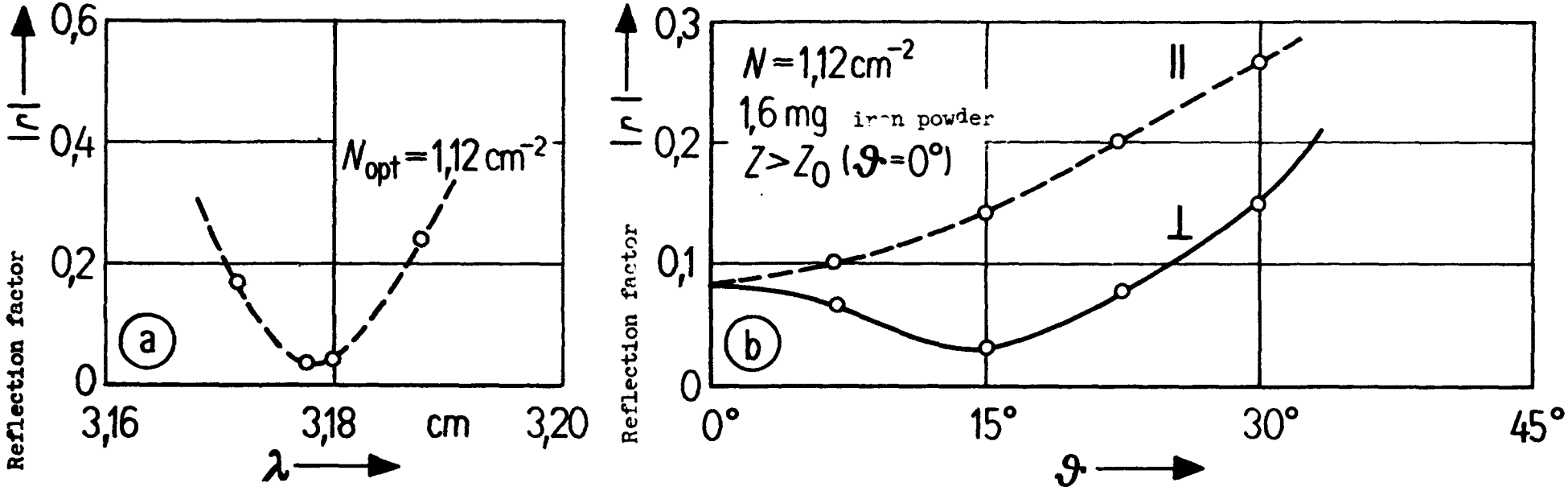
0,6
0,4
0,2
0
|r|
Reflection factor
$N_{opt} = 1{,}12\,cm^{-2}$
a
3,16
3,18
cm
3,20
λ
0,3
0,2
0,1
0
$N = 1{,}12\,cm^{-2}$
1,6 mg iron powder
$Z > Z_0$ ($\vartheta = 0°$)
∥
⊥
b
0°
15°
30°
45°
ϑ

Fig. 3.25

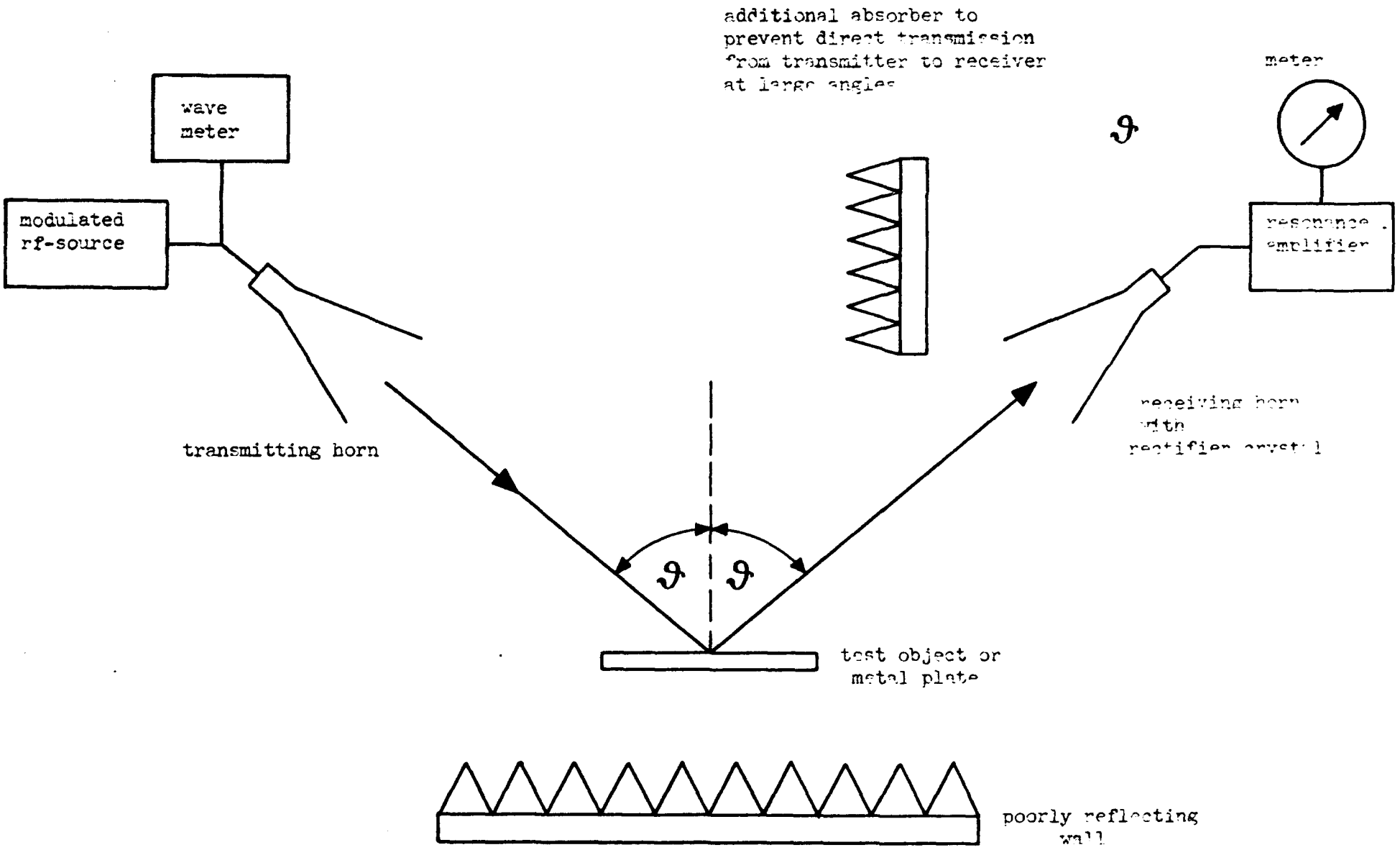
additional absorber to
prevent direct transmission
from transmitter to receiver
at large angles
meter
wave
meter
modulated
rf-source
resonance
amplifier
transmitting horn
receiving horn
with
rectifier crystal
test object or
metal plate
poorly reflecting
wall

Fig. 5.1

THIS
PAGE
IS
MISSING
IN
ORIGINAL
DOCUMENT

FIG. 5.2

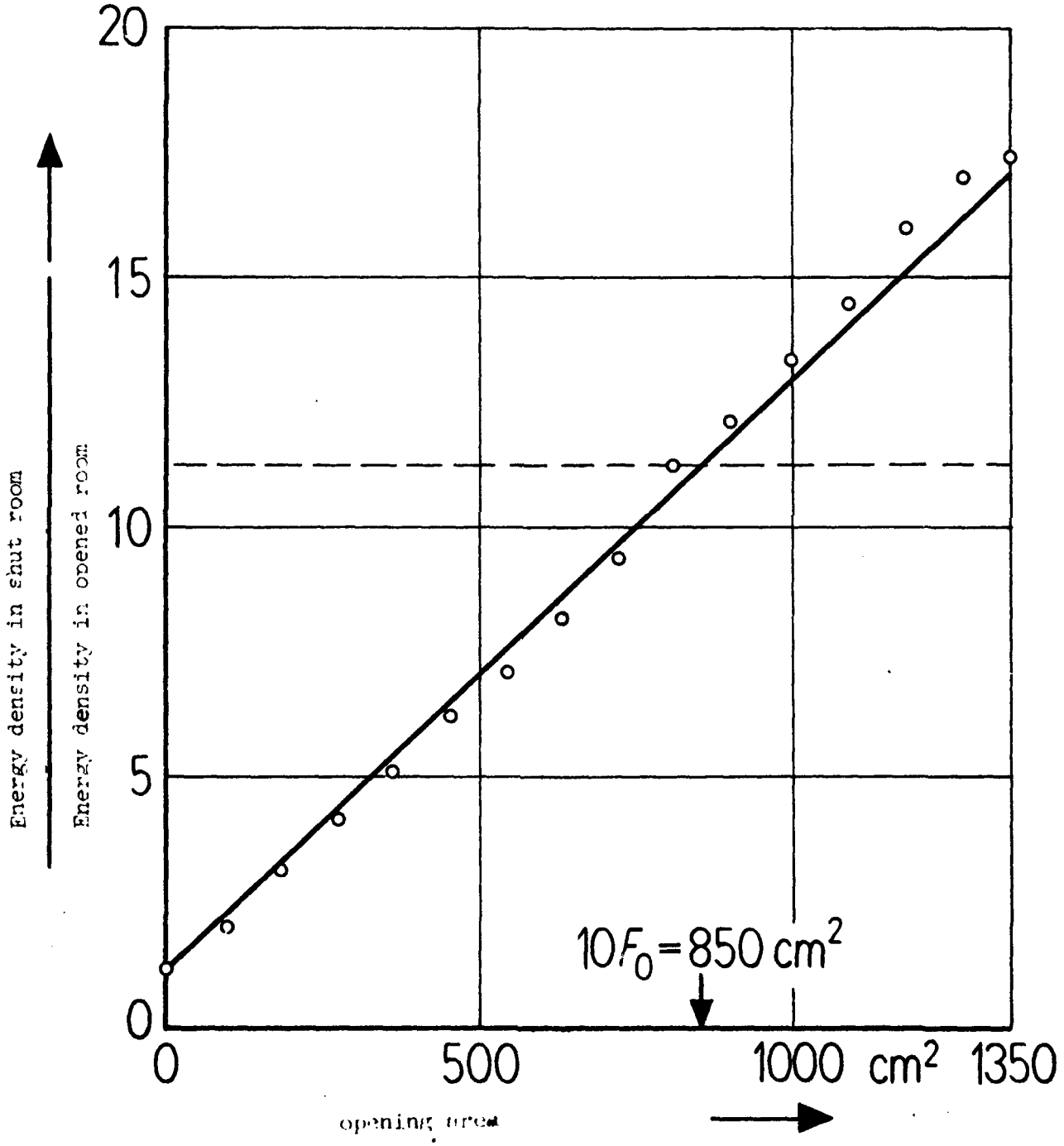
20
15
10
5
0
0
500
1000 cm²
1350
$10F_0 = 850\ cm^2$
Energy density in shut room
Energy density in opened room
opening area

Fig. 5.3

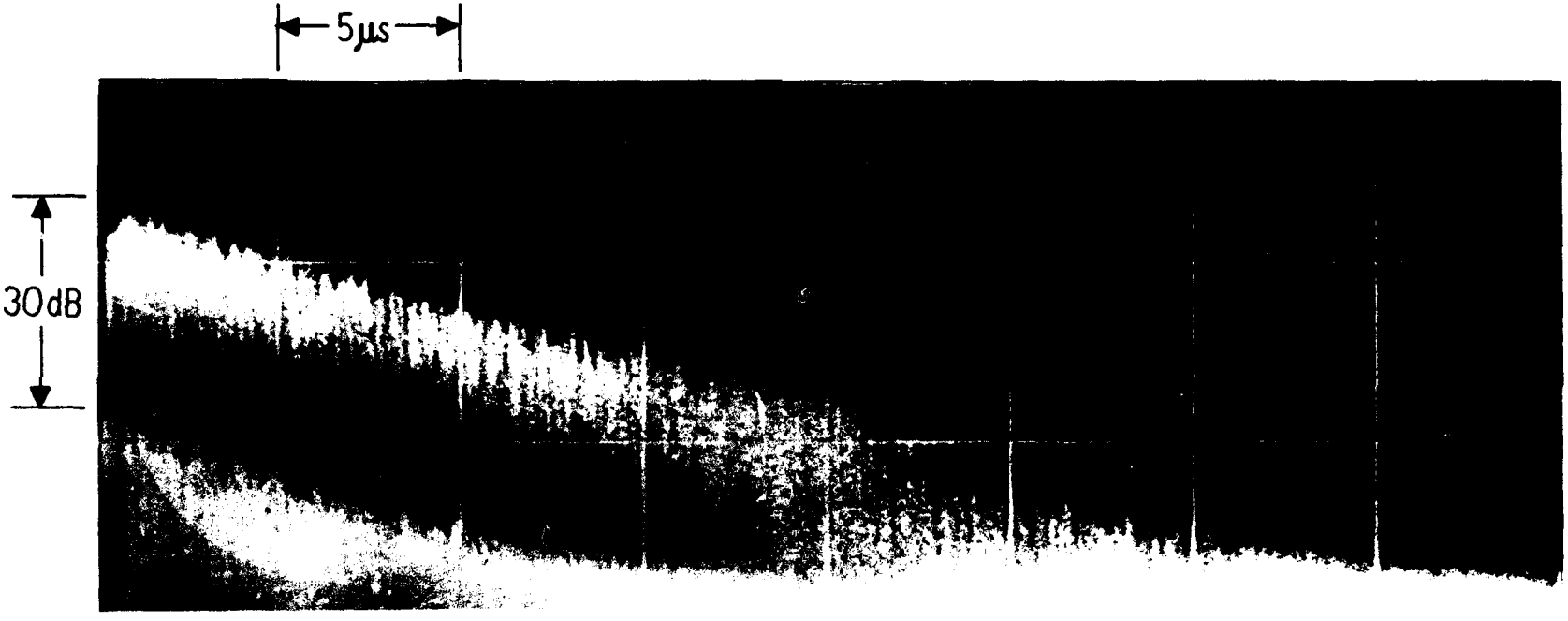

Fig. 5.4

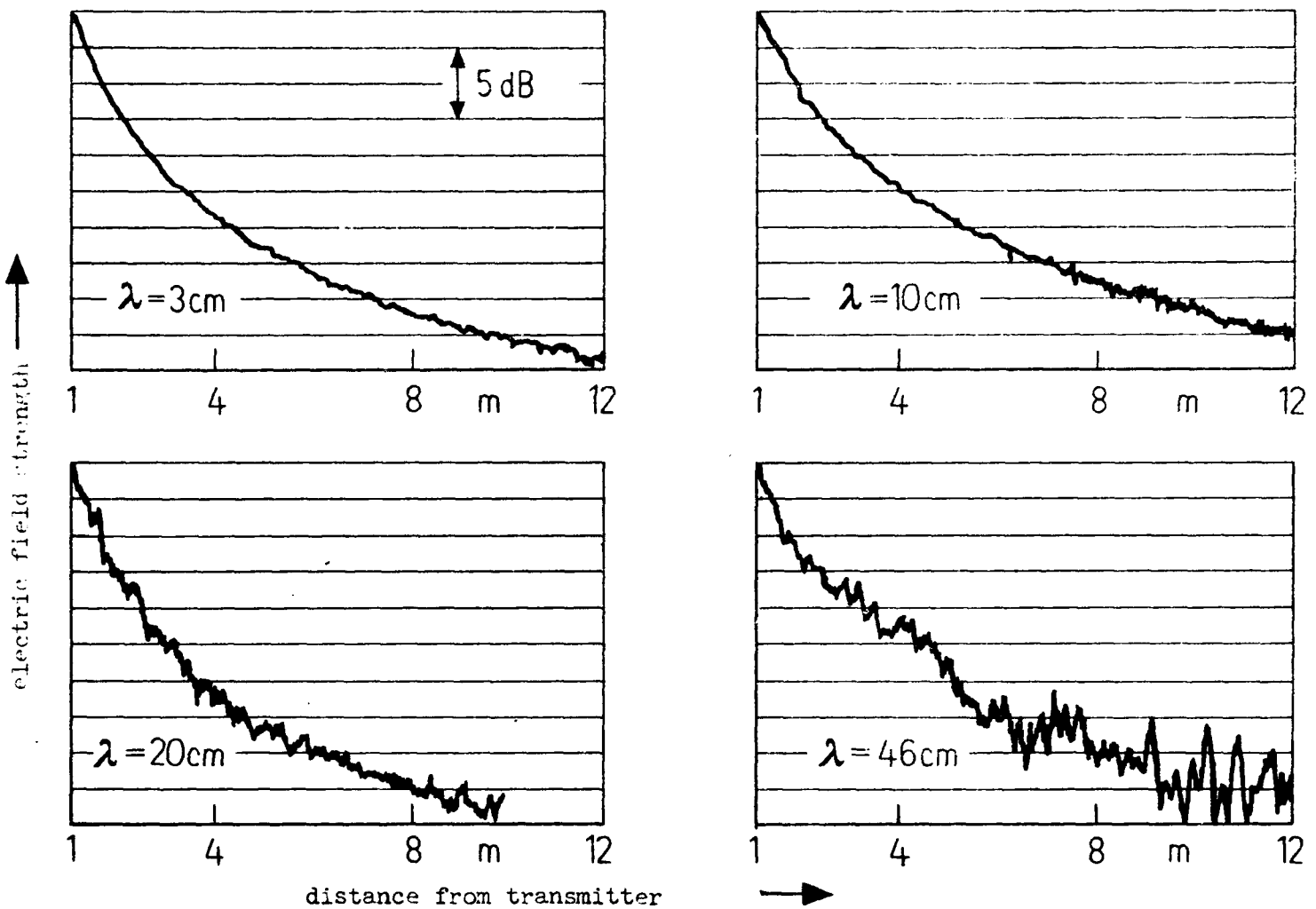
5 dB
λ=3cm
λ=10cm
λ=20cm
λ=46cm
1
4
8
m
12
electric field strength
distance from transmitter

Fig. 5.5

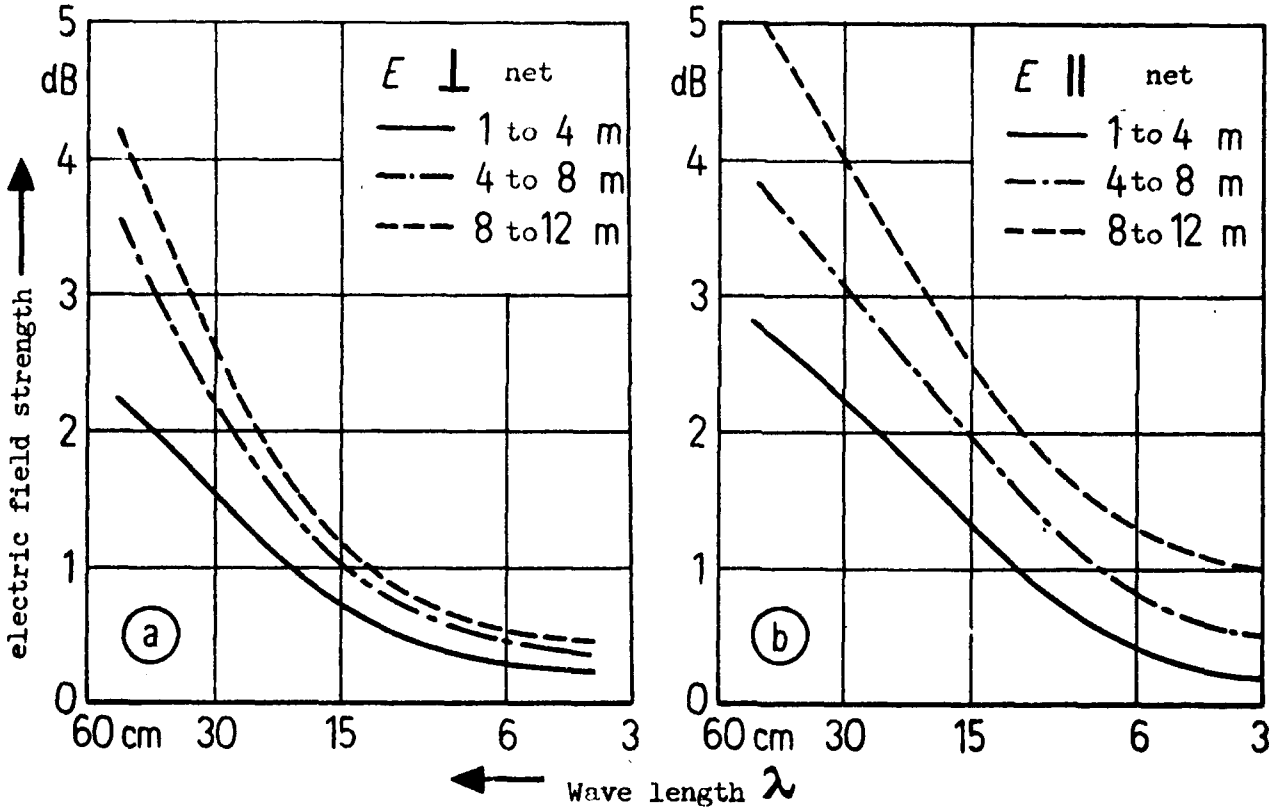
5
dB
4
3
2
1
0
electric field strength
E ⊥ net
1 to 4 m
4 to 8 m
8 to12 m
a
60 cm
30
15
6
3
E ∥ net
1 to 4 m
4 to 8 m
8 to 12 m
b
Wave length λ

Fig. 5.6

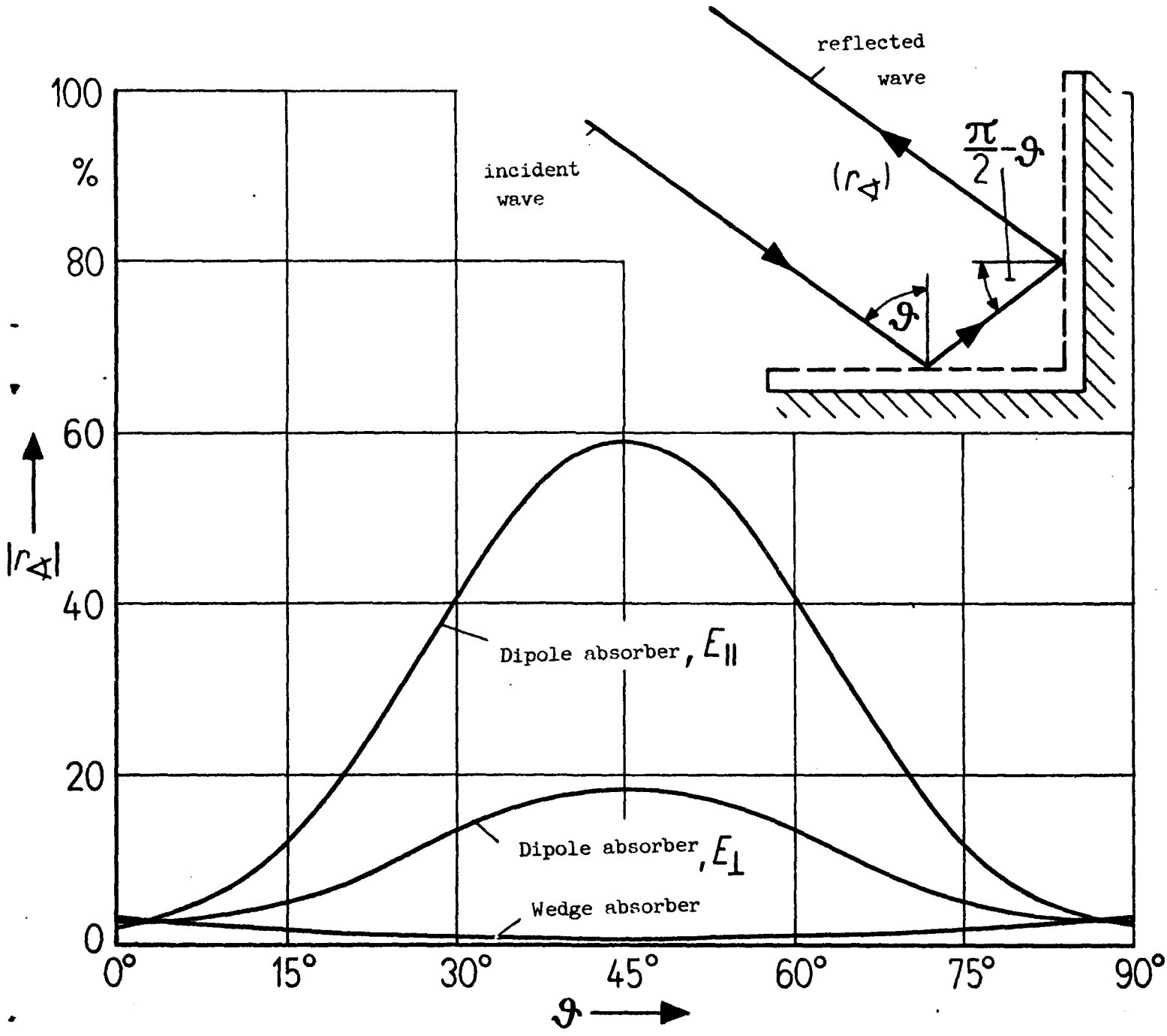
reflected
wave
incident
wave
$(r_\perp)$
$\frac{\pi}{2}-\vartheta$
ϑ
100
%
80
60
40
20
0
$|r_\perp|$
Dipole absorber, $E_\parallel$
Dipole absorber, $E_\perp$
Wedge absorber
0°
15°
30°
45°
60°
75°
90°
ϑ

Fig. 5.7